Lawrence Berkeley National Laboratory
Recent Work

Title
PRECISION ATOMIC-BEAM STUDIES OF THE ZEEMAN EFFECT IN THALLIUM AND GALLIUM (ELECTRONIC AND NUCLEAR MAGNETIC MOMENTS).

Permalink
https://escholarship.org/uc/item/2bn4r1k6

Author
Fowler, Thomas Richard

Publication Date
1968-08-01

eScholarship.org Powered by the California Digital Library
University of California

UCRL-18331
c. 2

University of California

Ernest O. Lawrence Radiation Laboratory

PRECISION ATOMIC-BEAM STUDIES OF THE ZEEMAN EFFECT
IN THALLIUM AND GALLIUM
(ELECTRONIC AND NUCLEAR MAGNETIC MOMENTS)

Thomas Richard Fowler

(Ph.D. Thesis)

August 1, 1968

RECEIVED
LAWRENCE
RADIATION LABORATORY
AUG 30 1968
LIBRARY AND
DOCUMENTS SECTION

TWO-WEEK LOAN COPY

This is a Library Circulating Copy which may be borrowed for two weeks. For a personal retention copy, call Tech. Info. Division, Ext. 5545

UCRL-18331
c. 2

DISCLAIMER

This document was prepared as an account of work sponsored by the United States Government. While this document is believed to contain correct information, neither the United States Government nor any agency thereof, nor the Regents of the University of California, nor any of their employees, makes any warranty, express or implied, or assumes any legal responsibility for the accuracy, completeness, or usefulness of any information, apparatus, product, or process disclosed, or represents that its use would not infringe privately owned rights. Reference herein to any specific commercial product, process, or service by its trade name, trademark, manufacturer, or otherwise, does not necessarily constitute or imply its endorsement, recommendation, or favoring by the United States Government or any agency thereof, or the Regents of the University of California. The views and opinions of authors expressed herein do not necessarily state or reflect those of the United States Government or any agency thereof or the Regents of the University of California.

UCRL-18331

UNIVERSITY OF CALIFORNIA

Lawrence Radiation Laboratory
Berkeley, California

AEC Contract No. W-7405-eng-48

PRECISION ATOMIC-BEAM STUDIES OF THE ZEEMAN EFFECT IN THALLIUM AND GALLIUM (ELECTRONIC AND NUCLEAR MAGNETIC MOMENTS)

Thomas Richard Fowler

(Ph.D. Thesis)

August 1, 1968

PRECISION ATOMIC-BEAM STUDIES OF THE ZEEMAN EFFECT
IN THALLIUM AND GALLIUM
(ELECTRONIC AND NUCLEAR MAGNETIC MOMENTS)

Contents

PRECISION ATOMIC-BEAM STUDIES OF THE ZEEMAN EFFECT IN THALLIUM AND GALLIUM (ELECTRONIC AND NUCLEAR MAGNETIC MOMENTS)

Thomas Richard Fowler

Lawrence Radiation Laboratory
University of California
Berkeley, California

August 1, 1968

ABSTRACT

The atomic beam method was used to measure the electronic and nuclear magnetic moments and the off-diagonal dipole interaction constants of gallium and thallium in both the ground state, $^2P_{1/2}$, and the metastable state, $^2P_{3/2}$.

The results for ^{69}Ga are:

$$g_{1/2} = -0.66579172(28)$$

$$g_{3/2} = -1.33405731(60)$$

$$g_I = +7.29530(33) \times 10^{-4}$$

$$a''' = -107.76(98) \text{ MHz}$$

$$\eta = 1.0886(290)$$

$$\Delta\nu_{1/2} = 2677.98716(20) \text{ MHz}$$

Also, the previous measurement of the hyperfine interaction constants by Holloway have been re-analyzed (see Appendix A).

For ^{205}Tl the results are:

$$g_{1/2} = -0.6656924(18)$$

$$g_{3/2} = -1.33410447(20)$$

$$g_I = 17.549(14) \times 10^{-4}$$

$$Na''' = -1.051(230) \times 10^3 \text{ MHz}$$

where N is a dimensionless relativistic correction factor of order unity.

For ^{203}Tl the results are:

$$g_{1/2} = -0.6656920(18)$$

$$g_{3/2} = -1.3341044(11)$$

$$g_I = 17.375(14) \times 10^{-4}$$

$$Na''' = -1.090(240) \times 10^{3} \text{ MHz} .$$

Both thallium isotopes (203 and 205) were measured to check for possible isotope shifts at Z = 81; none were found. All errors shown in parenthesis are two standard deviations. The sign convention for all g-factors is that the sign of g is the same as the sign of the magnetic moment.

Introduction

The subgroup III elements (Gallium, Indium, and Thallium) occupy a unique position in the theory of hyperfine structure because they have the simplicity of only one electron outside of closed shells yet have two relatively close lying electron states in the ground configuration which can interact with each other. Because of the ease of detection and production of both electronic states, Gallium has been the object of much research in Atomic Beams. By measuring the electronic g factors in both states Kusch and Foley[19] were able to infer the anomalous magnetic moment of the electron. Later, Daley and Holloway[33], by measuring all three zero field hyperfine separations in the upper $^2P_{3/2}$ state to great accuracy, were able to deduce the dipole, quadrupole, and octupole interaction constants. Unfortunately, to analyze the data of Daley and Holloway correctly - i.e. including the effects of the other nearby $^2P_{1/2}$ state - one needs to know the off-diagonal matrix elements of the dipole and quadrupole operators (the off-diagonal octupole elements are zero). Without data that is sensitive to these off-diagonal elements only theoretical estimates could be used in the analysis. Consequently, the results of Daley and Holloway contain a small untested correction. Later, Lurio[24] measured the zero field splitting ($\Delta\nu_{1/2}$) in the lower (ground) state.

This was the situation prior to the present work. The present work was undertaken in the hope of measuring these off-diagonal elements and obtaining a complete consistent analysis giving unique values for all parameters of interest (see section I-D). As discussed in that section, there are eleven parameters involved in the analysis of the two states. This is, of course, neglecting any other states of other configurations. These eleven parameters are $a_{3/2}$, b, c, $\Delta\nu_{1/2}$, a''', η, N, g_I, $g_{1/2}$, $g_{3/2}$, and δ where $a_{3/2}$, b, and c are the dipole, quadrupole, and octupole interaction constants of the upper $^2P_{3/2}$ state, $\Delta\nu_{1/2}$ the hyperfine(dipole) separation constant, $a'''$and ηb the off-diagonal dipole and quadrupole elements, N a relativistic correction factor near one, $g_{1/2}$, $g_{3/2}$, and g_I the g factors of the lower $^2P_{1/2}$ state, the upper $^2P_{3/2}$ state, and the nucleus respectively, and δ is the fine structure separation of the two states. Now, in order to determine all parameters uniquely, eleven different types of measurements must be made. That is, eleven measurements that depend differently on the parameters. Optical measurements give δ and we can set N equal to one since Z is only 31. This eliminates two parameters outright. Daley and Holloway's data are three independent measurements that are very sensitive to $a_{3/2}$, b, and c with only a slight correction due to the remaining parameters and Lurio's data gives $\Delta\nu_{1/2}$. However, it was necessary to remeasure $\Delta\nu_{1/2}$ more accurately for this work. Nuclear Magnetic Resonance measurements of the nuclear magnetic moment, however, could not be used for g_I since there may be a large

diamagnetic correction from Gallic ion solutions(in which the NMR measurements were made) to an atomic beam of free atoms. Consequently, it was necessary to measure g_I. It was also felt worthwhile remeasuring the electronic g factors($g_{1/2}$ and $g_{3/2}$) to a few parts per million, not only to complete the analysis, but also to compare the result with the theory of the Zeeman effect.

Summarizing, using the three independent measurements of Daley and Holloway we see that we need 9 minus 3 or 6 additional independent measurements to fit the 9 parameters of interest. By measuring the transitions listed below(some at different fields) we were able to get enough additional information to determine all 9 parameters.

Although Thallium is just as easy to detect as Gallium, the upper $^2P_{3/2}$ state is not produced in sufficient quantities in a thermal source. Consequently, it is much more difficult determining all the parameters of interest. The only precision measurements prior to the present work have been those of Gould[34] who measured $\Delta\nu_{3/2}$ and a series of measurements of $\Delta\nu_{1/2}$ the latest of which is by Beehler and Glaze[23] for ^{205}Tl and Lurio and Prodell[24] for ^{203}Tl. The purpose of the present measurements was to measure the electronic g factors to a few parts per million and to measure the off-diagonal dipole matrix elements and to compare them with theoretical estimates. Since the nuclear spins are one half there are no quadrupole or octupole elements. By measuring both isotopes we were also able to check for any isotope shifts in the

electronic g factors. Since Z is 81 for Thallium, we could not set N equal to one. Assuming $\Delta\nu_{1/2}$, $\Delta\nu_{3/2}$, and δ are known we are left(see section I-D) with the five parameters $g_{1/2}$, $g_{3/2}$, g_I, a''', and N. Since there are no "Doublet transitions" in the lower state(unlike Gallium) we were unable to get five independent measurements but only four. Consequently, the data was analyzed by assuming various values of N near one and fitting the remaining four parameters. Fortunately, the values of $g_{1/2}$, $g_{3/2}$, and g_I were, for all practical purposes, independent of N whereas a''' varied approximately inversely with N as shown in Figure III-7.

I. THEORY

A. Fine Structure

As is well known, the detailed structure of atoms is very complicated. For a neutral atom of atomic number Z, there are Z + 1 particles to consider, assuming the nucleus is rigid. For gallium, therefore, with Z = 31, we have a 32-body problem and for thallium we have an 82-body problem. Clearly, many approximations are necessary in order to make practical any calculations. A well-known approximate Hamiltonian, based on non-relativistic quantum mechanics, is

$$\mathcal{H}_0 = \sum_{i=1}^{Z}\left(\frac{P_i^2}{2m} - \frac{Ze^2}{r_i}\right) + \sum_{i>j}^{Z}\frac{e^2}{r_{ij}} + \sum_{i=1}^{Z}\xi_i(r_i)\vec{\ell}_i\cdot\vec{s}_i \qquad (1)$$

where r_i is the distance of the i^{th} electron from the nucleus, and r_{ij} is the distance between electron i and electron j. The second term on the right is the electrostatic interaction among the electrons. The last term on the right, denoted by $\mathcal{H}_{so}$, is the spin-orbit interaction. Clearly this Hamiltonian neglects any effects due to the finite size, mass, or spin of the nucleus. It also neglects orbit-orbit, spin-spin, and spin-other-orbit interactions among the electrons. Such higher order effects will be discussed later. The resulting atomic structure that one could calculate, in principle, from Eq. (1) is known as the fine structure of the atom. For many-electron atoms, even Eq. (1) is much too difficult to handle and one makes the central-field approximation; that is one assumes the first term on the right-hand side of Eq. (1) is much larger than the last two terms. One first solves the problem with:

$$\mathcal{H}_{\text{central}} = \sum_{i=1}^{Z} \left[\frac{P_i^2}{2m} + U_i(r_i) \right]$$

where $U_i(r_i)$ is spherically symmetric. A rigorous treatment of $U_i(r_i)$ leads to the Hartee-Fock equation if one uses his "self-consistency principle". Since $\mathcal{H}_{\text{central}}$ is spherically symmetric, the wave function will be of the form, for electron i,

$$\psi_i = \psi_i(r_i, \theta_i, \phi_i, m_s) = R_n(r_i) Y_\ell^{m_\ell}(\theta_i, \phi_i)\sigma$$

where $\sigma = \alpha$ if $m_s = +1/2$ and $\sigma = \beta$ if $m_s = -1/2$. The wave function for the electrons, consistent with the exclusion principle, can be written as

$$\psi = \frac{1}{\sqrt{N!}} \begin{vmatrix} \psi_1(1) & \cdots & \psi_1(N) \\ \vdots & & \vdots \\ \psi_N(1) & \cdots & \psi_N(N) \end{vmatrix}$$

where N is the total number of electrons (N equals Z if the atom is electrically neutral) and $\psi_i(j)$ is shorthand for $\psi_i(n,\ell,m_\ell,m_s)$. The energy is independent of m_ℓ and m_s. Each energy eigenvalue can be identified by $(n_1\ell_1)^{X(1)}(n_2\ell_2)^{X(2)} - - - - (n_N\ell_N)^{X(N)}$ [where X(1) is the number of times $(n_1\ell_1)$ occurs] and is called a configuration. For gallium we have for the ground state configuration $1s^2\ 2s^2\ 2p^6\ 3s^2\ 3p^6\ 3d^{10}\ 4s^2\ 4p$. Similarly, for thallium we have $1s^2\ 2s^2\ 2p^6\ 3s^2\ 3p^6\ 3d^{10}\ 4s^2\ 4p^6\ 4d^{10}\ 4f^{14}\ 5s^2\ 5p^6\ 5d^{10}\ 6s^2\ 6p$. As expected for subgroup III elements, only a p electron remains outside of closed shells. Of course, many excited configurations also exist.

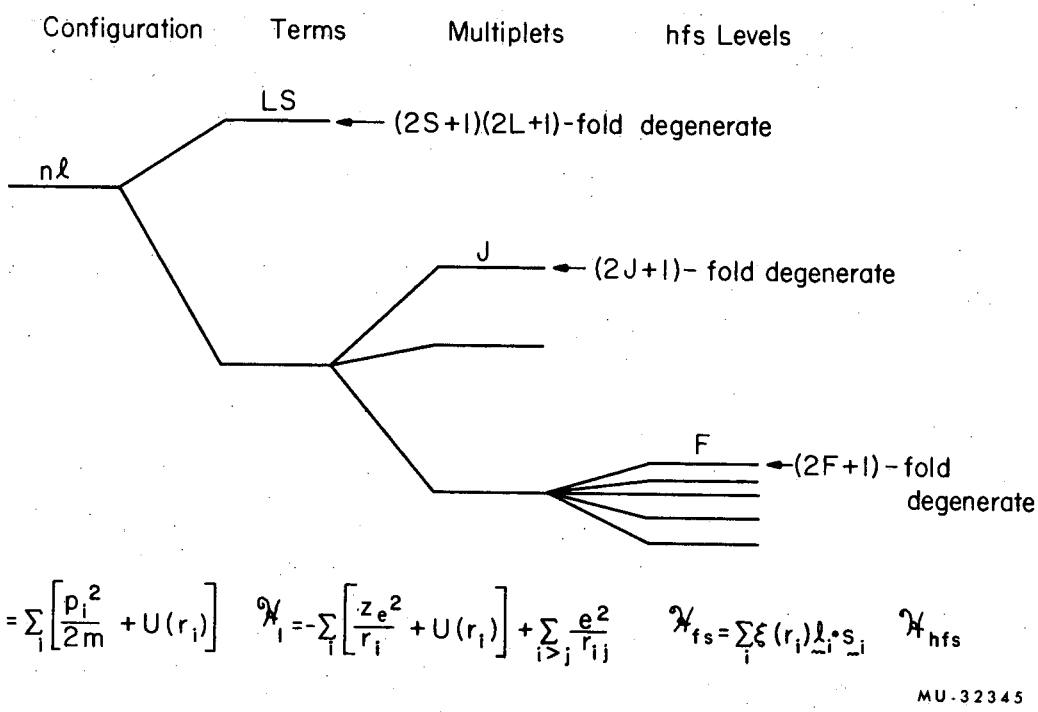

Fig. I-1. The effect of the inclusion of different terms in the Hamiltonian.

The remaining part of the Hamiltonian, $\mathcal{H}_0 - \mathcal{H}_{central}$, is handled by perturbation theory. If $e^2/r_{ij} >> \xi_i(r_i)\vec{\ell}_i \cdot \vec{s}_i$, we have the Russell-Saundars coupling scheme and we can neglect the spin-orbit interaction for a moment and consider only e^2/r_{ij}. Since $\vec{L} = \Sigma\vec{\ell}_i$ and $\vec{S} = \Sigma\vec{s}_i$ commutes with e^2/r_{ij}, $\vec{L}$ and $\vec{S}$ are good quantum numbers. Therefore, the electrostatic interaction splits each configuration into terms which can be labeled ^{2S+1}L, the degeneracy of which is $(2L+1)(2S+1)$. The spin-orbit interaction commutes with the total angular momentum of the atom, $\vec{J} = \vec{L} + \vec{S}$, and not $\vec{S}$ or $\vec{L}$ alone. Therefore, when the spin-orbit interaction is included the terms are split into levels $^{2S+1}L_J$ of degeneracy $2J+1$.

For gallium and thallium the ground-state configuration has only one term, the ^2P, since there is only one electron outside of closed shells. The ^2P term is split into $^2P_{1/2}$ and $^2P_{3/2}$ by the spin-orbit interaction with the $^2P_{1/2}$ becoming the ground state. The spin-orbit splitting between $^2P_{1/2}$ and $^2P_{3/2}$ is 826.24 cm^{-1} for gallium[2] and 7792.7 cm^{-1} for thallium[1].

For many heavy atoms, $e^2/r_{ij} << \xi_i(r_i)\vec{\ell}_i \cdot \vec{s}_i$ which leads to j-j coupling. The spin-orbit interaction is handled first coupling $\vec{\ell}_i$ and $\vec{s}_i$ to give $\vec{j}_i$. Both coupling schemes are approximations, of course, and one should diagonalize both the electrostatic and spin-orbit interactions simultaneously. J and the parity $(-1)^{\Sigma\ell_i}$ are always good quantum numbers and so can be used to label a state in any coupling scheme. For the ground state configurations of gallium and thallium we need not concern ourselves with coupling schemes since there is only one electron outside of closed shells. The fine structure of thallium

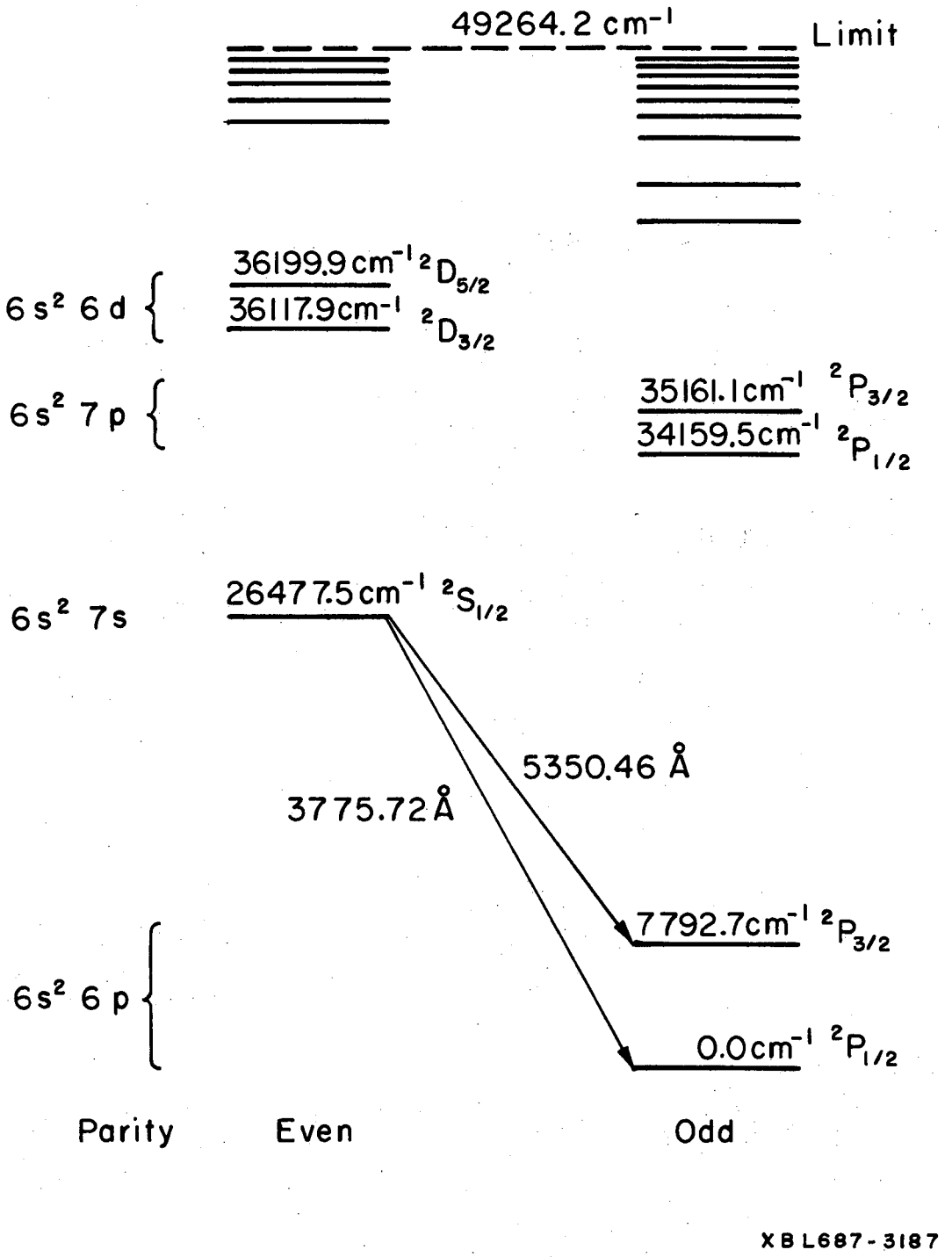

Fig. I-2. Atomic Fine-Structure Energy Levels of Thallium.

is shown in Fig. I-2[1]. For both Gallium and Thallium, $^2P_{1/2}$ is the ground state and all other states are unstable. The lifetime of these excited states depends upon several factors, the most important of which is the type of radiation emitted. For electric dipole transitions, the decay is very fast and lifetimes are of the order of 10^{-8} sec. The selection rules are $\Delta J = 0, \pm 1$, $J = 0 \not\to 0$ no, $\Delta L = 0, \pm 1$, $\Delta S = 0$, and parity must change. The L and S selection rules hold rigourously only for L-S coupling. For example, the $^2S_{1/2}$ level above the ground state can decay via electric dipole radiation and has a lifetime of the order of 10^{-8} sec.

Usually excited levels that cannot decay via electric dipole radiation have much longer lifetimes and are called metastable. For example, the $^2P_{3/2}$ state just above the ground state is metastable and decays by emitting magnetic dipole or electric quadrupole radiation. Higher orders than quadrupole can be neglected. The selection rules for magnetic dipole radiation are $\Delta J = 0, \pm 1$, $J = 0 \not\to 0$ no, $\Delta L = 0, \pm 1$, $\Delta S = 0, \pm 1$, and parity does not change. For the electric quadrupole case, for example, the rules are $\Delta J = 0, \pm 1, \pm 2$, $\Delta L = 0, \pm 1, \pm 2$, $\Delta S = 0$, and parity does not change and $0 \not\to 0$, $1/2 \not\to 1/2$, and $0 \not\to 1$ are forbidden for J and L. We see, therefore, that 6P $^2P_{3/2}$ can decay into 6P $^2P_{1/2}$ by emitting either magnetic dipole or electric quadrupole radiation. The lifetime of the 6P $^2P_{3/2}$ state is of the order of several milliseconds and is long enough so that an atomic beam in the $^2P_{3/2}$ state can traverse the length of the atomic beam machine without many decays.

B. Hyperfine Structure

If the nucleus has a spin, $\vec{I}$, there will be, in addition to the spherically symmetric Coulomb potential $Z\ e/r$, more complex potentials of non-spherical symmetry. It is the interaction of the electrons with these additional fields which gives rise to the hyperfine structure (hfs). The total angular momentum of the atom is given by $\vec{F} = \vec{J} + \vec{I}$ where $|I+J| \geq F \geq |I-J|$. Since $\vec{F}$ commutes with the Hamiltonian $\mathcal{H}_{fs} + \mathcal{H}_{hfs}$ for a free atom, each hyperfine level will be degenerate with a degeneracy of 2F+1. The hyperfine energy separations are much smaller than those of the fine structure. The former are of the order of 1 cm^{-1} or less while the latter are 10^3 cm^{-1} or more.

If we assume that the nucleus is made up of protons and neutrons, the electromagnetic potential of the nucleus will be given by

$$V(\vec{r}) = \int \frac{\rho(\vec{r}')}{|\vec{r}-\vec{r}'|}\, d\vec{r}'$$

and

$$\vec{A}(\vec{r}) = \frac{4\pi}{c} \int \frac{\vec{j}(\vec{r}')}{|\vec{r}-\vec{r}'|}\, d\vec{r}'$$

where

$$\rho(\vec{r}') = e \left\langle \psi_N \middle| \sum_{i=1}^{A} g_{\ell i}\, \delta(\vec{r}_i - \vec{r}') \middle| \psi_N \right\rangle$$

and

$$\vec{j}(\vec{r}') = \vec{j}_c(\vec{r}') + \vec{j}_s(\vec{r}')$$

with

$$\vec{j}_c(\vec{r}') = e \left\langle \psi_N \middle| \sum_{i=1}^{A} g_{\ell i}\, \vec{v}_i\, \delta(\vec{r}_i - \vec{r}') \middle| \psi_N \right\rangle$$

and

$$\vec{j}_s(\vec{r}') = \text{Curl}\ \left(\left\langle \psi_N \right| \sum_{i=1}^{A} g_{si} \frac{e\hbar}{2m_i}\ \vec{s}_i\ \delta(\vec{r}_i - \vec{r}') \left| \psi_N \right\rangle\right)$$

ρ, $\vec{j}$, $\vec{j}_c$, and $\vec{j}_s$ are the charge, total current, convection current, and spin current densities of all the A nucleons in the nucleus. For protons $g_\ell = 1$ and $g_s \cong +.00304$ and for neutrons $g_\ell = 0$ and $g_s \cong -0.00208$ where the sign of these g factors(in Bohr Magnetons) are the same as the sign of the corresponding magnetic moment.

In order to use the theory of angular momentum it is convenient to transform the above expression into a multipole expansion in spherical tensor form. Now,

$$\frac{1}{|\vec{r}-\vec{r}'|} = \sum_k r_<^k\ r_>^{-k-1}\ C^{(k)}(\theta,\phi)\cdot C^{(k)}(\theta',\phi')$$

where

$$C_\mu^{(k)}(\theta,\phi) = \sqrt{\frac{4\pi}{2k+1}}\ Y_\mu^k(\theta,\phi)$$

and are spherical tensors of rank k and parity $(-1)^k$. We have used the tensor product defined by

$$C^{(k)} \cdot C^{(k)} = \sum_\mu C_\mu^{(k)}\ C_{-\mu}^{(k)}\ (-1)^\mu \quad .$$

With this expansion we have

$$V(\vec{r}) = \sum_k r^{-k-1}\ C^{(k)}(\theta,\phi)\cdot Q^{(k)}$$

with

$$Q^{(k)} = e \left\langle \psi_N \right| \sum_{i=1}^{A} g_{\ell i}\ r^k\ C^{(k)}(\theta,\phi) \left| \psi_N \right\rangle$$

Since $Q^{(k)}$ has parity $(-1)^k$ and the nucleus has definite parity we see that only terms with k even will be non-zero.

Using the operator $\vec{L} = -i\vec{r} \times$ grad., C. Schwartz[3] has shown it is also possible to write $\vec{A}$ in the form

$$\vec{A}(\vec{r}') = \sum_k \frac{1}{ik} r^{-k-1} [\vec{L}\, C^{(k)}(\theta,\phi)] \cdot M^{(k)}$$

where

$$M_\mu^{(k)} = \mu_N \langle \psi_N | \sum_{i=1}^{A} [\vec{\nabla} r^k C^{(k)}(\theta,\phi)] \cdot [g_{i\ell} \frac{1}{k+1} \vec{L}_i + g_{is} \vec{S}_i] | \psi_N \rangle .$$

Now $M^{(k)}$ has parity $(-1)^{k+1}$ so only terms with k odd are non-zero.

We have assumed here that the nuclear and electronic wave functions do not overlap, i.e. that the nuclear volume can be ignored. The finite nuclear volume will slightly change the magnitude of the hyperfine interaction. The effect will be different for various isotopes and is called the hyperfine structure anomaly[4] and is $\lesssim$10% in the heaviest atoms.

We now wish to consider the effect of these multipole fields upon the sole valence electron of thallium and gallium. For this purpose we will assume that the core is spherically symmetric (i.e. no configuration interaction) and with the nuclear Coulomb potential Ze/r produces a potential V_c which we assume is already known. The motion of one valence electron in a spherically symmetric potential V_c (generated by the nucleus and the core electrons) is governed by the Dirac equation (which we assume has already been solved)

$$(c\vec{\alpha} \cdot \vec{P} + \beta mc^2 - eV_c)\psi = E\psi$$

where

$$\psi = \begin{pmatrix} \Psi \\ \phi \end{pmatrix} \equiv |J\ m_J\rangle$$

and

$$\Psi = \frac{f(r)}{r} y_{\ell jm} \quad \text{and} \quad \phi = \frac{g(r)}{ir} y_{\bar{\ell} jm}$$

and $\bar{\ell} = \ell \pm 1$, $j = \ell \pm 1/2 = \bar{\ell} \mp 1/2$, and

$$y_{\ell jm} = \sum_{m_\ell m_s} (2j+1)^{1/2} \begin{pmatrix} \frac{1}{2} & \ell & j \\ m_s & m_\ell & -m \end{pmatrix} Y_\ell^{m_\ell} \chi_{\frac{1}{2}}^{m_s} (-1)^{1/2-\ell+m}$$

where χ is a two-component spinor and $\begin{pmatrix} \frac{1}{2} & \ell & j \\ m_s & m_\ell & -m \end{pmatrix}$ is a 3-j symbol[45] and is a known real valued function of its six arguments. With this factorization of ψ the equations for f and g are

$$\left(\frac{d}{dr} - \frac{\kappa}{r}\right) f = \frac{1}{\hbar c} (mc^2 + E + eV_c) g$$

and

$$\left(\frac{d}{dr} + \frac{\kappa}{r}\right) g = \frac{1}{\hbar c} (mc^2 - E - eV_c) f$$

where $\kappa = j + 1/2$ if $j = \ell + 1/2$ and $\kappa = -(j + 1/2)$ if $j = \ell - 1/2$.

The hyperfine interaction Hamiltonian is then

$$\mathcal{H}_{hfs} = -e(V-V_c) + e\vec{\alpha}\cdot\vec{A} \quad .$$

With the spherical tensor form of V and $\vec{A}$ we see that $\mathcal{H}_{hfs}$ is of the form

$$\mathcal{H}_{hfs} = \sum_k \mathcal{H}_e^{(k)} \cdot \mathcal{H}_n^{(k)}$$

where $\mathcal{H}_e^{(k)}$ operates only on the electron space and $\mathcal{H}_n^{(k)}$ operates only the nuclear space. Because of the parity selection rules, terms for k even (odd) are understood to be electric (magnetic). An interaction

arising from the k^{th} term is said to be due to a multipole moment of order 2^k. Therefore, the possible terms are electric monopole, magnetic dipole, electric quadrupole, magnetic octupole, etc. The electric monopole term is just the Coulomb interaction which has already been included in V_c and, therefore, need not be considered. Introducing wave functions of the total system $|IJFm_F\rangle$ by the well known prescription

$$|IJFm_F\rangle = \sum_{m_I m_J} (-1)^{I-J+m_F} (2F+1)^{-1/2} \delta_{m_F, m_I+m_J} \begin{pmatrix} I & J & F \\ m_I & m_J & -m_F \end{pmatrix} |Im_I\rangle |Jm_J\rangle \qquad (4)$$

we can use a very powerful theorem due to Racah[4] to obtain the general matrix element

$$\langle IJFm_F | \mathcal{H}_{hfs} | IJ'Fm_F \rangle = \sum_k (-1)^{I+J+F} \begin{Bmatrix} F & J & I \\ k & I & J' \end{Bmatrix} \langle J \| \mathcal{H}_e^{(k)} \| J' \rangle \langle I \| \mathcal{H}_n^{(k)} \| I \rangle$$

where the reduced matrix elements are defined by the Wigner-Eckhart theorem

$$\langle Jm_J | \mathcal{H}_\mu^{(k)} | J'm_{J'} \rangle = (-1)^{J-m_J} \begin{pmatrix} J & k & J' \\ -m_J & \mu & m_J \end{pmatrix} \langle J \| \mathcal{H}^{(k)} \| J' \rangle$$

The quantity $\begin{Bmatrix} F & J & I \\ k & I & J' \end{Bmatrix}$ is a 6-j symbol[45] and, like the 3-j symbol, is a known real valued function of its six arguments. Now, the 6-j symbol vanishes unless k is less than or equal to the lesser of 2I and 2J. For example, if I = 1/2 (as for thallium) then k = 1 is the only non-zero term. For I = 3/2, as for gallium, k = 3 and only terms up to magnetic octupole need be considered. If J<I than similar restrictions will apply. J = 1/2 in the $^2P_{1/2}$ state in gallium, so for this state only the magnetic dipole term is present. However, if one includes effects of the $^2P_{3/2}$ state on the $^2P_{1/2}$ state the quadrupole interaction in the

former state will affect the $^2P_{1/2}$ state via off-diagonal quadrupole matrix elements. Also, the 6-j symbol puts restrictions on $|J-J'|$. For k = 1 we have $|J-J'| = 0, \pm 1$. For k = 2, $|J-J'| = 0, \pm 1, \pm 2$; and for k = 3, $|J-J'| = 0, \pm 1, \pm 2, \pm 3$ and so on. If we consider only the $^2P_{1/2}$ and $^2P_{3/2}$ states of the ground configuration in gallium and thallium we see that these conditions on $|J-J'|$ have no effect.

Although, in principle, the hyperfine interaction mixes nuclear states of different I, as it does for electronic states of different J, one can completely ignore such effects because of the very large nuclear energy level separations. These are typically of the order of 1 Mev which is about 10^6 times larger than any electronic level separations. Consequently, effects on the hyperfine structure due to excited nuclear levels will be 10^6 times smaller than effects due to excited electronic levels which are around 1 $cm^{-1}/10^3$ cm^{-1} or one part in 10^3. Therefore, excited nuclear levels will result in energy level shifts of around one part in 10^9. The atomic beam machine used in the present work is not sensitive to level shifts of one part in 10^9 and, therefore, we will ignore matrix elements off diagonal in I.

Now, using the relation

$$\begin{pmatrix} I & k & I \\ -I & 0 & I \end{pmatrix} = (2I)!/\sqrt{(2I-k)!\,(2I+k+1)!}$$

and the Wigner-Eckhart theoreum with $\mu = 0$ we can immediately write down the reduced nuclear matrix elements which are (up to k = 3)

$$\left\langle I \| \mu_n^{(1)} \| I \right\rangle = \sqrt{\frac{(I+1)(2I+1)}{I}}\ \mu_I$$

$$\langle I \| \mathcal{M}_n^{(2)} \| I \rangle = 1/2 \sqrt{\frac{(2I+3)(2I+1)(I+1)}{I(2I+1)}}\, Q$$

$$\langle I \| \mathcal{M}_n^{(3)} \| I \rangle = -\sqrt{\frac{(2I-3)!(2I+4)!}{(2I)!(2I)!}}\, \Omega$$

where

$$\mu_I \equiv \langle II | \sum_{i=1}^{A} \mu_N [\vec{\nabla} r C^{(1)}(n)] \cdot [-g_{i\ell} \vec{L}_i + g_{is} \vec{S}_i] | II \rangle$$

$$Q \equiv 2 \langle II | \sum_{i=1}^{A} e\, g_{\ell i}\, r^2\, C^{(2)}(n) | II \rangle$$

and

$$\Omega \equiv -\langle II | \sum_{i=1}^{A} \mu_N [\vec{\nabla} r^3 C^{(3)}(n)] \cdot [-g_{i\ell} 1/2\, \vec{L}_i + g_{is} \vec{S}_i] | II \rangle$$

are the nuclear magnetic dipole, electric quadrupole, and magnetic octupole moments respectively. These moments can be calculated only if the nuclear wave function, $|Im_I\rangle$, is known which is not the case at the present time. We can now calculate the reduced electronic matrix elements in the same way. However, as the angular dependence of the electronic wave function is known, only radial matrix elements will be left undetermined. If ℓ is the orbital angular momentum ($\ell = 1$ for Ga and Tl) we can specify a state $|Jm_J\rangle$ as $|1/2\ell\ J\ m_F\rangle$ where $J = \ell \pm 1/2$. From Schwartz[3] we have the dipole elements

$$\langle J \| \mathcal{M}_e^{(1)} \| J \rangle = -\sqrt{\frac{(2J+1)(2J+1)}{J}} \left(\frac{4e\kappa}{2J+2} \int_0^\infty r^{-2} f g dr \right)$$

$$\langle J \| \mathcal{M}_e^{(1)} \| J-1 \rangle = -\sqrt{\frac{(2J+1)(2J-1)}{4J}} \left(e \int_0^\infty r^{-2} (f''g' + g''f') dr \right)$$

where fg = f'g' if J = ℓ + 1/2 and fg = f"g" if J = ℓ - 1/2. In general, primes will refer to the J = ℓ + 1/2 state and double primes refer to the J = ℓ - 1/2 state.

For the quadrupole elements we have

$$\left\langle J \| \mathcal{H}_e^{(2)} \| J \right\rangle = \sqrt{\frac{(J+1)(2J+1)(2J+3)}{J(2J-1)}} \frac{e(2J-1)}{2(2J+2)} \int r^{-3}(f^2+g^2)dr$$

$$\left\langle J \| \mathcal{H}_e^{(2)} \| J-1 \right\rangle = -\sqrt{\frac{3(2J+1)(2J-1)}{16J(J+1)(J-1)}} \; e \int r^{-3}(f'f''+g'g'')dr$$

For the octupole elements we have

$$\left\langle J \| \mathcal{H}_e^{(3)} \| J-1 \right\rangle = \sqrt{\frac{(2J+4)(2J+3)(2J+2)(2J+1)}{2J(2J-2)(2J-1)}} \frac{2e\kappa(2J-1)}{(2J+4)(2J+2)} \int r^{-4} fgdr$$

For ℓ = 1, $\left\langle J \| \mathcal{H}_e^{(3)} \| J-1 \right\rangle$ vanishes. It is customary to define the following

$$a_J = -2e\mu\mu_0 \frac{\kappa}{IJ(J+1)} \int_0^\infty r^{-2} fgdr$$

$$a''' = -\frac{e\mu\mu_0}{2IJ} \int_0^\infty r^{-2}(f''g'+g''f')dr$$

$$b_J = \frac{eQ(2J-1)}{2J+2} \int_0^\infty r^{-3}(f^2+g^2)dr$$

$$c_J = -\Omega \frac{2e\kappa(2J-1)}{(2J+4)(2J+2)} \int_0^\infty r^{-4} fgdr$$

a_J and a''' are the diagonal and off-diagonal magnetic dipole interaction constants. b_J and c_J are the electric quadrupole and magnetic octupole interaction constants. Since b_J and c_J exist for only the $^2P_{3/2}$ state, we will drop the subscript J and use b and c. Rather than define an off-diagonal quadrupole interaction constant b''', we will introduce η defined by

$$\eta \equiv \frac{\int_o^\infty r^{-3}(f'f''+g'g'')dr}{\int_o^\infty r^{-3}(f^2+g^2)dr} \quad .$$

Later on we will need the ratios $a_{1/2}/a_{3/2}$ and $a'''/a_{3/2}$. We can get reasonable values for these if we assume that most of the contribution to the radial integrals comes from the region near the nucleus where $V_c \cong Ze/r$. With this and assuming $V_c << m_e c^2$ we have the solution

$$f = C\ [\tfrac{1}{2}\ X\ J_{2\rho+1}(X) - (\rho+\kappa)\ J_{2\rho}(X)]$$

$$g = \alpha Z\ C\ J_{2\rho}(X)$$

where J_p is a Bessel function and $X = \sqrt{8Zr/a_o}$, $\rho = \sqrt{\kappa^2-\alpha^2Z^2}$, and $a_o = e^2/\hbar c$. If $J = \ell + 1/2$ then $C = C'$ and if $J = \ell - 1/2$ then $C = C''$. The normalization constants C' and C'' are best obtained from the $^2P_{1/2}$ - $^2P_{3/2}$ spin-orbit splitting (δ). With these assumptions Schwartz[3] has shown

$$\int_o^\infty r^{-2} fg\,dr = C^2 \frac{\hbar}{2mc} \left(\frac{2Z}{a_o}\right)^2 \frac{F}{(2\ell+1)[\mp(2\ell+1)-1]}$$

where $\mp$ for $j = \ell \pm 1/2$, and

$$\int_o^\infty r^{-2}(f'g''+g'f'')\ dr = -C'C'' \frac{\hbar}{2mc} \left(\frac{2Z}{a_o}\right)^2 \frac{G}{\ell(2\ell+1)(2\ell+2)}$$

where F and G are correction factors of order unity and $C' \cong -C''$. For a ^2P doublet we then have

$$a_{1/2}/a_{3/2} \cong 5\theta$$

and

$$a'''/a_{3/2} \cong -5/16\ \xi$$

where $\theta = (F_{1/2}/F_{3/2})(C''/C')^2$ and $\xi = (G/F_{3/2})|C''/C'|$. Casimir[5] has calculated θ, ξ, and η . He finds for gallium $\theta \cong 1.103$, $\xi \cong 1.02$, and $\eta \cong 1.04$. For thallium he finds $\theta \cong 2.416$ and $\xi \cong 1.11$.

We are now in a position to write down all the hyperfine matrix elements which will be needed for the description of the hyperfine energy levels. They are (using $\ell = 1$ and for the off-diagonal elements $J \equiv 3/2$, $J-1 \equiv 1/2$):

$$\langle IJFm_F|\mathcal{H}^{(1)}_{hfs}|IJFm_F\rangle = \frac{a_J}{2}[F(F+1)-J(J+1)-I(I+1)]$$

$$\langle IJFm_F|\mathcal{H}^{(1)}_{hfs}|IJ-1Fm_F\rangle = \frac{a'''}{2}[(F+J-I)(F+I-J+1)(F+J+I+1)(J+I-F)]^{\frac{1}{2}}$$

$$\langle IJFm_F|\mathcal{H}^{(2)}_{hfs}|IJFm_F\rangle = \frac{b}{2}\left[\frac{3a^2+(3/2)a-I(I+1)J(J+1)}{I(2I-1)J(2J-1)}\right]$$

(with $b = 0$ for $J = 1/2$)

$$\langle IJFm_F|\mathcal{H}^{(2)}_{hfs}|IJ-1Fm_F\rangle = -\frac{15}{32}\eta b\frac{[F(F+1)-I(I+1)-J^2+1]}{J(J+1)(J-1)I(2I-1)}[(I+J-F)(J-I+F)(I-J+F+1)(I+J+F+1)]^{\frac{1}{2}}$$

$$\langle IJFm_F|\mathcal{H}^{(3)}_{hfs}|IJFm_F\rangle = c\left\{\frac{10a^3+20a^2+2a[-3I(I+1)J(J+1)+I(I+1)+J(J+1)+3]}{I(I-1)(2I-1)J(J-1)(2J-1)} - \frac{4I(I+1)J(J+1)}{I(I-1)(2I-1)J(J-1)(2J-1)}\right\}$$

where $a = 1/2[F(F+1)-I(I+1)-J(J+1)]$.

A list of these interaction constants that have been previously measured in gallium and thallium are shown in Appendices A, B, and C.

C. Zeeman Effect

The addition of a uniform magnetic field to the above system results in the complete removal of the F degeneracy. Every hyperfine level splits into 2F + 1 levels. Of course, m_F is still a good quantum number. The Zeeman Hamiltonian can be written

$$\mathcal{H}_{Zeeman} = -\mu_o g_I \vec{I}\cdot\vec{H} - e\,\vec{\alpha}\cdot\vec{A}$$

where $\vec{A} = 1/2\ (\vec{H}\times\vec{r})$ and $\vec{H} = H\hat{z}$. Matrix elements of the first term depend only on the nuclear wave functions and are easily seen to be

$$\langle Im_I | -\mu_o g_I \vec{I}\cdot\vec{H} | Im_I' \rangle = -\mu_o g_I H m_I \delta_{m_I, m_I'}$$

Similarly, matrix elements of the second term depend only upon the electronic wave functions and, according to Clendenin[6], are

$$\langle Jm_J | -e\vec{\alpha}\cdot\vec{A} | Jm_J \rangle = -\mu_o g_J H m_J$$

$$\langle Jm_J | -e\vec{\alpha}\cdot\vec{A} | J\text{-}1m_J \rangle = \frac{\mu_o H N}{2\ell+1} \left[(\ell+\tfrac{1}{2})^2 - m_J\right]^{\frac{1}{2}}$$

where

$$N = \int_o^\infty g' g'' dr$$

$$g_J = g_J' \left(1 - \frac{4k}{2k-1} \int_o^\infty f^2 dr\right)$$

where $k = -\ell - 1$ for $J = \ell + 1/2$ and $k = \ell$ for $J = \ell - 1/2$. In the non-relativistic limit N becomes the normalization which is unity. We will assume N = 1 for gallium. For thallium we will leave it to be determined. g_J' is called the Lande g-factor and is given by

$$g_J' = g_\ell \frac{J(J+1)+L(L+1)-S(S+1)}{2J(J+1)} + g_s \frac{J(J+1)+S(S+1)-L(L+1)}{2J(J+1)}$$

where, for the free electron, $g_\ell = -1$ and $g_s = -2.002319114$.[42] For the $^2P_{3/2}$ state we have $g_{3/2} = 2/3g_\ell + 1/3g_s = -1.3341064$ and for the $^2P_{1/2}$ state, $g_{1/2} = 4/3g_\ell - 1/3g_s = -0.6658936$. In the case of $v/c \ll 1$ where v is the speed of the electron it can be shown that[7]

$$\int_0^\infty f^2 dr = \langle T \rangle$$

where $\langle T \rangle$ is the average kinetic energy of the electron. This approximation should be excellent for both gallium and thallium and will be used later to calculate this correction. The correction to g_J, Δg_R, for a 2p electron can be shown for the above to be

$$\Delta g_R = + \frac{16}{15} \alpha^2 \langle T \rangle .$$

$\langle T \rangle$ is in atomic units and α is the fine structure constant ($\sim 1/137$). This correction is called the relativistic correction and is caused by the variation of the mass of the electron with its speed. A list of g-factors that have been previously measured for gallium and thallium are shown in Appendices A, B, and C.

Now, using the above matrix elements (in a $|IJm_I m_J\rangle$ representation) one can easily calculate the matrix elements of $\mathcal{H}_{Zeeman}$ in the representation $|IJFm_F\rangle$ given by Eq. (4). The selection rules on $\langle IJFm_F|\mathcal{H}_{Zeeman}|IJ'Fm_F'\rangle$ are $\Delta F = 0, \pm 1$, $\Delta J = 0, \pm 1$, and $\Delta m_F = 0$. That is, the Zeeman operator mixes states in a collection of hyperfine levels that have the same m_F value and F and J differing by 0 or ±1. In

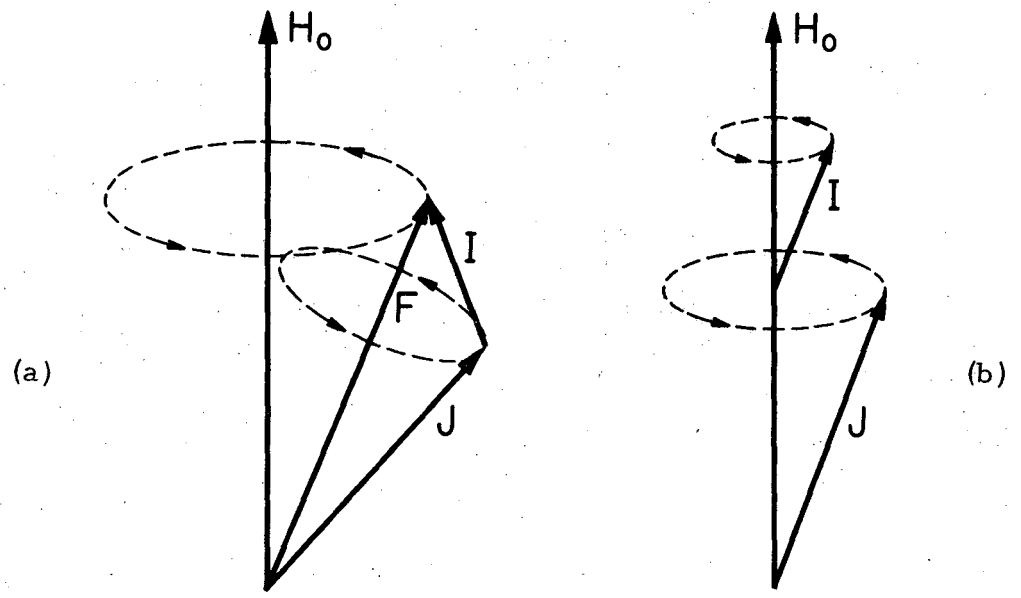

Fig. I-3. The precession of $\vec{I}$ and $\vec{J}$ in the presence of (a) a weak, and (b) a strong field.

Figs. I-4 through I-7, for example, we have labelled the states by $|IJFm_F\rangle$. In reality, of course, this is correct only for H = 0. At non-zero fields the states are linear combinations of states satisfying the selection rules. Only the states $|IJ_{max}F_{max}\pm F_{max}\rangle$ are "pure". A general state will be given by

$$\psi_{hfs}(m_F) = \sum_{F,J} a(F,J,H)\,|IJFm_F\rangle \quad .$$

At large fields $\vec{I}$ and $\vec{J}$ will precess abouth $\vec{H}$ separately rather than couple together to form $\vec{F}$ which precesses about $\vec{H}$ (see Fig. I-3). At such fields the hyperfine levels are very nearly eigen-states of the representation $|IJm_Im_J\rangle$. The selection rules for the high field case then are $\Delta m_J = 0, \pm 1$ and $\Delta m_I = 0, \pm 1$. At high fields the valence electron and the nucleus are acting like separate systems and a transition satisfying $\Delta m_J = \pm 1$, $\Delta m_I = 0$ flips just the electron and the transition satisfying $\Delta m_J = 0$, $\Delta m_I = \pm 1$ flips only the nucleus. Since the $|IJFm_F\rangle$ and $|IJm_Im_J\rangle$ representations both form a complete set of states, it does not make any difference which one one chooses to calculate the matrix elements. Both representations are only eigen-functions for the H = 0 and large H cases respectively. The eigen-functions for the general case of arbitrary H can be obtained only by diagonalizing the complete energy matrix, the elements of which have been calculated using a convenient complete set of states such as $|IJFm_F\rangle$ or $|IJm_Im_J\rangle$. From the above it is clear that the hyperfine matrix elements are most easily calculated in the $|IJFm_F\rangle$ representation and that the Zeeman matrix elements are most easily calculated in the $|IJm_Im_J\rangle$ representation. We have chosen to use the $|IJFm_F\rangle$ set of states purely as a matter of overall computational convenience.

D. The Energy Matrix

The complete Hamiltonian for our problem can be written $\mathcal{H} = \mathcal{H}_{so} + \mathcal{H}_{hfs} + \mathcal{H}_{Zeeman}$. From this we want the energy of each hyperfine level in the ^2P doublet of the ground configuration as a function of g_J, H, g_I, $a_{1/2}$, $a_{3/2}$, a''', etc. From previous measurements we know we must include perturbation effects between the $^2P_{3/2}$ and $^2P_{1/2}$ states. From perturbation theory we know the effect of one level, i, on another level, j, is given by

$$\Delta E \sim \frac{\langle \psi_i | \mathcal{H} | \psi_j \rangle}{E_i - E_j} \quad .$$

Consequently, the effects of other states upon levels in the ^2P term should be very small because of the large energy separations. Therefore, we will consider only the hyperfine levels in the ^2P doublet. We will consider thallium first since it is simpler.

1. Thallium. In the $^2P_{1/2}$ state with I = 1/2, we have F = 0 and 1. For $^2P_{3/2}$ with I = 1/2 we have F = 2 and 1. The total number of hyperfine levels is $1 + 2\cdot1+1 + 2\cdot2+1 + 2\cdot1+1 = 12$. Therefore, our energy matrix will be a 12 × 12 matrix. Since m_F is a good quantum number this matrix breaks up into smaller submatrices along the diagonal as shown in Fig. I-4. To calculate the eigenvalues of the $^2P_{1/2}$ state we measure the energy from the center of gravity of the $^2P_{1/2}$ multiplet. $\mathcal{H}_{so}$ adds an energy δ to all the diagonal $^2P_{3/2}$ matrix elements. Since δ is much larger than any other elements in the matrix we can approximate the diagonal $^2P_{3/2}$ elements by δ. By adding and subtracting rows and columns we can eliminate

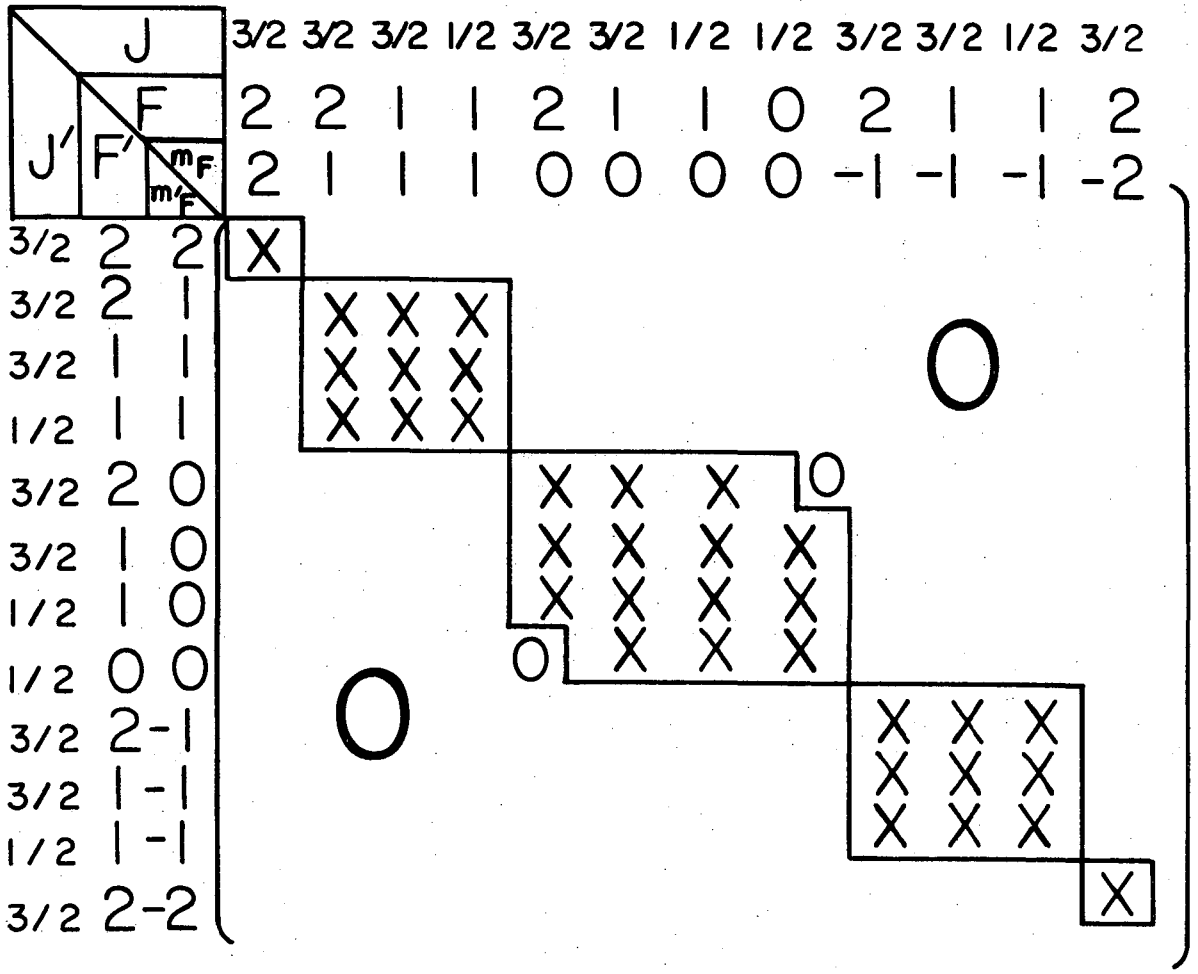

XBL 687-1325

Fig. I-4. Structure of the Thallium Energy Matrix.

the $^2P_{3/2}$ eigenvalues to order $1/\delta$ by the method of pivotal condensation.[8] The result for the $^2P_{1/2}$ state[6]

$$\nu-\nu_o = -\frac{\Delta\nu_{1/2}}{2(2I+1)} - g'_I\frac{\mu_o H m_F}{h} \pm \frac{\Delta\nu_{1/2}}{2}\sqrt{1+\frac{4m_F x}{2I+1}+x^2} - \frac{2(a''')^2 I(2I+1)}{\delta} - \frac{2\mu_o{}^2H^2N^2}{9h^2\delta} \tag{5}$$

where

$$\Delta\nu_{1/2} = (I+1/2)\,[a_{1/2} - 2(a''')^2/\delta]$$

and

$$g'_I = g_I\left(1+\frac{4Na'''}{3g_I\delta}\right)$$

and

$$x = (g'_I - g_J)\frac{\mu_o H}{h\Delta\nu_{1/2}} \quad .$$

The first and last two terms on the right in Eq. (5) are independent of F and m_F and therefore are unobservable for the transitions observed in our experiments and can be ignored.

For the $^2P_{3/2}$ state we measure the energy from the center of gravity of the $^2P_{3/2}$ multiplet. $\mathcal{H}_{s\text{-}o}$ adds $-\delta$ to all the diagonal $^2P_{1/2}$ state matrix elements. As above, we can eliminate the $^2P_{1/2}$ eigenvalues to order $1/\delta$. The result given by Clendenin[6] for the $^2P_{3/2}$ state is

$$\nu-\nu_o = -\frac{\Delta\nu_{3/2}}{2(2J+1)} - g_J\frac{\mu_o H m_F}{h} \pm \frac{\Delta\nu_{3/2}}{2}\sqrt{1-\frac{4m_F x}{2J+1}+x^2+\Gamma}+\Lambda \tag{6}$$

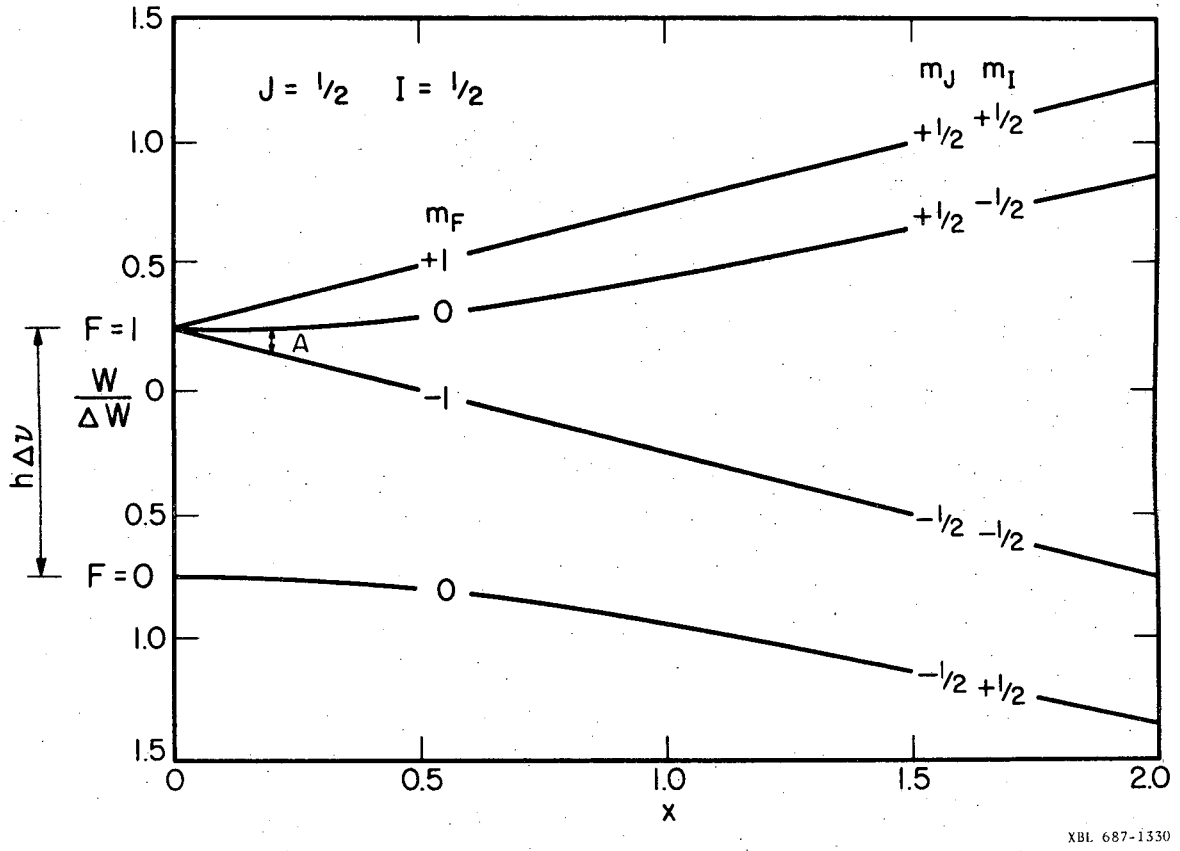

Fig. I-5. Hyperfine Zeeman Levels of Thallium in the $^2P_{1/2}$ State ($X \cong H(\text{Gauss})/22{,}400$).

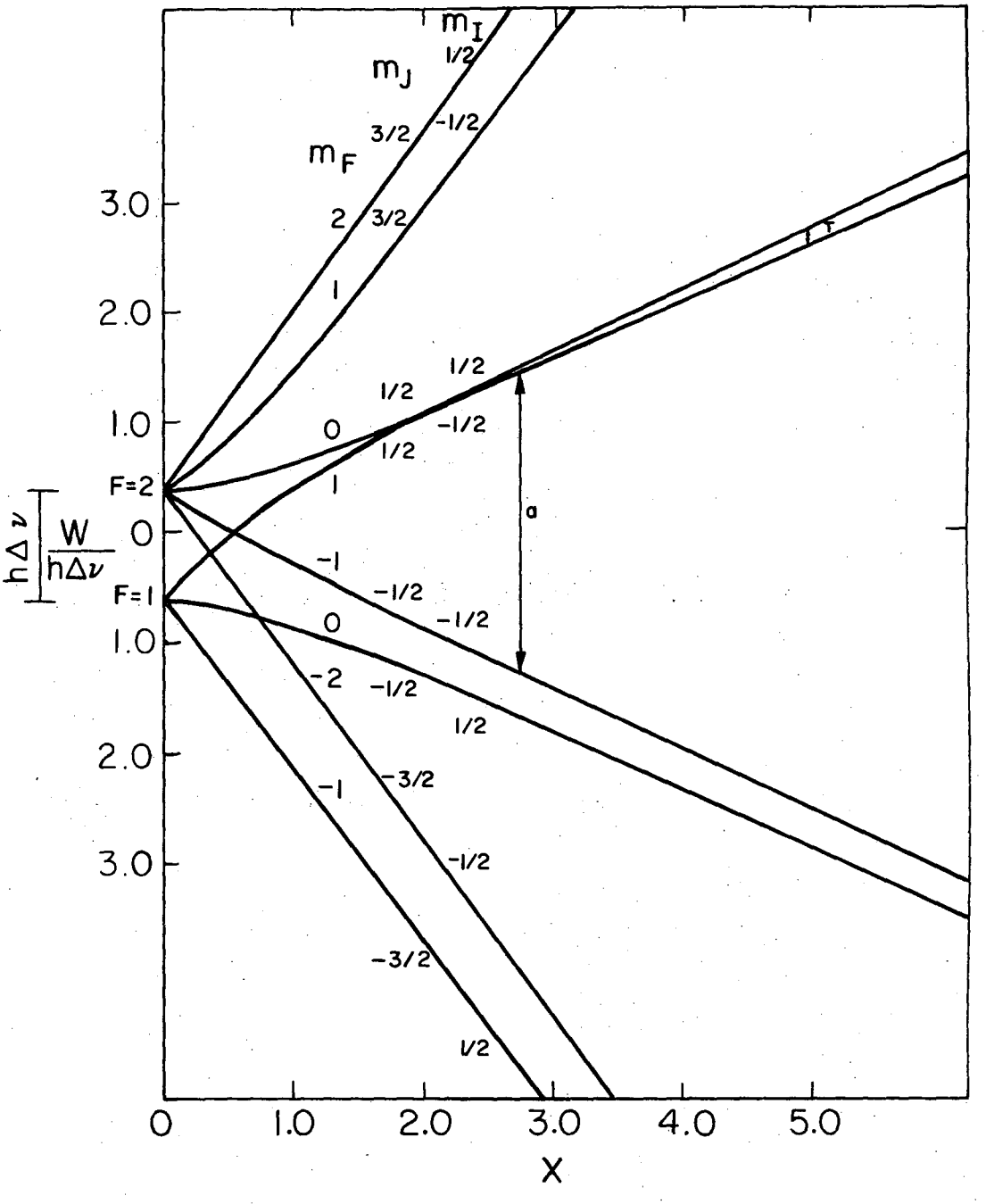

Fig. I-6. Hyperfine Zeeman Levels of Thallium in the $^2P_{3/2}$ State ($X \cong H(\text{Gauss})/286$).

where

$$\Gamma = \frac{4}{\delta}\left[-m_F a''' y + \left(\frac{m_F{}^2 \Delta\nu_{3/2}}{J+1/2} y^2 - a'''(2-m_F{}^2)\, xy - m_F \Delta\nu_{3/2} xy^2\right)\right],$$

$$\Lambda = \frac{1}{\delta}\left[-3/2(a''')^2 + \left(m_F a''' \Delta\nu_{3/2} y + \Delta\nu_{3/2}{}^2 (2-m_F{}^2) y^2\right)\right],$$

$$x = (g_I - g_J)\frac{\mu_o H}{h\Delta\nu_{3/2}},$$

$$y = \frac{N\mu_o H}{3h\Delta\nu_{3/2}}, \text{ and } \Delta\nu_{3/2} = [J + 1/2][a_{3/2} - (a''')^2/\delta].$$

Just as in Eq. (5), terms in Eq. (6) that are independent of F and m_F can be ignored. Graphs of these levels for the $^2P_{1/2}$ and $^2P_{3/2}$ states are shown in Figs. I-5 and I-6 respectively. Terms of order $1/\delta^2$ are extremely small and can be neglected. In both Eqs. (5) and (6) the plus sign is for the F = I + 1/2 or J + 1/2 levels. Of course we are expressing energies in frequency units (MHz).

2. Gallium. For gallium we have a total of 24 hyperfine levels so our energy matrix is 24 × 24. The dimensions of the non-zero submatrices are 6, 5, 3, and 1. An expression for the $^2P_{1/2}$ state levels accurate to the order of $1/\delta$ can be obtained as in the thallium case. The result, due to A. Lurio[9,10], is

$$\nu - \nu_o = -\frac{\Delta\nu_{1/2}}{2(2I+1)} - g_I' \frac{\mu_o H m_F}{h} \pm \frac{\Delta\nu_{1/2}}{2}\left[1 + \frac{4m_F x}{2I+1} + x^2 + \frac{\eta bN}{3I(2I-1)(g_I'-g_J)\delta}\left(\frac{16I(I+1)}{2I+1} m_F x + 12 m_F{}^2 x^2 - (4I^2+4I+3)x^2\right)\right]^{1/2} + \phi \qquad (7)$$

where

$$\Delta\nu_{1/2} = a_{1/2}(I+1/2) - \frac{(2I+1)}{\delta}\left[\left(\frac{5}{16}\xi\zeta\, a_{3/2}\right)^2 + \frac{5}{16}\xi\zeta\, a_{3/2}\eta b\frac{(2I+3)}{2I} - \frac{3}{16}\frac{\eta^2 b^2}{I^2}\frac{(2I+3)}{(2I-1)}\right] ,$$

$$x = (g_I' - g_J)\frac{\mu_o H}{h\Delta\nu} ,$$

$$g_I' = g_I\left[1 + \frac{4Na'''}{3g_I\delta} + \frac{\eta bN}{I(2I-1)g_I\delta}\right] , \text{ and}$$

$$\phi = -\left[\frac{5}{16}\xi\zeta\, a_{3/2}\right]^2\frac{2I(I+1)}{\delta} - \frac{\eta^2 b^2(I+1)(2I+3)}{8I(2I-1)\delta} - \frac{2}{9}\frac{\mu_o{}^2N^2H^2}{h^2\delta} .$$

ϕ and the first term on the right in Eq. (7) are not observable with our observations, since they are independent of F and m_F and will be ignored. The ± sign is handled just as for thallium. Figure I-7 shows the hyperfine structure for the $^2P_{1/2}$ state in gallium.

Eliminating the $^2P_{1/2}$ eigenvalues we are left with reduced submatrices or order 1, 2, 3, and 4. The $m_F = -2$ submatrix was solved with the quadratic formula. The $m_F = -1$ and 0 submatrices were left as is and the eigenvalues calculated using a standard matrix diagonalization program.[11] For our set of observations (see Appendix E) only the eigenvalues for the $m_F = 0$, -1, and -2 levels were needed in the $^2P_{3/2}$ state. For the $m_F = 0$ submatrix we needed (except for Holloway's Data) the second largest eigenvalue. For $m_F = -1$ and -2 cases we wanted the largest eigenvalues. The reduced -2, -1 and 0 submatrices are shown in Appendices G, H, and I. The hyperfine structure of the $^2P_{3/2}$ state is shown in Fig. I-8.

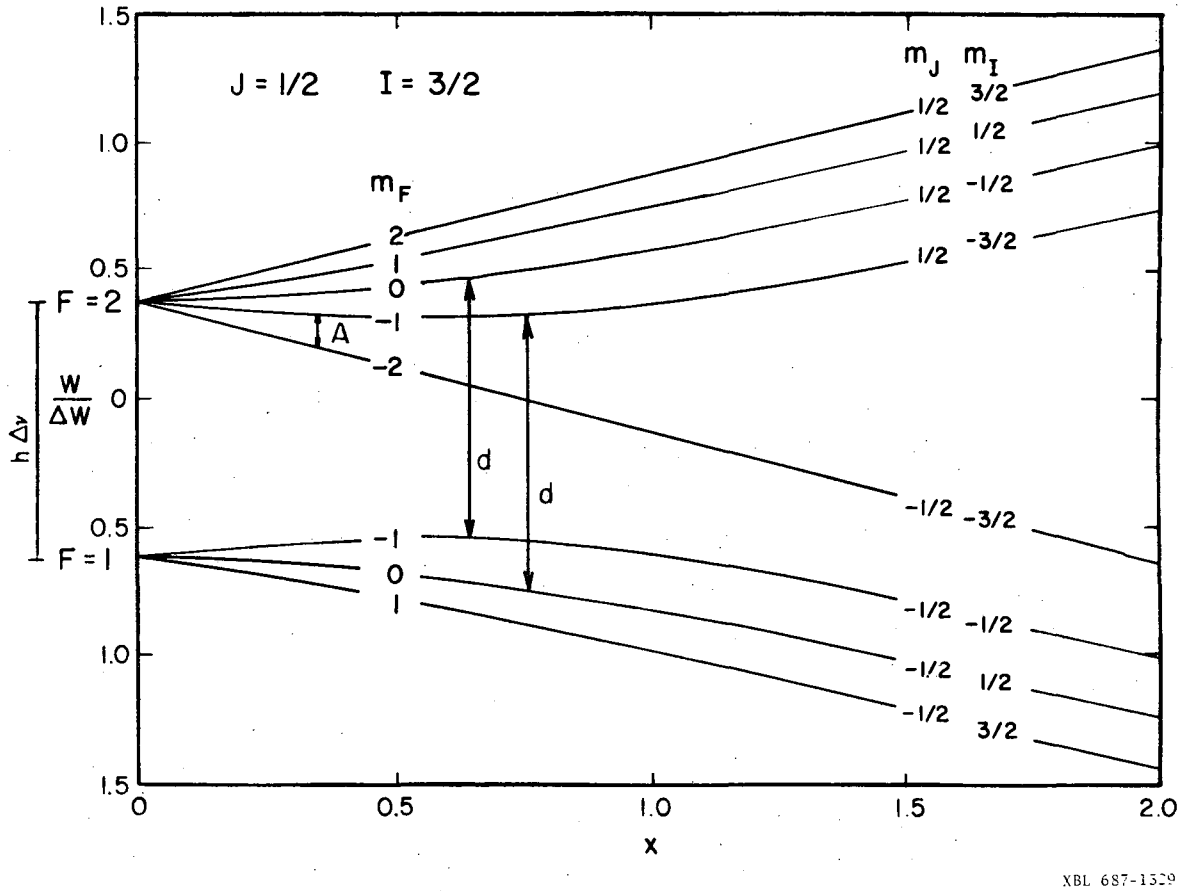

Fig. I-7. Hyperfine Zeeman Energy Levels of Gallium in the $^2P_{1/2}$ State ($X \cong H(\text{Gauss})/2865$).

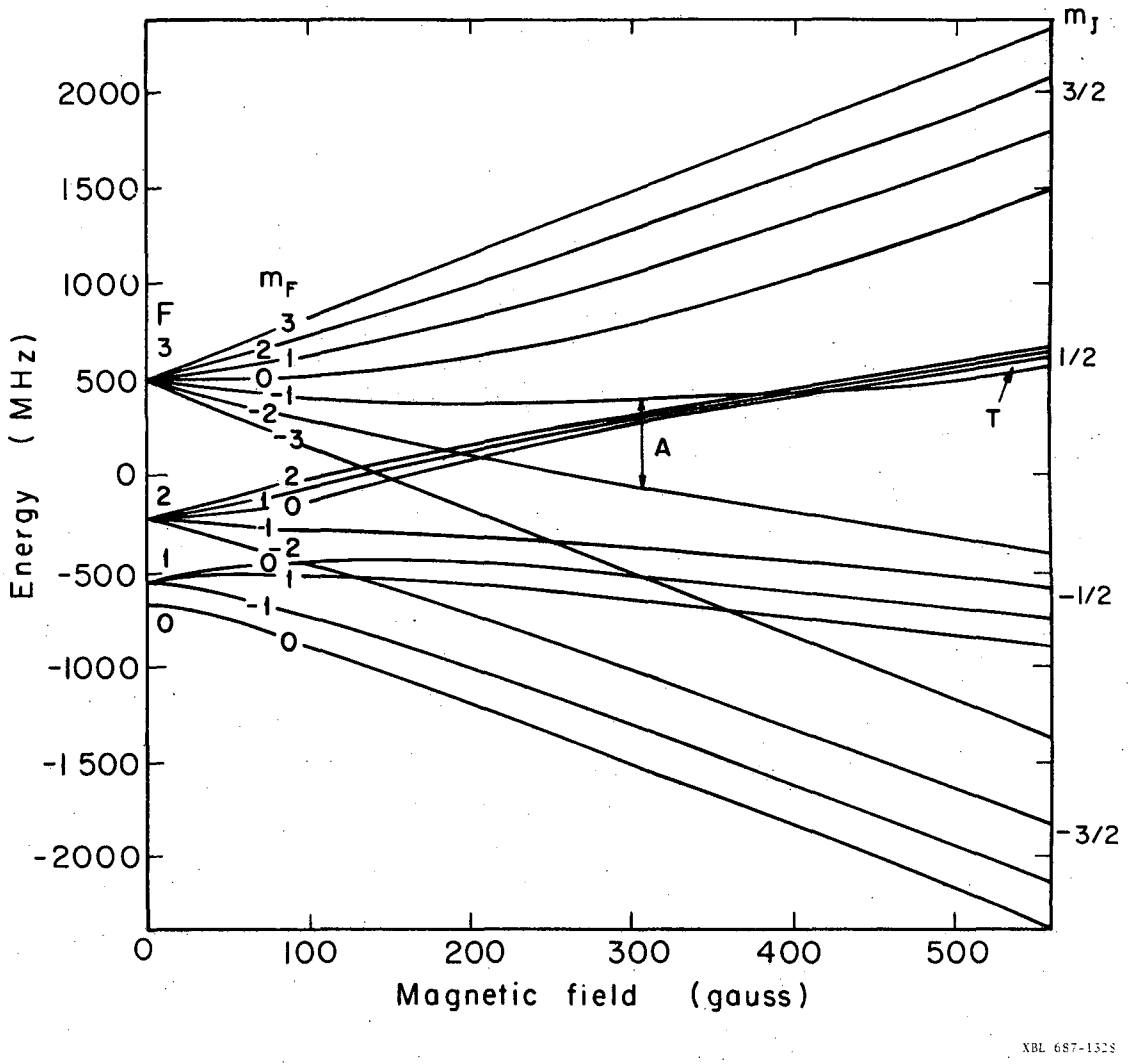

Fig. I-8. Hyperfine Zeeman Levels of Gallium in the $^2P_{3/2}$ State.

E. Higher Order Corrections

1. Finite Mass and Size of the Nucleus. The effect of a finite mass for the nucleus is to change the orbital g-factor of the electron from one to[12]

$$g_\ell = -(1-\frac{m}{M}) + \frac{m}{ML_z} \left\langle Jm_J \left| \frac{1}{\hbar} \sum_{i<j} (\vec{r}_i \times \vec{p}_j + \vec{r}_j \times \vec{p}_i) \right| Jm_J \right\rangle$$

$$\equiv -1 + \frac{m}{M}(1+\Phi)$$

where m and M are the electronic and nuclear masses, L_z is the component of the orbital angular momentum in the direction of H. For gallium $M \cong 69*1836\ m$, so we have $m/M \cong 8 \times 10^{-6}$ and for thallium $M \cong 205*1836\ m$ and $m/M \cong 2.5 \times 10^{-6}$. Φ involves matrix elements between the valence ^2P electron and one election in each closed shell of opposite parity from the odd parity of the shell of the valence electron. Two such electrons will contribute if they have the same spin, opposite parity, and m_ℓ differing by ±1. Only exchange terms are non-zero and they give negative contributions. Also, we expect Φ to be of order unity. If Φ is negative and of order unity than $\Delta g_\ell \lesssim m/M$. The resulting correction to g_J for thallium is probably not observable in this experiment. For gallium it is possible that there is a slight by observable shift. In any case, since the other corrections to be discussed can be calculated only to accuracies of the order of 1 part in 10^5, there is little point in determining Δg_ℓ more accurately since it is smaller than these other corrections as we shall see.

The finite size of the nucleus will spread out the charge and magnetic moment densities and thereby slightly reduce the interaction

constants. The effect can reach a few percent in the heaviest atoms. Since we are interested in predicting a''' in terms of the observed diagonal dipole constant, $a_{3/2}$, most, if not all, of this effect will already be included in our estimate. In any case, the effect will be too small to be observed in gallium and because of the uncertainty in N can be ignored in thallium where the effect is about one percent.

2. Other Relativistic and Diamagnetic Corrections to g_J. Abragam and Van Vleck[13] have considered in detail the corrections to the Zeeman effect arising from additional terms in the relativistic Hamiltonian. They find, in addition to the relativity correction discussed above, the following corrections for a $2\ ^2P_{3/2}$ valence electron

$$\Delta g_{\text{Lamb}} = +\frac{2}{9}\alpha^2(\langle W\rangle_{2p} - \frac{1}{5}\langle V\rangle_{2p})$$

$$\Delta g_{\text{orbit-orbit}} = +\frac{2}{9}\alpha^2(\langle W\rangle_{2p} + \langle V\rangle_{2p})$$

For a $2\ ^2P_{1/2}$ electron the corrections are

$$\Delta g_{\text{Lamb}} = +\frac{2}{9}\alpha^2(\langle W\rangle_{2p} - \frac{4}{5}\langle V\rangle_{2p})$$

$$\Delta g_{\text{orbit-orbit}} = +\frac{4}{9}\alpha^2(\langle W\rangle_{2p} + \langle V\rangle_{2p})$$

α is the fine structure constant ($\cong 1/137$) and

$$V(r) = 1/r^3 \int_o^r r'^4 \rho(r')dr'$$

and

$$W(r) = \int_r^\infty r'\rho(r')dr' \quad .$$

We have assumed here that the charge density, $\rho(r')$, of the core is spherically symmetric. $\langle V\rangle$ and $\langle W\rangle$ are in atomic units.

3. Configuration Interaction.

A. Dipole Interaction Constants. In general, the valence electron will distort the core from spherical symmetry by means of the electrostatic interaction e^2/r_{ij}. Of course, other interactions such as orbit-orbit, spin-other-orbit, etc. can contribute to this effect but are smaller than the electrostatic interaction and will be ignored. If the core is asymmetric it is no longer possible to characterize the atom as an inert core with a valence electron having the only degrees of freedom left to the atom. That is, the assignment of an atomic ground state to a particular configuration is no longer meaningful. For example, we have written the ground configuration of gallium as [core] $(4p)^1$. If configuration interaction is present we must allow other configurations to be present such as [core] $(4s)^1(4p)^2(5s)^1$.

In principle one must include all possible configurations since only then can one be assured of having included all possible perturbations upon the atomic state in question. Fortunately, however, only a few configurations are important and usually one configuration will dominate over all the rest. For example, in gallium, the ^2P ground state doublet is overwhelmingly due to the configuration [core] $(4p)^1$.

Since the electrostatic interaction is diagonal in S, L, J and the parity only those states in the two "interacting" configurations that have the same S, L, J, and parity can interact. This greatly simplifies the problem. As in all perturbation problems, the amount a state in an "interacting" configuration is mixed into another state is proportional to the matrix element connecting the two states and inversely proportional to the energy separation. With this in mind the most important configuration in addition to $(4p)^1$ [dropping the core] to consider for subgroup

III elements are $(4s)^1(4p)^1(5s)^1$, $(4s)^1(4p)(4d)$, $(3d)^9(4p)(4d)$, and $(3p)^5(4p)(5p)^1$. Of these (4s)(4p)(5s) [henceforth called s→s' mode] is most important in affecting the magnetic dipole interaction constants because of the presence of two unpaired s-electron spins. Also, because of the spherical symmetry of s electrons, the s→s' mode will not affect the quadrupole or octupole interaction constants. Since the diagonal multipole interaction constants have already been measured we are interested only in calculating the effect of configuration interaction upon the off-diagonal interaction constants. For the off-diagonal quadrupole interaction constants $b''' = \eta b$ we will assume the correction is negligible and for the off-diagonal dipole element that the correction is due only to the s→s' mode. Schwartz[14,15] has given an analysis of the s→s' mode based on angular momentum considerations. He showed that if β is the fractional contribution to $a_{3/2}$ due to s→s' configuration interaction then the observed a values are given by

$$a_{3/2} = (1+\beta)\, a^{th}_{3/2}$$

$$a_{1/2} = (1-\beta/5\theta)\, a^{th}_{1/2}$$

$$a''' = (1-16/5\xi\ \beta)\, a'''^{th}$$

where a^{th} are those values calculated in Sec. I-B. Using the relations $a^{th}_{1/2} / a^{th}_{3/2} = 5\theta$ and $a'''^{th}/a^{th}_{3/2} = -5/16\ \xi$ and the observed ratio $a_{1/2} / a_{3/2}$ one can calculate β and a'''. For ^{69}Ga we have $a_{1/2} / a_{3/2} = 7.02$, $\theta = 1.1$, and $\xi = 1.02$ from which we conclude $\beta = -0.190$ and $a''' = -120$ MHz. We see $a_{1/2}$, $a_{3/2}$, and a''' are changed by +3.5%, -19%, and +60% respectively by s→s' configuration interaction.

For ^{205}Tl we have $a_{1/2} / a_{3/2} = 80.5$, $\theta = 2.42$, and $\xi = 1.11$ so that we have $\beta = -0.839$ and $a''' = -1930$ MHz. $a_{1/2}$, $a_{3/2}$, and a''' are changed by +7%, -84%, and +242%. From these figures we can readily see that configuration interaction is not a small effect. The calculated a''' values will be compated with the data later.

B. Electron g Factors. Since g_J is a function of only S, L, and J one would not expect any configuration interaction corrections becuase the electrostatic interaction is diagonal in S, L, and J. However, M. Philips[16] has shown that in the 4^{th} order there is a non-zero effect. The spin-orbit coupling mixes states of different L and S in the excited configuration which in turn gets mixed into the ground state. The s→s' mode does not contribute at all to this effect because there are no ^2P doublets in (4s)(5s) to mix into the ^2P state of the 4p electron. The two most likely to contribute are $(3d)^9(4p)^1(4s)^1$ and $(3d)^9(4p)(4d)$ which will be called d→s and d→d respectively. Owing to the large energy separations, effects due to exciting a deeper lying s or p electron should be very small. Now, Philips claims that d→s gives very little effect so we will consider only d→d. If ζ is the spin-orbit parameter for the ^2D term of $(nd)^9$ and E is the energy between the ground state ^2P and the excited ^2P terms of $(nd)^9[(n+1)p]^1$ $[(n+1)d]^1$, then she showed

$$\Delta g_{1/2} = -(-5G_1^2 + 14F_2G_1)\ \zeta^2/E^4$$

$$\Delta g_{3/2} = -(-0.6F_0G_1 - 2.5G_1^2)\ \zeta^2/E^4$$

where the F's and G's are the corresponding Slater integrals.

Estimates of $(\zeta/E)^2$ are 1.6×10^{-5} and 1.2×10^{-3} for gallium and thallium respectively. Unfortunately, the Slater integrals are unknown although Philips claims F_0G_1 is probably negative. If this is the case then we would expect $g_{3/2}$ to be slightly decreased and $g_{1/2}$, of course, will be slightly increased. As we shall see later, the unexpected result for $g_{3/2}$ of thallium may be explained by this effect. It appears that the other g_J's measured are not detectably perturbed by this effect.

II. EXPERIMENTAL METHOD

A. Atomic Beam Apparatus

All measurements were done on a flop-in type atomic beam machine that has been described elsewhere.[17] A schematic diagram of the machine is shown in Fig. II-1. Neutral atoms produced in the buffer or oven chambers travel past the A, C, and B magnets and then are detected. The A and B magnets are highly inhomogeneous with $\partial B/\partial z \cong 10{,}000$ G/cm and $B \cong 10{,}000$ G. Neutral atoms see a force in such a field given by

$$F_z = -\frac{\partial W}{\partial z} = -\frac{\partial W}{\partial H}\frac{\partial H}{\partial z} = \mu_{eff}\frac{\partial H}{\partial z}$$

where μ_{eff} is the negative of the slope of the hyperfine energy level at the field H. For 10,000 G, μ_{eff} is usually of the order μ_o (μ_o is the Bohr magnetron). The A and B fields and gradients are in the same direction so that only atoms that change the sign of μ_{eff} (i.e. change the hfs level) in the C magnetic region can be refocused to the detector. Very slow atoms can not be focused since they run into the collimator or magnetic pole faces. Very fast molecules are purposely stopped by a "stop wire" since they are very slightly deflected and only contribute a large background. Since the source of neutral atoms is a hot (i.e. $kT >> \Delta\nu_{hfs}$) oven in quasi-equilibrium, all hyperfine levels in a given fine structure state are equally populated. The C-field which must be homogeneous and well regulated to obtain narrow resonance lines is obtained from a Varian Associates V40/2A with 12-inch pole faces. Although the power supply (Varian V2100) for this electromagnet is very well regulated, is was necessary further to stabilize the C-field

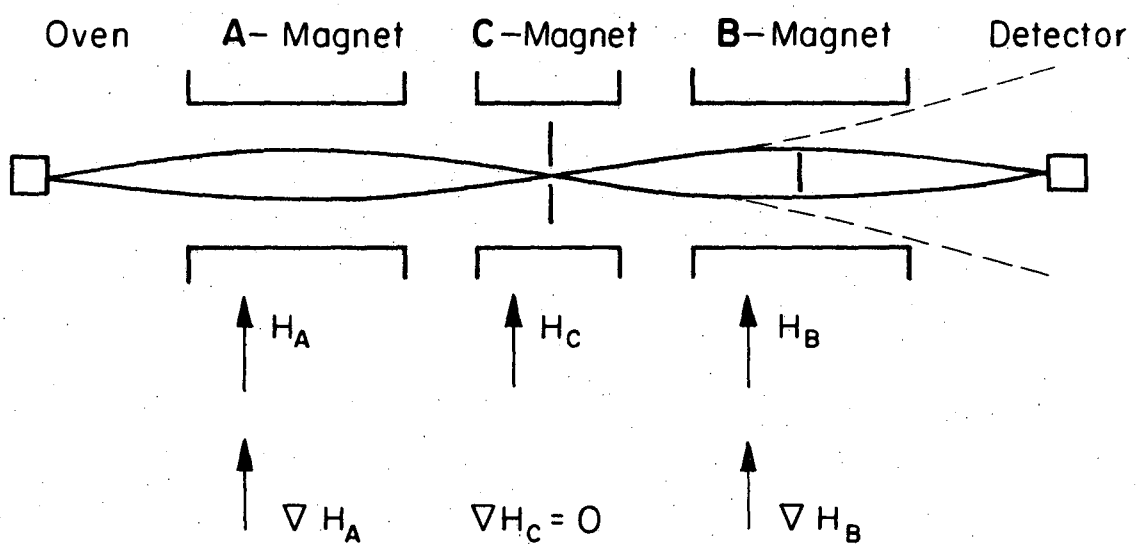

Fig. II-1. Schematic atomic-beam apparatus of the flop-in type.

by means of a nuclear magnetic resonance (NMR) field regulator (Harvey-Wells FC-502). Resonances of protons in water were usable from 800 to 7000 Gauss. A very stable oscillator (a Schlumberger FS-30) was weakly coupled to the marginal oscillator of the NMR regulator to reduce drift. Stabilities were typically a few parts per million per hour. Although the marginal oscillator frequency gives a crude value for the C-field (within 1/2 Gauss) the field can be measured by looking at a resonance of an isotope with a known hyperfine structure. The alkali elements (Rb, Cs, and K) usually serve this purpose.

B. Hyperfine Transitions

Transitions between hyperfine levels are induced in the C-magnet region. Because of the parity selection rule, transitions between hyperfine levels within a fine structure level are magnetic dipole to lowest order. The selection rules are $\Delta m_J = \pm 1, 0$, $\Delta m_I = \pm 1, 0$, $\Delta F = \pm 1, 0$, and $\Delta m_F = \pm 1, 0$. It should be pointed out that the transition rate for spontaneous emission for these transitions is very small so that for our purposes, each excited hyperfine level can be considered to have an infinite half-life. The half-lives are usually of the order of many thousands or even millions of years. Transitions satisfying $\Delta m_F = 0$ (± 1) are called $\sigma(\pi)$ transitions and require $H_{rf} \parallel (\perp)$ to H_0 where H_{rf} is the magnetic field in the hairpin due to the radio-frequency generator and H_0 is the C-field. Due to curvature of H_{rf} in our hairpins, both σ and π transitions can be seen.

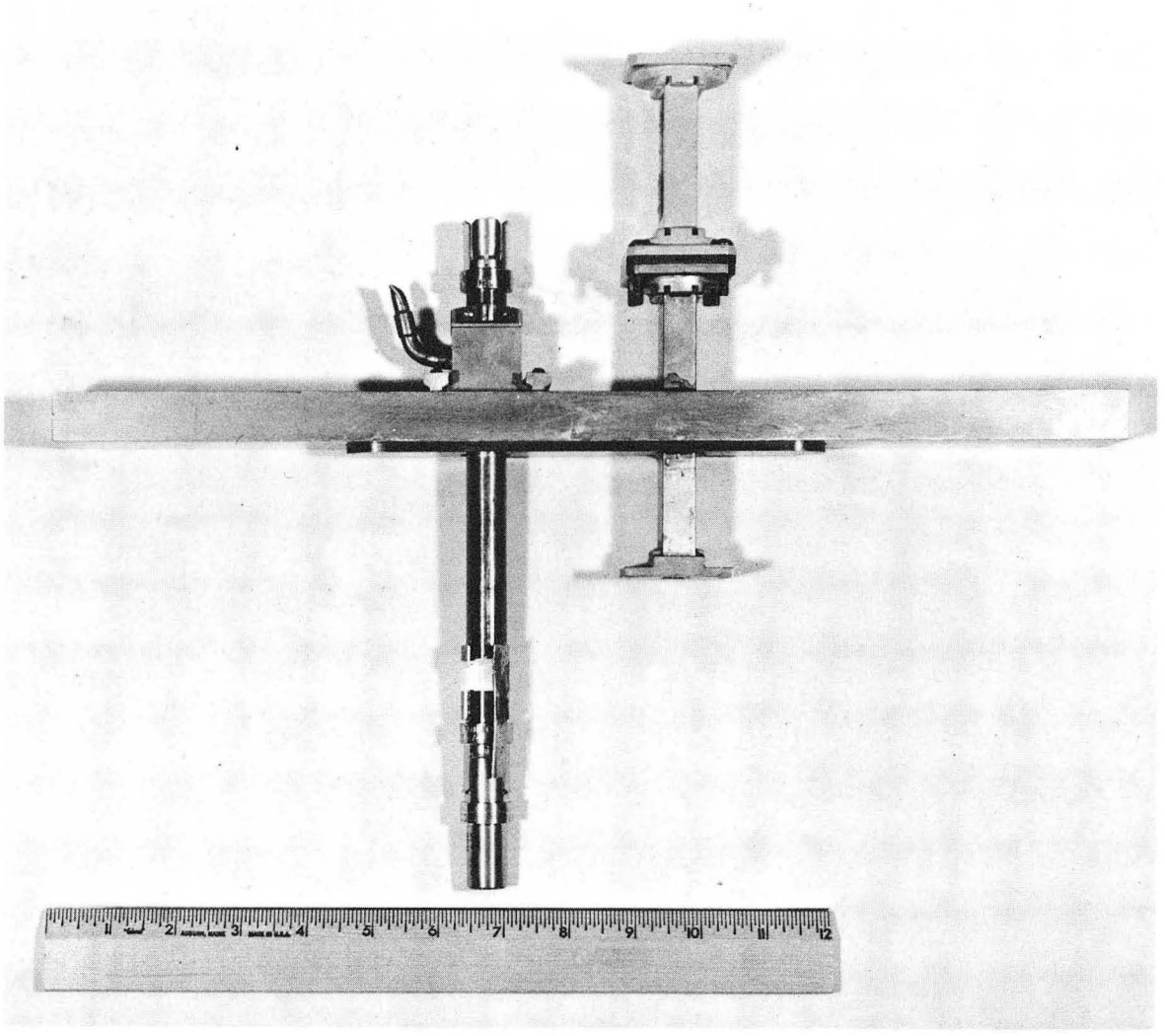

XBB 677-4015

Fig. II-2. Standard coaxial hairpin.

Radiofrequency energy is introduced by means of rf-loops or "hairpins". The coaxial hairpin shown in Fig. II-2 was used to observe all field dependent transitions. It is terminated with a matched 50 Ω load. This hairpin gives good results up to 12.4 GHz, which was the highest frequency used in any of the experiments. The minimum resonance line width one can achieve with a hairpin of length ℓ is given by the uncertainty relation and is

$$\Delta\nu \cong V/\ell$$

where V is the velocity of the atoms traveling through the hairpin. For the coaxial hairpin ℓ = 1 cm. C-field inhomogeneities will alter the observed resonance line width depending on $\partial\nu/\partial H$ for the transition under observation. These coaxial hairpins were used to observe the "standard" transitions in all four atomic states. These "standard" transitions are $(F_{max}, m_F = -F_{max}+1) \leftrightarrow (F_{max}, m_F = -F_{max})$ and are labelled "A" in Figs. I-4 through I-7.

A note about power levels is in order. Fig. II-3 shows the relationship between the resonance height and the power introduced into the hairpin in arbitrary units. The curve results from the weighting of the transition probability, which is proportional to $\sin^2$ at where a is a constant and t is the time the atom spends in the transition region, by the velocity distribution of the beam. As is well known, line broadening and asymmetric shifts can result from "saturating" (using more than about 1 unit of power in Fig. II-3) the resonant line. To help minimize such effects for the field dependent line measurements both the experimental resonance and the calibration resonance (also a

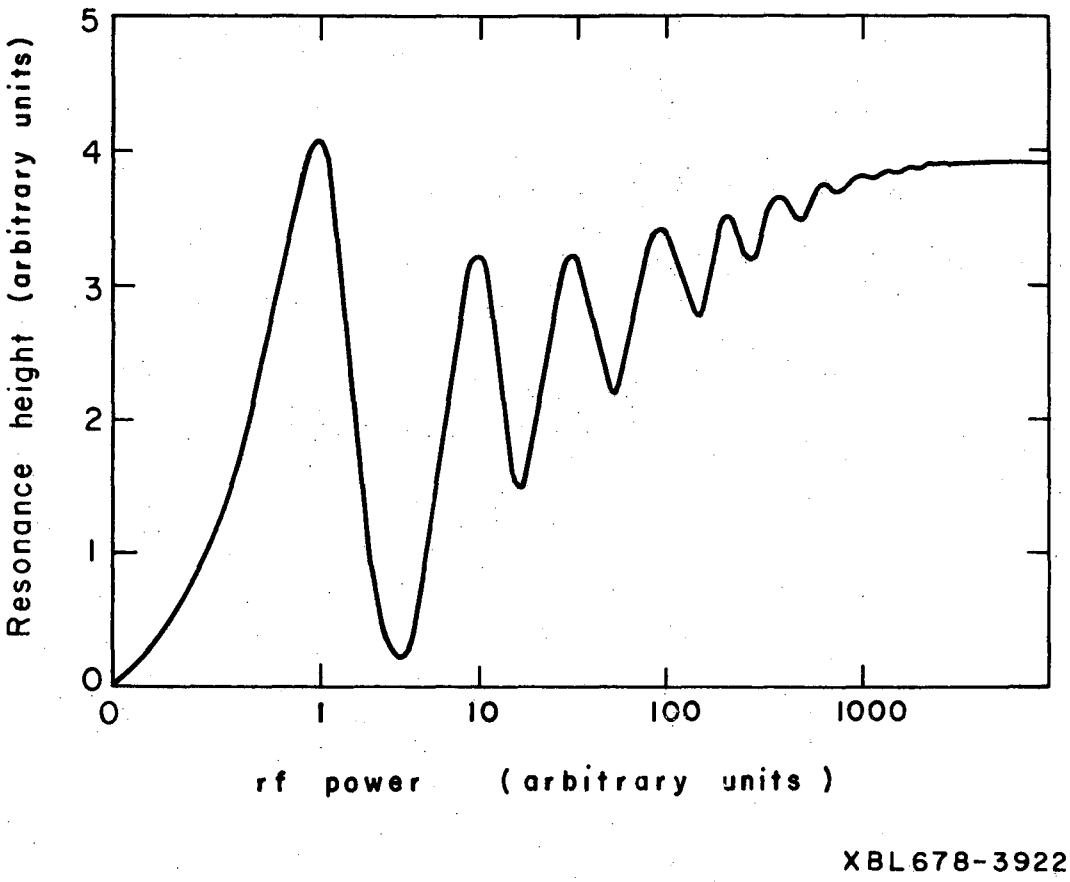

Fig. II-3. Resonance signal versus input power.

standard transition) were observed at the same percentage of peak power (1 unit in Fig. II-3). For example, if the gallium resonance ($^2P_{3/2}$) peaked at 80 mw and the calibration resonance at 90 mw, 62 mw and 70 mw would be used respectively. All runs were done at around 80% of peak power.

Two major reasons prevent one from using a longer hairpin to obtain narrower resonance lines. First, it is very difficult to construct reliable hairpins of non-coaxial geometry which are broad banded for frequencies above 1 GHz. Standing waves will sample the atomic beam at different points in space which will introduce uncontrollable calibration errors and asymmetries in the line shape since the calibrating frequency is not the same as the experimental frequency. The small space between the C-magnet pole faces prevent one from making larger coaxial hairpins. Secondly, field inhomogeneities in the C-magnet will increase the line width as ℓ is increased. In mose cases this broadening will overwhelm any gains of a longer hairpin. A modification of the Ramsey method has recently been developed by Y. Chan[18] which does allow one to obtain narrow line widths for these field dependent transitions.

For field independent transitions there are two ways to get narrower line widths. First, the Ramsey method of separated loops will work for any radio frequency. This method was used to observe the "doublet" transitions in the $^2P_{1/2}$ state of gallium which are $(F=2, m_F=-1) \leftrightarrow (F=1, m_F=0)$ and $(F=2, m_F=0) \leftrightarrow (F=1, m_F=-1)$. The two doublet frequencies together are very sensitive to the magnetic dipole interaction constant and the nuclear magnetic moment. Both hairpins were fed by the same radiofrequency oscillator. A typical Ramsey pattern is shown in Fig. III-2.

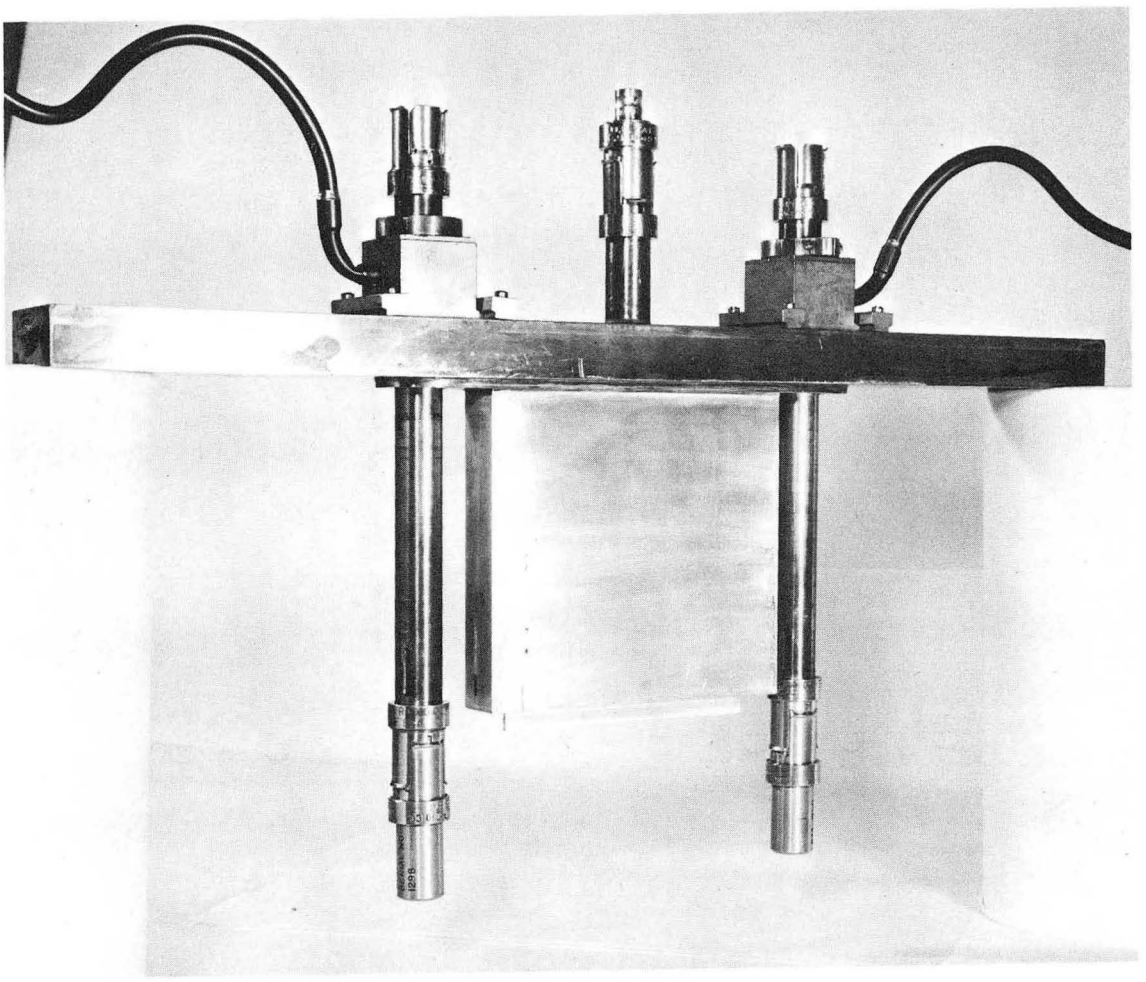

CBB 678-4801

Fig. II-4. Hairpin setup used to observe gallium triple loop resonance.

The width of the central maximum (or minimum) is given by $\Delta\nu \cong 0.65\ V/L$. In our measurements L = 6 in. giving $\Delta\nu \approx 1.6$ KHz for Ga. The pattern is symmetrical only if the phase, ϕ, between the rf fields in the two loops is 0° or 180°. When $\phi = 0°$ there is a maximum and for $\phi = 180°$ there is a minimum at the center of the pattern. The phase was adjusted by changing the length of one of the arms feeding the outer hairpins until the pattern was symmetrical about the central maximum or minimum.

In order for the method to work, the magnetic field must be the same in the two loops. The C-field was shimed in order to satisfy this condition. Also, the frequency of the central peak must correspond to the average field between the two hairpins. If $(\Delta\nu)_1$ is the difference between the resonance frequency in the hairpins and in the average intermediate region, the resonance is asymmetrically shifted approximately $(\ell/L)(\Delta\nu)_1$.[19] For the field independent transitions that were observed in gallium, this shift was less than 1 Hz and could be neglected.

For field independent transitions of frequency less than around 1500 MHz, the large center hairpin shown in Fig. II-4 may be used. For such frequencies, the wavelength is much larger than the hairpin and variations in the field strength over and along the beam are small and no asymmetries or calibrating errors are introduced. These hairpins were used to observe the transition $(F=2, m_F=0) \leftrightarrow (F=3, m_F=-1)$ in the $^2P_{3/2}$ state of gallium and the transition $(F=1, m_F=1) \leftrightarrow (F=2, m_F=0)$, $^2P_{3/2}$ state of thallium. These transitions (henceforth called direct transitions and labeled "T" in the energy level diagrams) do not satisfy the focusing condition discussed earlier and cannot be observed with only one hairpin. Using the triple loop[20,21] arrangement shown in Fig. II-4

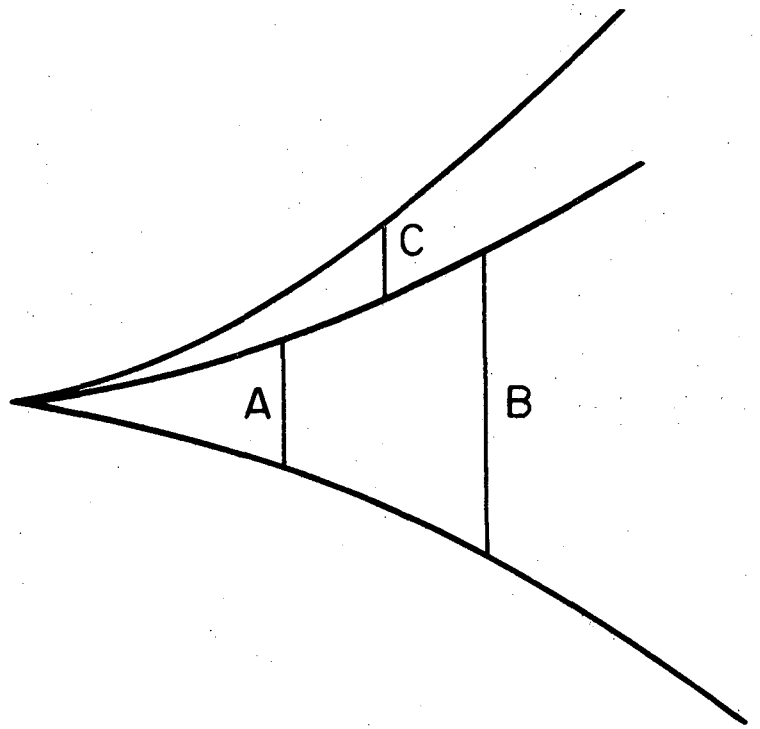

MUB-8117

Fig. II-5. Triple loop signal relations.

$$S_A \propto P_A$$

$$S_{AB} \propto (P_A + P_B - 2P_AP_B)$$

$$S_{ABC} \propto (P_A + P_B - 2P_AP_B + P_AP_BP_C)$$

one can observe these transitions. The outer two hairpins are used to induce the standard A and B transitions (see Fig. II-5) while the center hairpin is used to induce the transition, C. Let P_A, P_B, and P_C be the probability of inducing the transitions A, B, and C respectively. Then with just the two outer hairpins, the signal is $\propto 2P_A(1-P_B)+2P_B(1-P_A)$. With the central hairpin included, the signal is $\propto P_C P_A P_B+2P_A(1-P_B)$ $+2P_B(1-P_A)$. The optimum condition is $P_A = P_B = 1$ — i.e. the outer resonances are maximized. Since one radiofrequency oscillator was used for both of the outer hairpins it was necessary to shim the C-magnetic field. Such shiming had pronounced effects on the C-magnetic field homogeneity and it was not always possible to peak both outer resonances with our traveling wave tube amplifier Hewlett-Packard 495A or 493A (output $\sim$1 watt). Both of these direct transitions were observed at high enough fields so the J and I were decoupled. When I and J are decoupled the representation $|IJm_I m_J\rangle \equiv |m_I m_J\rangle$ is a much more accurate representation than $|IJFm_F\rangle$. In fact, in the limit where I and J are completely uncoupled m_I and m_J are good quantum numbers. Now, the triple loop transition is given by $|1/2 - 1/2\rangle \leftrightarrow |1/2 - 3/2\rangle$ for Ga and $|1/2\ 1/2\rangle \leftrightarrow |1/2 - 1/2\rangle$ for Tℓ. In such a case only the nucleus is flipped and because of the much smaller transition probability to flip a nucleus than an electron, much more power was needed to see these transitions than was required to see the standard transitions. Usually 2 to 5 watts were used. Understandably, these direct transitions are very sensitive to the nuclear magnetic moment. In all of the above transitions all four combinations of hairpin order along the beam and

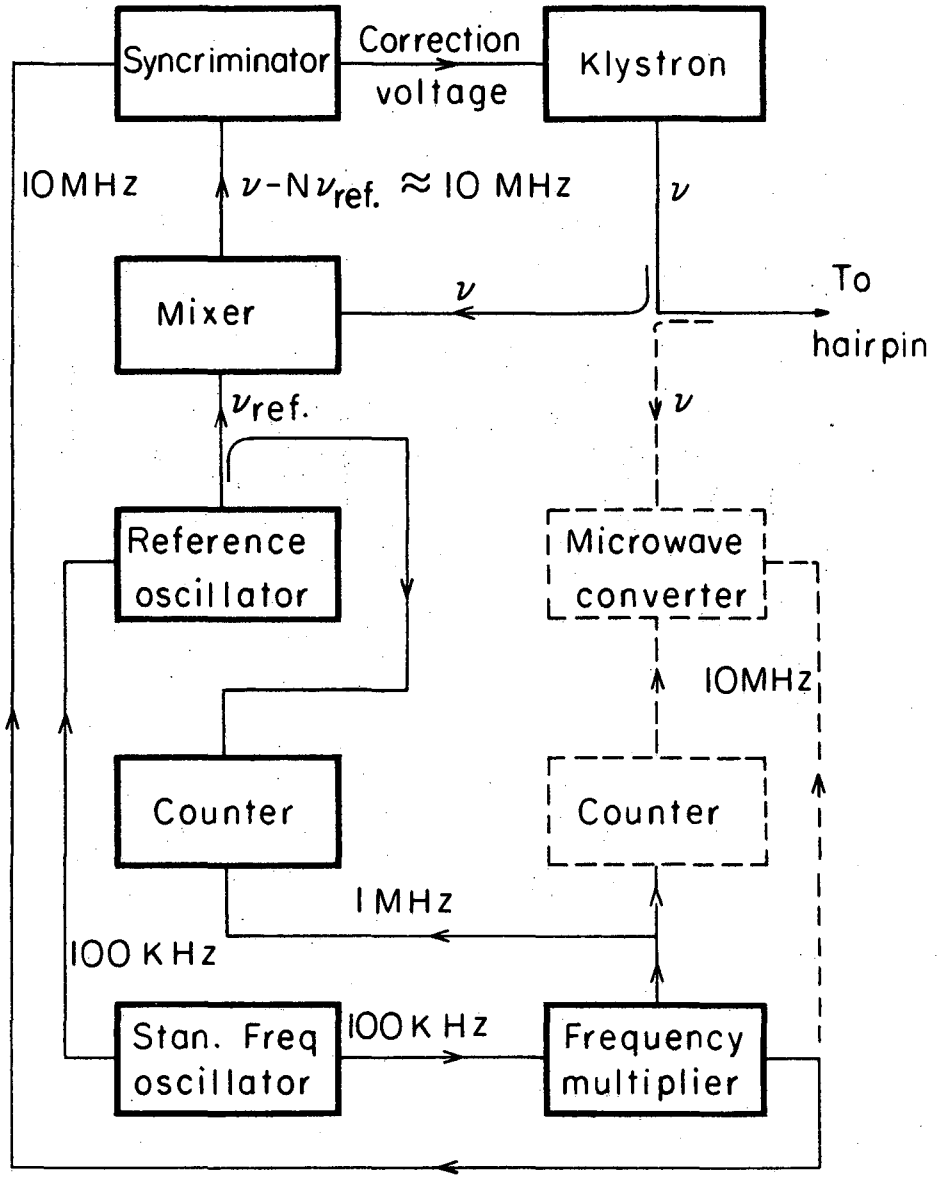

Fig. II-6. Block diagram of the klystron phase-locking circuit and frequency-measuring circuit.

C-magnet field directions were investigated to detect any systematic errors. No systematic errors were found.

C. Radiofrequency Equipment

Two signal synthesizers were available. A Schomandl Model FD-3 generated 300 - 1000 MHz. A Schlumberger type DO-1001 with plug-ins generated 1 to 1500 MHz. For transition frequencies less than 4 GHz the output of these generators were either directly amplified (using an Electron-International AP-502R, and Applied Microwave A100, or a Boonton Model 230A) or increased to the proper frequency by crystal doublers and then amplified with traveling wave tube amplifiers. For frequencies greater than 4 GHz these generator outputs were used to phase lock reflex klystrons with a Dymec Model 2650A or a Schomandl FDS-3 syncriminator. All frequencies were measured with Hewlett-Packard Model 5245L counters and power levels were measured with a General Microwave AR Model 454. In most cases the experimental resonance frequency and the calibration frequency were sufficiently separated that two independent frequency generating setups were required. A complete block diagram of a frequency setup using a reflex klystron is shown in Fig. II-6.

The linewidths and frequencies in these experiments demanded that all frequencies be accurate to 1 part in 10^8 at least. Consequently, all signal generators, phase locking devices, and frequency counters were locked to an external 100 KHz quartz-crystal oscillator (J. Knight FS1100T with specified drift less than 5 parts in 10^{10} per 24 hours.

This standard was compated with WWVB (60 KHz carrier) every two or three days with a Gertsch PCR-1 VLF phase comparison receiver and was reset if the offset was 1 part in 10^8 or more. The actual drift rate was around 5 parts in 10^{11} per 24 hours.

D. Beam Production and Detection

1. Gallium Beam. Although gallium metal melts at only 30°C it requires a temperature of around 1200°C to get a vapor pressure of 1 mm which is required for a sufficiently intense beam. From the Boltzmann equation

$$\frac{n_1}{n_2} = e^{-(E_1-E_2)/kT}$$

relating the number of atoms in level 1 to the number in level 2 separated by an energy E_1-E_2 (n_2 is the ground state say) at a temperature T (°K). We see that with $^2P_{3/2}$ lying 826.24 cm^{-1} above the $^2P_{1/2}$ ground state, approximately 45% of the beam will be in the $^2P_{3/2}$ state at 1470°K (1200°C). Consequently, both states can be easily observed. Electron bombardment was used to heat up the gallium oven. Since gallium wets most metals, it was necessary to use a carbon oven with a tight fitting lid. A bare carbon oven tended to erode near the filament. To prevent this a tantalum oven was built with an inner carbon oven to hold the gallium. The tantalum oven was cylindrical in shape with diameter 12 mm and length 15 mm. This oven worked very well. A satisfactory beam was obtained with about 75 watts into the oven. The slit size was .005 in. by 1/16 in. Once the electron filament (0.015 in. thoriated tungsten) stabilized, the beam was very stable.

2. Thallium Beam. Thallium metal melts at 303°C and a satisfactory beam can be obtained at around 850°C. A standard resistive heated iron oven was used with a slit size of .005 in. by 1/16 in. The oven was cubical in shape and about 1/2 in. on a side. One loading of thallium metal produced enough beam to do all the runs described later. Beam stability was excellent. The heating element was a single coil made of .010 in. tantalum wire. Approximately 180 watts (90 volts at 2 amps) were required to get a satisfactory beam. Unlike gallium, the large fine structure separation (7792.2 cm^{-1}) and the low temperature (850°C) leads to only .005% of the atoms in the beam being in the $^2P_{3/2}$ state. Consequently, some means had to be found that would pump some thallium atoms from the $^2P_{1/2}$ state into the $^2P_{3/2}$ state.

Electron bombardment of the oven slit was first tried. The hope was that the electrons would excite the thallium atoms in the oven slit up into higher states in which some would decay into the $^2P_{3/2}$ state. Although a bright green discharge (indicating production of the $^2P_{3/2}$ state) was observed in the slit no $^2P_{3/2}$ resonance could be found.

It was then decided to excite the thallium atoms optically with an electrodeless discharge thallium lamp placed in the buffer chamber. This chamber was located between the A magnet and the main oven chamber and contained, in addition to the lamp, three ovens containing calibration isotopes (see below). Although such a lamp produces many excited states and their corresponding decay radiations, the primary exciting radiation is the 3775.72 Å line shown in Fig. I-2. Since the degeneracy of the $^2P_{3/2}$ state is 8 and that of the $^2P_{3/2}$ state, 4, 2/3 of the atoms in $7\ ^2S_{1/2}$ will decay into the $^2P_{3/2}$ state and 1/3 will return to the

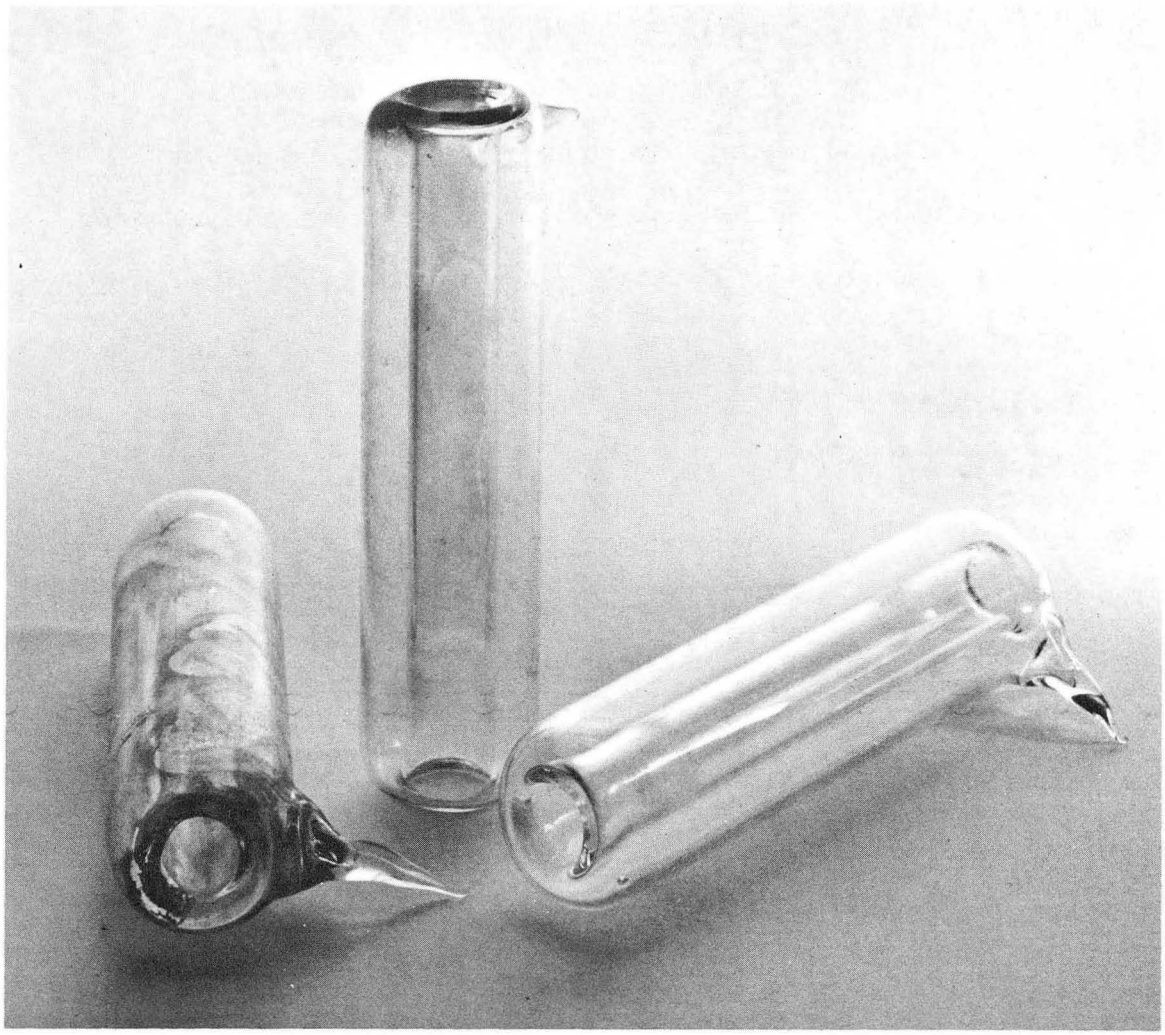

XBB 677-4019

Fig. II-7. Thallium electrodeless discharge lamps.

ground state. For example, if all beam atoms were excited by the 3775.72 Å radiation the emerging beam would be 67% $^2P_{3/2}$ and 33% $^2P_{1/2}$. A picture of some of these lamps is shown in Fig. II-7. The lamp was aligned in the buffer chamber so that the Tℓ beam passed directly down the axis of the lamp. This lamp configuration greatly increased the probability of exciting the beam. The lamps were made out of 4 mm thick quartz tubing and were 8 cm long. The outside diameter of the tubing was 21 mm and 12 mm for the outer and inner tubes respectively. The lamp contained 1 mm of argon and a small amount of $T\ell C\ell_3$ (about 50 μg). The lamps were mounted on the end of the moveable loader that also supported the calibrating ovens. Rather than move the loader back and forth between each observation and calibration, it was decided that the $^2P_{1/2}$ state would be used as the calibrating resonances for the $^2P_{3/2}$ measurements. The lamp could then be aligned and left along throughout the run. The output of a Litton L-3506 (5.6 GHz, 110 watt) magnetron was fed directly to the buffer chamber via waveguide and a microwave horn. An insulated wire, one end of which was a few millimeters from the lamp and the other end connected to a vacuum feed-through, was used to get the lamp started. It was only necessary to touch the wire with a Tesla coil exciter to get the argon to discharge. The argon would discharge immediately. With the lamp in a vacuum and supported by a quartz cradle, the thermal conductivity was very low and so, after about 10 minutes, the argon discharge would warm up the lamp to the point where the thallium vapor pressure would be high enough so that the thallium would begin to

discharge. At this point, the lamp rapidly heated up and produced a bright green glow easily visible from the detector end of the machine. The lamps were filled using the well known techniques described by McDermott and Novick.[22] An estimate of the amount of $^2P_{3/2}$ atoms produced will be made in Sec. III-B. Under the best conditions, about one-third or so of the beam was in the $^2P_{3/2}$ state.

3. Calibrating Beams. For measurements of the $^2P_{3/2}$ state in thallium the standard transition in the $^2P_{1/2}$ of thallium was used as the calibrating resonance as mentioned above. Also, the "a transition" in $^2P_{3/2}$ of ^{69}Ga (see Fig. I-8) was used to calibrate the field in the measurements of the triple loop resonance in the $^2P_{3/2}$ state of ^{69}Ga. All the remaining runs used an alkali beam of either K^{39}, Rb^{85}, Rb^{87}, or Cs^{133} as the standard. The standard mixture of the alkali halide and calcium powder was used in a resistive heated oven. The buffer chamber could hold three such ovens. Consequently, two or three different alkali beams were available if necessary, although only one beam was available at a time since each oven contained only one alkali. With 50 watts input, a satisfactory beam was achieved after a 20 minute warm-up. The geometry of the buffer and oven chambers was such that the experimental beam of gallium or thallium would pass directly over the top of the calibrating oven. Consequently, both beams were present simultaneously and it was not necessary to adjust the machine in any way during a run.

4. Beam Detection. The experimental beams of gallium and thallium as well as the alkali calibrating beams were detected on an oxidized tungsten hot wire (.015 in.).

Neutral atoms falling upon the hot wire are ionized. A voltage (12 VDC) between the hot wire and a metal collector sweeps these ions to the collector where they are measured with an electrometer. With the ionization potential of gallium and thallium being 6.00 e.v.[2] and 6.106 e.v.[1] respectively, very little would be detected on an ordinary W wire with a work function of 4.5 e.v. However, it is well known that a layer of oxygen will greatly increase the work function of tungsten. How and why oxygen does this and the chemical state of the oxygen on the surface is unknown. Once "oxidized" the wire will remain sensitive for about 12 hours of continuous running. It is also important to note that the speed of the hot wire detector depends upon the average time a neutral atom sits on the wire before becoming ionized. This time, known as the sitting time, is very temperature dependent and forces one to keep the temperature near 1000°C after the oxidizing is finished to keep the sitting time less than 0.1 second or so. The oxidizing procedure used is described by Beehler and Glaze.[23] The hot wire is maintained at around 900°C while O_2 is leaked into the detector chamber. The leak is increased until the pressure reaches 1000 microns of Hg. This pressure is maintained for about 90 seconds during which the vacuum is still being pumped upon so that a steady state is achieved. After 90 sec. the O_2 leak is closed and the vacuum is allowed to return to the operating pressure near 3×10^{-7} mm Hg -- all the while the hot wire temperature is kept at around 900°C. The whole oxidizing procedure takes only around 5 minutes. It is very important that the W wire be very clean before oxidation. This was achieved by maintaining the wire at 1500°C under a high vacuum (3×10^{-7} mm Hg) until the background was

reduced to 10^{-11} amperes or less. It sometimes took 12 hours or more to get the background down to this level. After oxidation the background increased to 3 to 7 × 10^{-10} amperes. Fortunately, after an hour or so this noise would become very steady and could be bucked out by the electrometer which was a Keithley Model 417. The beam resonances were generally 10^{-10} amperes or less and, therefore, smaller than the background on the wire. Fortunately, as long as the background was steady, beam resonances could be monitored on high sensitivity ranges of the electrometer without difficulty after the background was bucked out. That is, after a bucking current equal to the background current but opposite in direction was fed into the electrometer input essentially eliminating the constant component of the input.

E. Method of Measurement

For the field dependent measurements it was very important to calibrate the field before and after every measurement of the experimental isotope. Therefore, a run for a particular orientation of hairpin and C-field directions, consisted of n experimental resonance measurements placed between n + 1 calibration isotope measurements where n was around 15. Each run took about 30 minutes if everything went well. Each measurement consisted of sitting on the resonance 6 times, 3 times above the peak and 3 times below and symmetrically placed and recording the frequency each time. The average of the 6 frequencies was taken to be the resonance frequency. The average frequencies seemed to be independent of the 3 signal levels used to measure the six frequencies. An observation is defined as a measurement of the experimental resonance

and the corresponding field by means of the average frequency of the calibrating resonance taken before and after the experimental resonance measurement.

For field independent transitions (doublet and direct transitions) the calibrating problem was much less severe. Usually around 10 observations were made of the experimental resonance between each set of calibrating observations. Field drift between calibrations had no observable effect on the measured field independent transition frequencies.

III. EXPERIMENTAL RESULTS

A. Gallium-69

The gallium data is summarized in Appendix E. All observations are shown for each run, except for runs 144, 145, and 146 where Holloway's[33] three zero-field splittings ($\Delta F = \pm 1$ transition) as quoted in his paper were used as the observations. The total number of observations was 255. The first four runs were standard transitions in the $^2P_{3/2}$ state. The next five runs were standard transitions in the $^2P_{1/2}$ state. These nine runs were made with the standard coaxial hairpin. For all these runs the frequency error in Appendix D is an estimate of the reproducibility of the data at the magnetic field in question. In addition to these runs of the standard transition at 2000 Gauss as above, several runs were made below 2000 Gauss. However, due to non-reproducibility (of the order of a line width) these runs were rejected. The next observation (run 133) was the "doublet" transition in the $^2P_{1/2}$ state. The Ramsey method of separated loops was used. The outer hairpins were coaxial and terminated with a 50 Ω load. The field was calibrated by observing the standard transition in ^{133}Cs in the center hairpin. Although this hairpin was also coaxial, it was shorted rather than terminated with a 50 Ω load because of the location of the NMR probe which projected into the C-magnet. Run 132 was the direct transition $(F=2, m_F=0) \leftrightarrow (F=3, m_F=-1)$ in the $^2P_{3/2}$ state. The triple loop method was used using the hairpins shown in Fig. II-6. The half-width of the resonance was 5 KHz. The center hairpin was 4.5 in. long. The calibrating resonance (which was the a transition in ^{69}Ga in the $^2P_{3/2}$ state [see Fig. I-8]) was observed in the center hairpin.

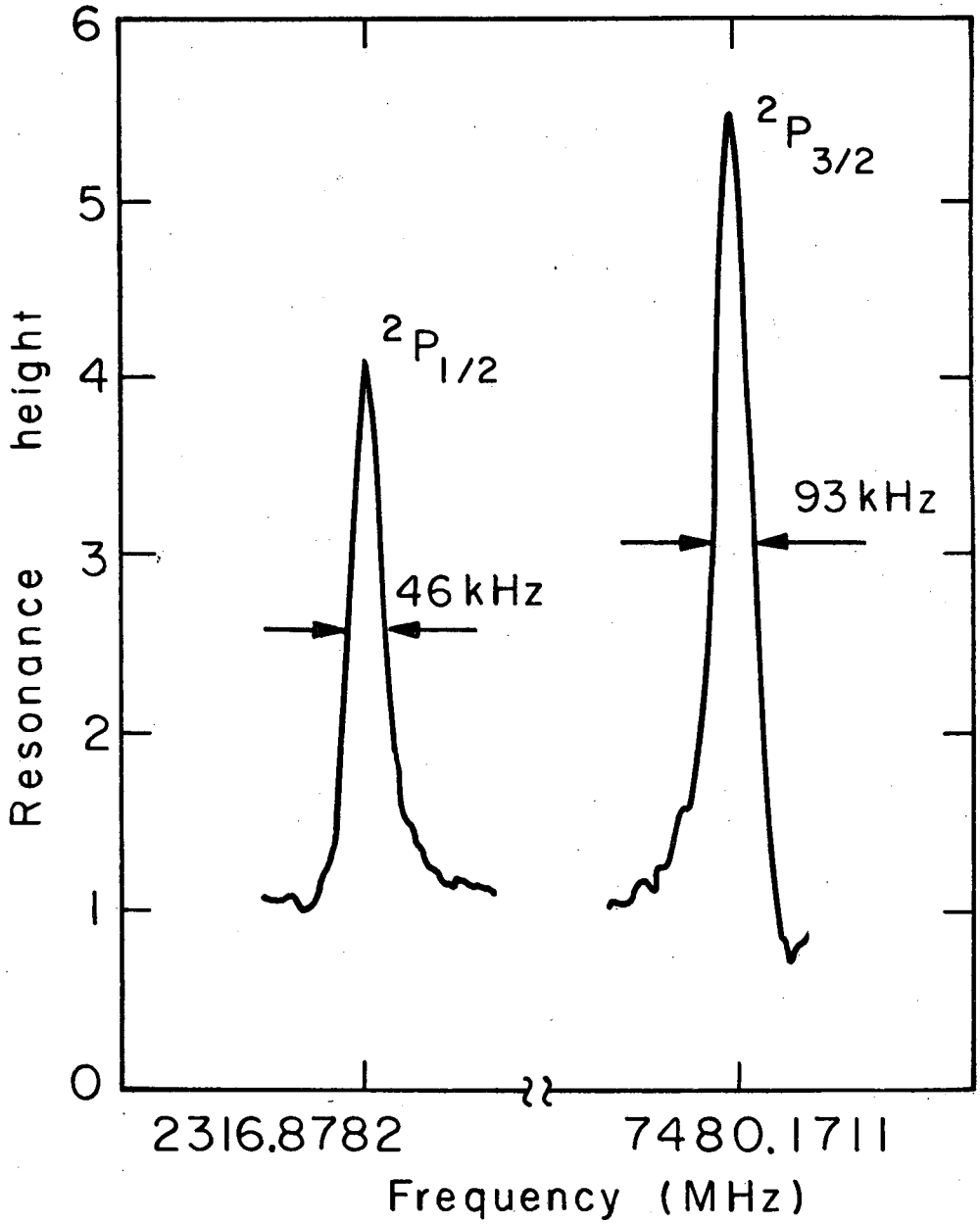

Fig. III-1. Chart-Recorder Tracings of the ^{69}Ga Standard Transition Resonances at 4000 G.

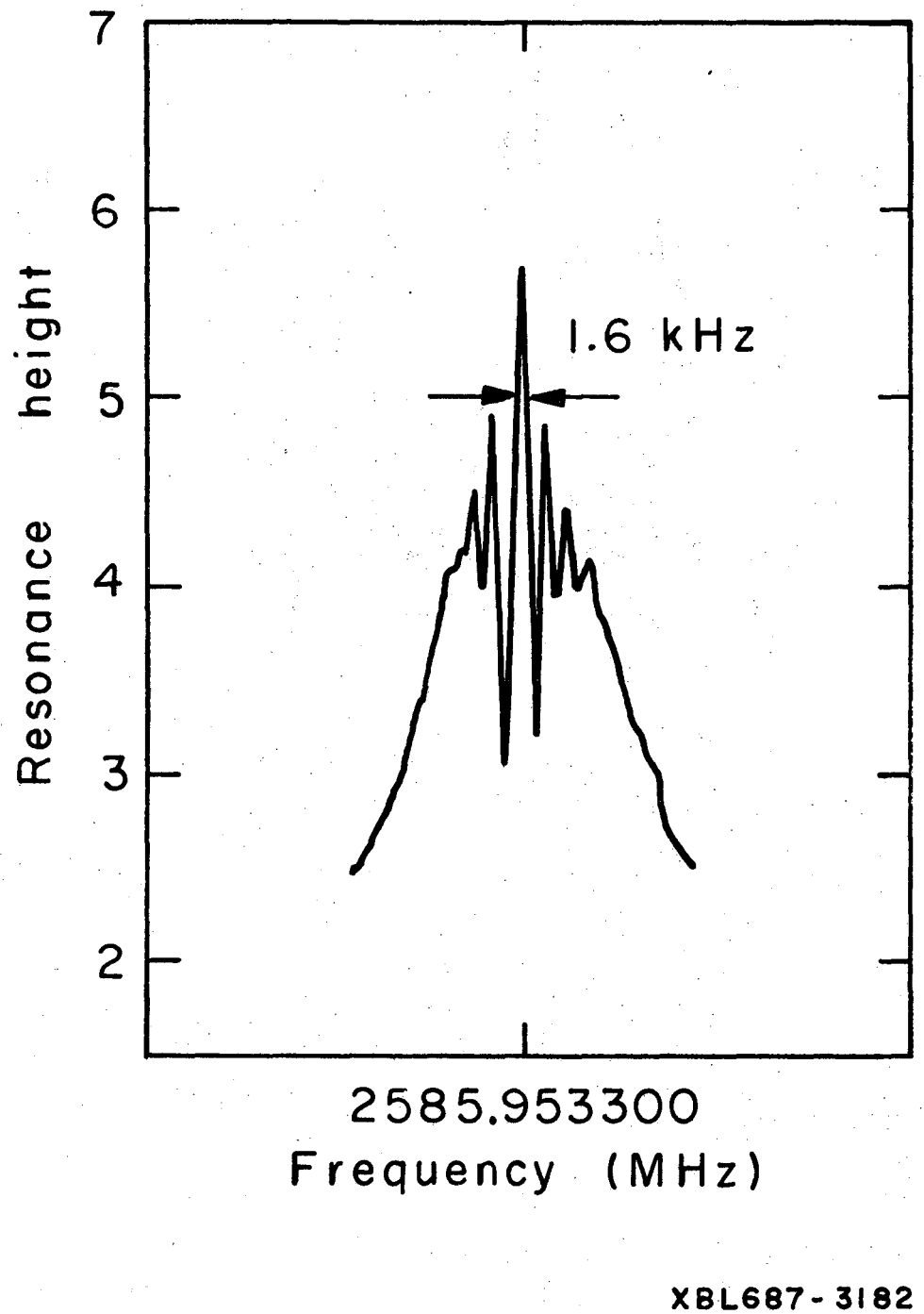

Fig. III-2. Chart-Recorder Tracings of ^{69}Ga Doublet Resonances.

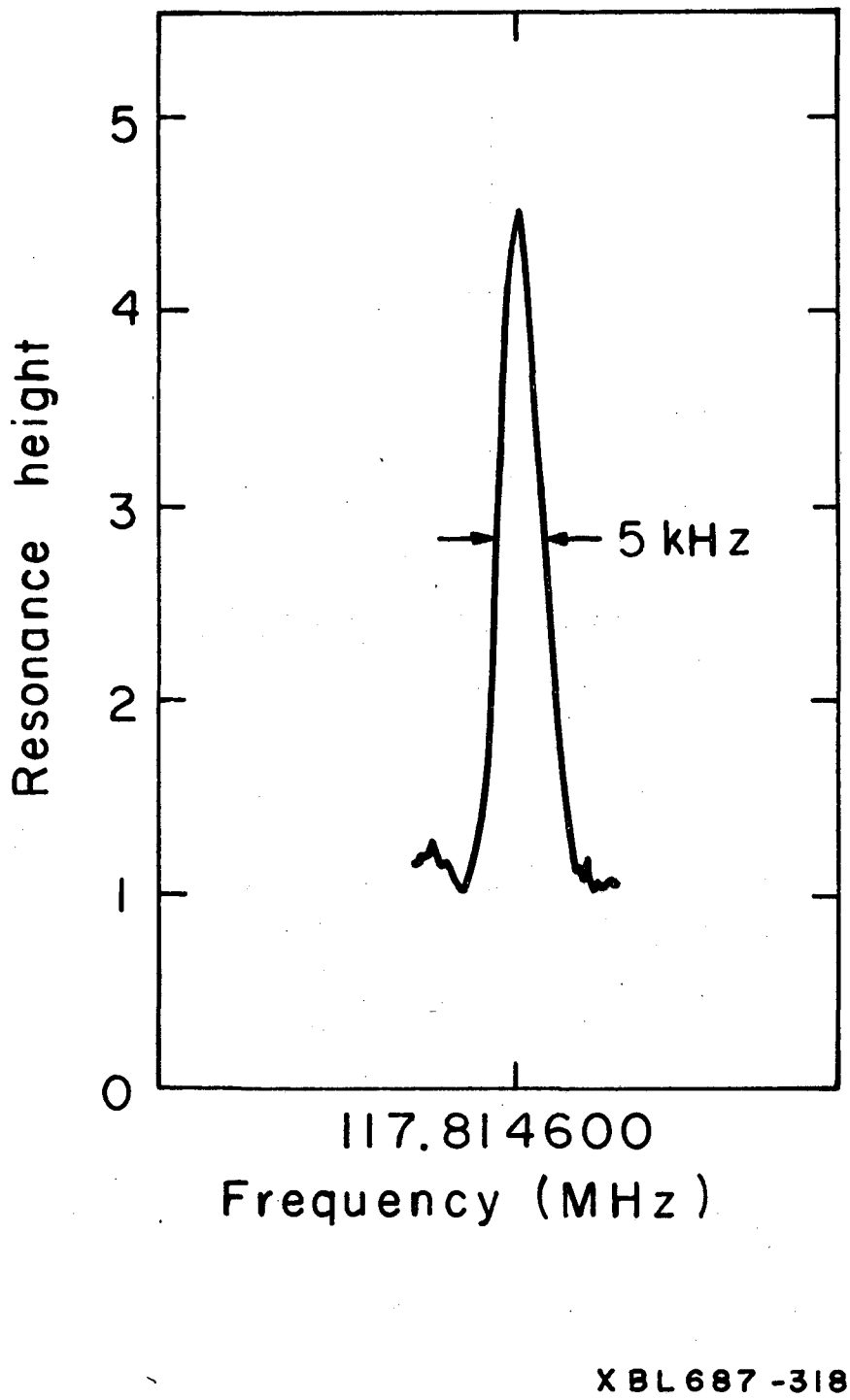

Fig. III-3. Chart-Recorder Tracings of the ^{69}Ga Triple Loop Resonance.

Although the line was very broad and asymmetric the line width was, nevertheless, small enough to give an adequate calibration. The equivalent uncertainty in the field was 0.11 Gauss. This was an adequate calibration because of the fact that as far as several gauss from the field where the measurements were made, no frequency changes in the resonance were observable. Run 133A was a measurement of the transition $(F=2, m_F=0) \leftrightarrow (F=1, m_F=-1)$ in the $^2P_{1/2}$ state of 0.3 Gauss. The set up was the same as for run 132. This runs was very sensitive to $\Delta\nu_{1/2}$. The last three ites labeled runs 144-146 are Holloway's data[33] which he used to calculate $a_{3/2}$, b, and c. Since these three interaction constants can be calculated from the observed zero-field separations only if the off-diagonal dipole and quadrupole (η) elements are known, it is necessary to recalculate $a_{3/2}$, b, and c consistent with our new experimental observations. The errors in the observations are those quoted by Holloway. Figures III-1 to III-3 show typical gallium resonances. We now want to least squares fit 9 of the eleven parameters that enter into the energy matrix to all the observations. We will assume N=1 and δ = 826.24 cm^{-1}. That leaves the following 9 parameters to be fitted -- $a_{3/2}$, b, c, $\Delta\nu_{1/2}$, $g_{1/2}$, $g_{3/2}$, g_I, a''', and η. Rather than vary all nine simultaneously, we will take advantage of the fact that runs 133A, 144, 145, and 146 give $\Delta\nu_{1/2}$ and $a_{3/2}$, b, and c very accurately with only a relatively small dependence upon the other five parameters. The procedure used was as follows: Runs 133A, 144, 145, and 146 were analyzed giving $\Delta\nu_{1/2}$, $a_{3/2}$, b, and c assuming reasonable

values for the other five parameters -- i.e. their theoretical or previously measured values. Using these four fitted values we fitted the remaining five parameters. These were used in turn to calculate new values for $\Delta\nu_{1/2}$, $a_{3/2}$, b, and c. The process was then repeated until all nine parameters converged. It was found that three iterations were sufficient to obtain a consistent solution. The resulting values are

^{69}Ga:

$$\Delta\nu_{1/2} = 2677.98716(20)\ \text{MHz}$$
$$a_{3/2} = 190.79436(11)\ \text{MHz}$$
$$b = 62.52319(23)\ \text{MHz}$$
$$c = 90(6)\ \text{Hz}$$
$$g_{1/2} = -0.66579172(28)$$
$$g_{3/2} = -1.33405731(60)$$
$$g_I = 7.29530(33) \times 10^{-4}$$
$$a''' = -107.76(98)\ \text{MHz}$$
$$\eta = 1.0886(290)$$

χ^2 was 73 and the total number of observations was 255. The errors are twice the least square errors -- i.e. two standard deviations.

$\Delta\nu_{1/2}$ has been measured by Lurio and Prodell[24] who obtained $\Delta\nu_{1/2}$ = 2677.9875(10) MHz which is consistent with the new result. The previously measured values for $a_{3/2}$, b, and c are shown in Appendix A. As can be seen the major change is in b where the new result is 723 Hz larger than the old. This is about twice as large as the error in b as quoted by

Holloway and seven times the error derived from his original data with our analysis.

From the observed a-values one can calculate the expected off-diagonal element, a''', on the basis of only the $s \rightarrow s'$ mode. Above, we found $\beta = -0.190$ and $a''' = -120$ MHz. We see that our observed value is about 11% smaller than this expected value. This discrepance is probably due to other types of configuration interaction. The measured value of η is 4.8% greater than the value calculated by Schwartz which is accurate to about 5%.[25]

The g_I value means there is a -778(44) ppm diamagnetic shift between the free atom and gallic ion in aqueous solution in which the NMR measurements were made.[26] The mechanism for this shift may be the same as in thallium which is well known for its large diamagnetic shifts.[27] The experimental work on thallium solutions indicate that the thallic ion tends to form complexes in solution whereas thallous ion has a much smaller tendency to do so. It appears that this effect accounts for the -1900 ppm diamagnetic shift between these two ions in solution. It appears that the g_I value inferred from the thallous ion solutions are much closer to the free atom values than the values obtained from thallic ion solutions. Unfortunately, gallous ion is unstable and no direct comparison can be made of the diamagnetic shift between gallic and gallous ion solutions and, therefore, all NMR measurements have had to be made on gallic ion. However, it appears reasonable to suppose gallic ion behaves somewhat like thallic ion and therefore we would expect a large shift like the one observed. Since only order of magnitude calculations can be made for these large shifts, no attempt will be made to calculate them.

Table 1. Gallium g_J Comparison

		Hartree	Herman et Al
$P_{3/2}$:	Δg_{Rel}	$= +25.8 \times 10^{-6}$	$+54.4 \times 10^{-6}$
	Δg_{Lamb}	$= +14.7 \times 10^{-6}$	$+20.0 \times 10^{-6}$
	$\Delta g_{orbit\text{-}orbit}$	$= +38.6 \times 10^{-6}$	$+44.5 \times 10^{-6}$
	Δg_{total}	$= +79.0 \times 10^{-6}$	$+118.9 \times 10^{-6}$
	g_{theory}	$= g_{3/2} + \Delta g_{total}$	$g_{3/2} + \Delta g_{total}$
		$= -1.3340274$	-1.3339875
	$g_{observed}$	$= -1.3340573$	-1.3340573
	Discrepancy	$= -0.000030$	-0.000070
		$= -22$ ppm	-52 ppm
$P_{1/2}$:	Δg_{Rel}	$= +25.8 \times 10^{-6}$	$+54.4 \times 10^{-6}$
	Δg_{Lamb}	$= +2.8 \times 10^{-6}$	$+7.7 \times 10^{-6}$
	$\Delta g_{orbit\text{-}orbit}$	$= +77.1 \times 10^{-6}$	$+89.0 \times 10^{-6}$
	Δg_{total}	$= +105.7 \times 10^{-6}$	$+151.1 \times 10^{-6}$
	g_{theory}	$= g_{1/2} + \Delta g_{total}$	$g_{1/2} + \Delta g_{total}$
		$= -0.6657879$	-0.6657425
	$g_{observed}$	$= -0.6657917$	-0.6657917
	Discrepancy	$= -0.0000038$	-0.0000492
		$= -5.7$ ppm	-74.0 ppm

The electronic g-factors are consistent with the previous measurements of Kusch and Foley[28] (see Appendix A). Two different wave functions were used to calculate the correction factors discussed in Secs. I-C and D. Table 1 shows the results. As can be seen, Hartree's wave functions[29] give satisfactory agreement. The main difference between the wave functions of Hartree and those of Herman et al[30] is the use of the free electron exchange approximation for the latter. As was pointed out by Herman et al, the free-electron exchange approximation is least accurate in the outer parts of an atom. From Table 1 it would appear that the correction factors of interest are very sensitive to the wave functions and that the free electron approximation makes matters worse for the present purposes.

B. Thallium

A summary of the ^{205}Tl and ^{203}Tl runs are shown in Appendix F. For all the field dependent transitions the frequency error was taken to be 1/10 of a line width. As was stated earlier, the $^2P_{1/2}$ standard transition was used as the calibrating frequency for the $^2P_{3/2}$ measurements.

Unlike all the other runs, the triple loop resonances were measured by setting the frequency at the center of the resonance line and recording the frequency. The signal to noise ratio was around 2 or 3 to one and prevented sitting six times on each observation. The calibrating problem was not severe so 20 to 30 measurements were taken between calibrations. A total of 200 to 300 peak measurements were made at each field setting. The line widths were 3.5 kHz and the total spread in the various measurements was 1 kHz. The average of all measurements at each field (for a given

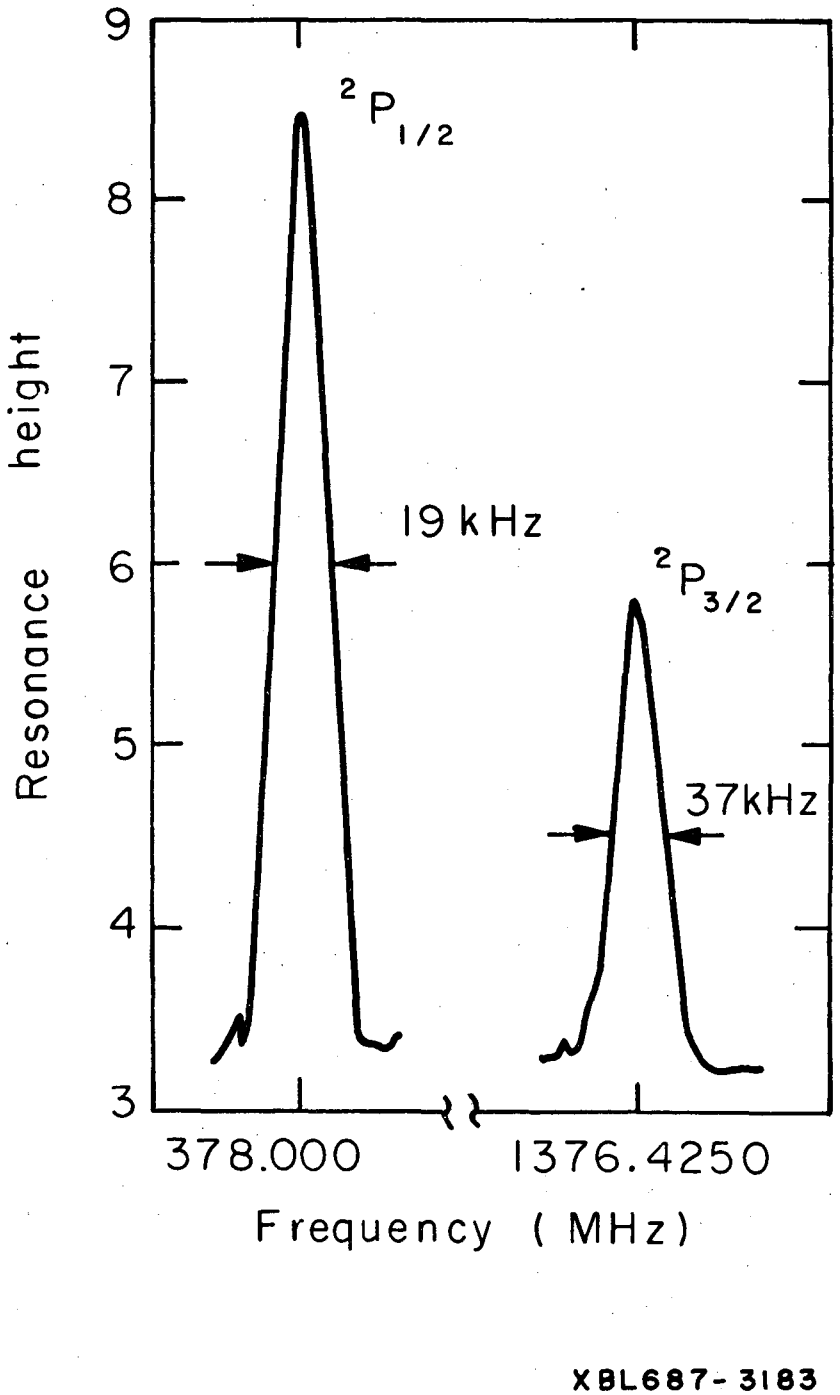

Fig. III-4. Chart-Recorder Tracings of ^{205}Tl Standard Transitions at 800 G.

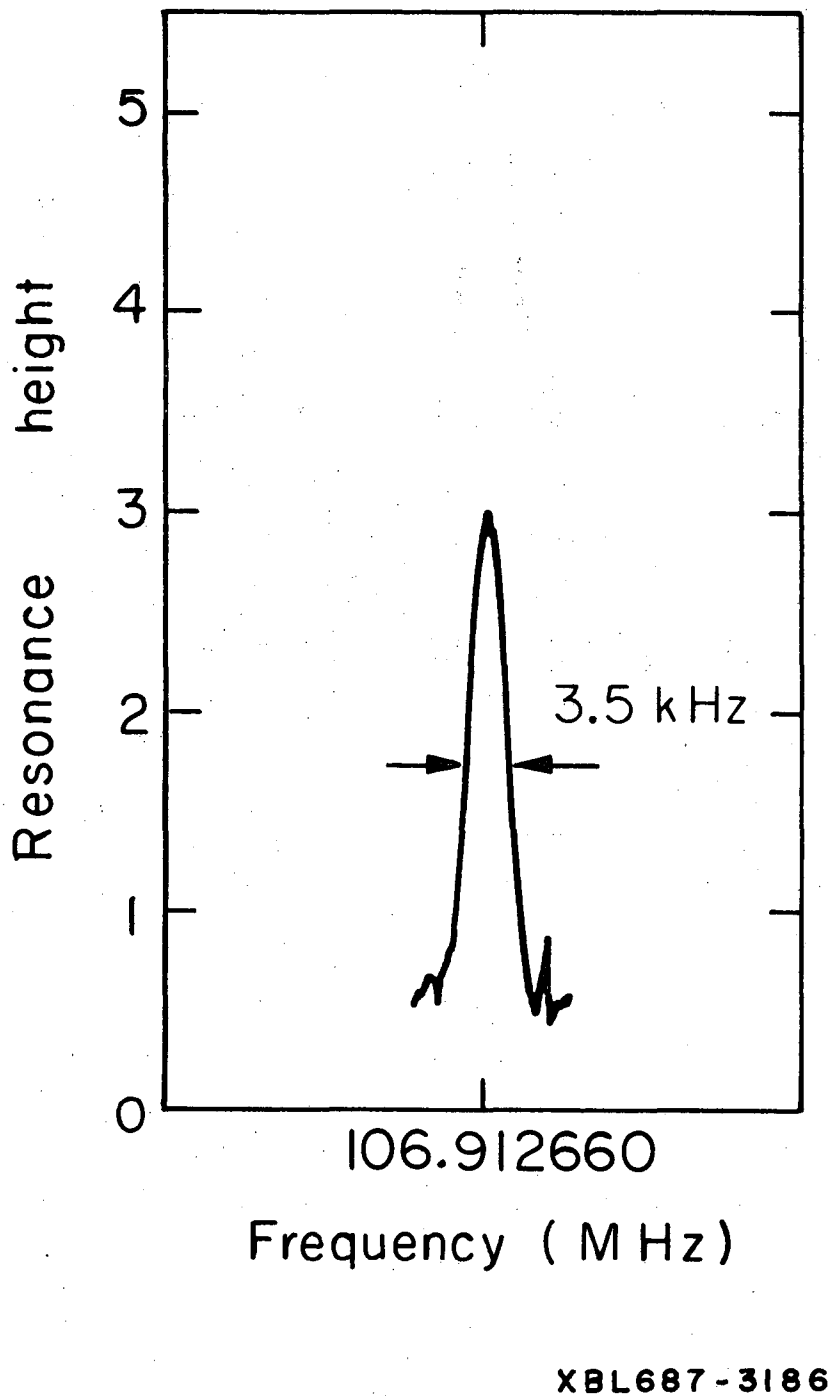

Fig. III-5. Chart-Recorder Tracings of $^{205}T\ell$ Triple Loop Resonance.

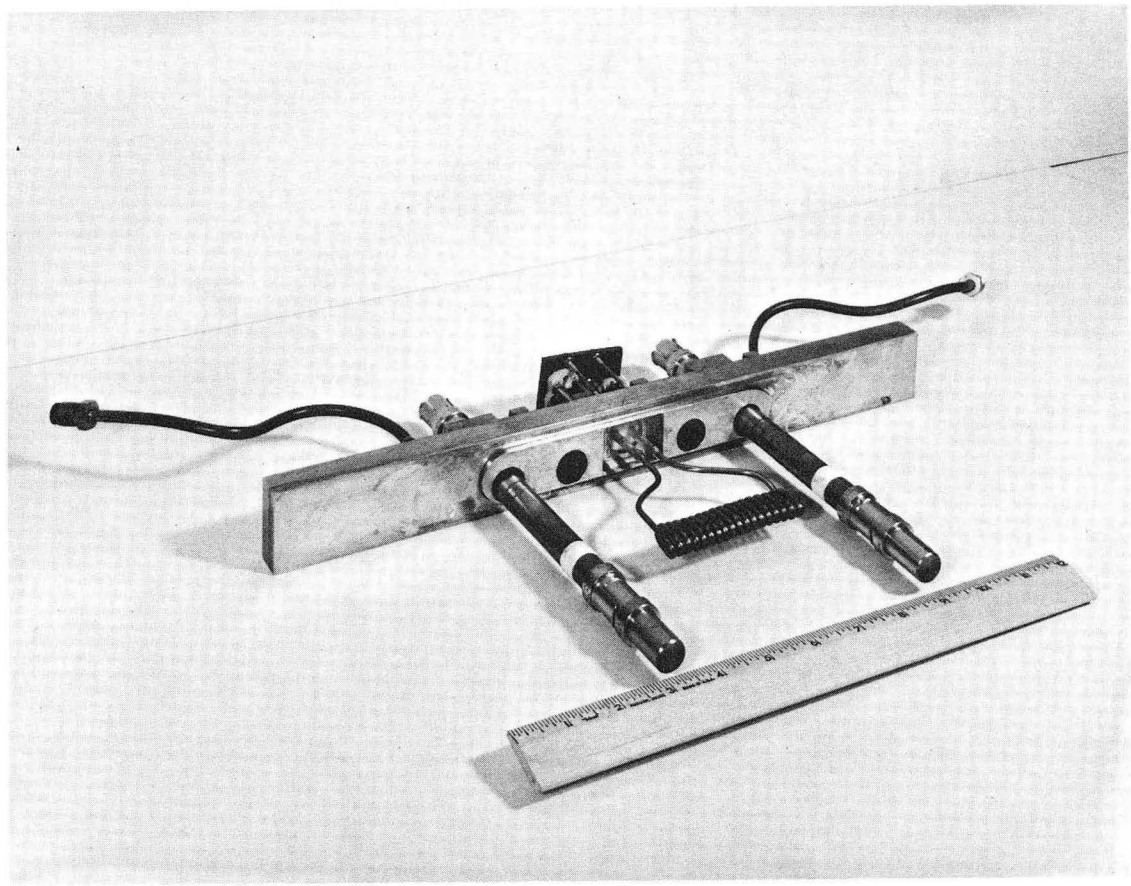

XBB 677-4013

Fig. III-6. Hairpin setup used to observe triple loop resonance in thallium.

hairpin and field orientation) was used as the observed frequency for that field. The error in this frequency was taken as 200 Hz. Figs. III-4 and III-5 show typical thallium resonances. The resonances for ^{203}Tl were one third as large as the ^{205}Tl resonances shown. The hairpin setup used to observe the triple loop signal is shown in Fig. III-6. From Fig. III-4 we see that the ratio, R, of the $^2P_{3/2}$ resonance height to the $^2P_{1/2}$ resonance height is about 0.5. If we knew the ratio of the detection efficiencies for the two states we could calculate the percentage of the beam that is excited up into the metastable ($^2P_{3/2}$). There are two possibilities. First, the $^2P_{3/2}$ atoms could de-excite on the wire first and then be detected like $^2P_{1/2}$ atoms. In this case the detection efficiencies should be equal for the two states. Therefore, the ratio of $^2P_{3/2}$ to $^2P_{1/2}$ atoms striking the wire is 8R/4. The factor 8/4 comes from the fact that for each state, the atoms are evenly distributed over the hyperfine levels with a corresponding loss in resonance height. Now, if α is the percentage of the beam that absorbs a 3775.72 Å photon then $2/3\alpha$ will end up in the $^2P_{3/2}$ state and $1/3\alpha + (1-\alpha)$ will be in the ground state, $^2P_{1/2}$, as the beam leaves the lamp. Equating 2R to $2/3\alpha \,/\, (1-2/3\alpha)$ and solving for α with R = 1/2, we get $\alpha = 0.75$. That is 75% of the beam is excited by 3775.72 Å radiation and 50% of the beam is in the $^2P_{3/2}$ state.

The other possibility is that the 1 e.v. difference in the ionization potentials of the $^2P_{3/2}$ and $^2P_{1/2}$ state will result in a much higher efficiency for the $^2P_{3/2}$ state. As is well known, the detector efficiency (ratio of ionized atoms to total number of atoms striking the wire) is given by[19] for $I > \phi$

$$d = e^{-(I-\phi)/kT}$$

where I is the ionization potential of the incoming atoms (6.1 V for $^2P_{1/2}$ and 5.1 volts for $^2P_{3/2}$), ϕ is the work function of the wire (about 6.0 volts for oxidized tungsten[19], and T is the temperature (about 1000°C). In e.v. units kT = 0.1, so for $^2P_{1/2}$, $d \cong e^{-(0.1)/0.1} \cong e^{-1} \cong 1/3$. For $^2P_{3/2}$ d is very near 1. So, the ratio of $P_{3/2}$ to $P_{1/2}$ atoms striking the wire is (8R/3)(1/3) -- solving for α again with R = 1/2 we get α equal to 9/15. Therefore, 38% of the beam atoms are excited by the 3775.72 Å radiation and 25% of the beam is in the $^2P_{3/2}$ state. It must be emphasized that this calculation is very approximate since the result is very sensitive to the work function on oxidized tungsten and this is not known very accurately. In any case, approximately 25% to 50% of the beam was in the $^2P_{3/2}$ state.

Unfortunately, there is not enough information to vary the five parameters, $g_{1/2}$, $g_{3/2}$, g_I, N, and a"' simultaneously. Instead four parameters were varied for various values of N which should be near 1. Fortunately, $g_{1/2}$, $g_{3/2}$, and g_I were essentially indendent of N in the range N = 1/2 to 1+1/2. Their values are for ^{205}Tl

$$g_{1/2} = -0.6656924(18)$$
$$g_{3/2} = -1.33410447(20)$$
$$g_I = +17.549(14) \times 10^{-4}$$

and for ^{203}Tl:

$$g_{1/2} = -0.6656920(18)$$
$$g_{3/2} = -1.3341044(11)$$
$$g_I = +17.375(14) \times 10^{-4} \quad .$$

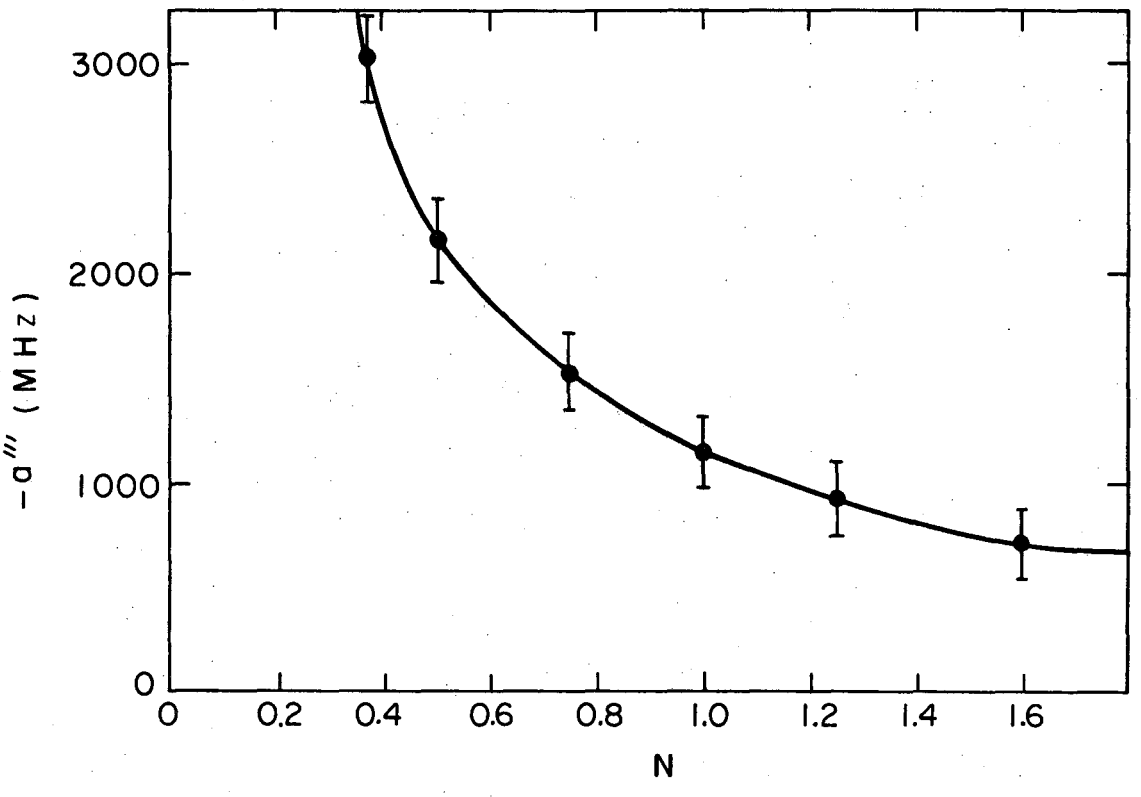

Fig. III-7. a'''versus N for $^{205}T\ell$.

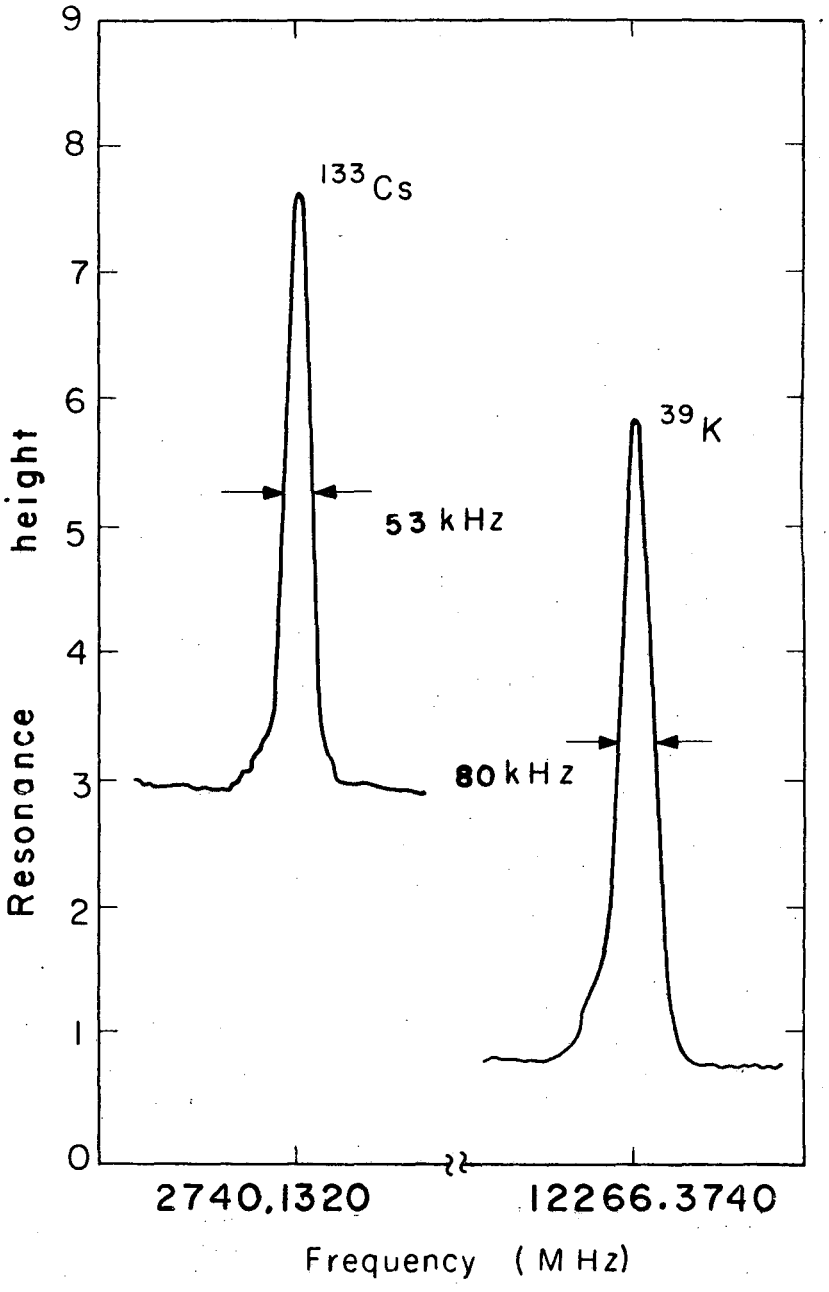

Fig. III-8. Chart-Recorder Tracings of the Standard Transition in ^{133}Cs and ^{39}K at 4500 G.

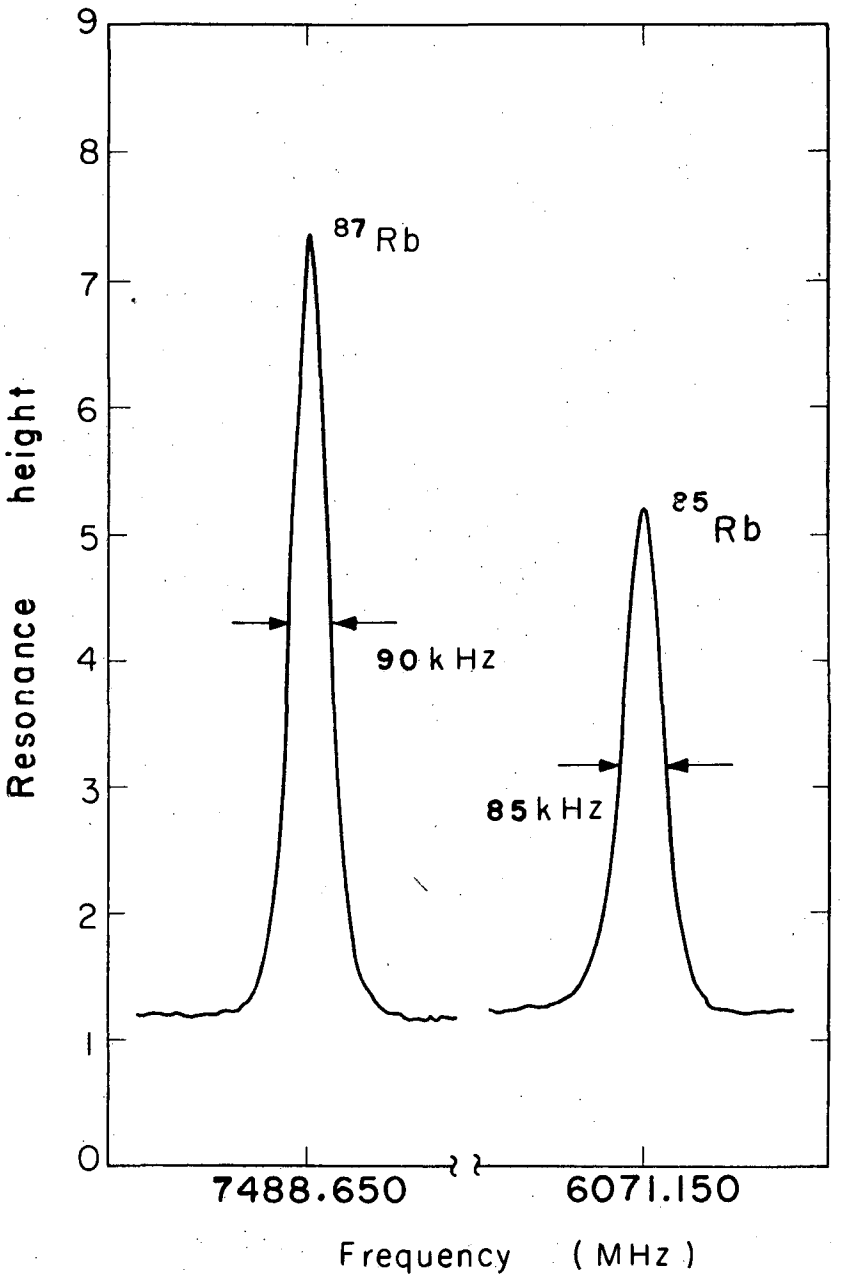

Fig. III-9. ^{85}Rb and ^{87}Rb Resonances at 3000 G.

Naturally these parameters did change somewhat, but well within 1/10 of the quoted errors (which are two standard deviations). a''', on the other hand, was strongly dependent on N. Fig. III-7 shows a''' as a function of N for $^{205}T\ell$. χ^2 for all these fits was 178 with 357 observations for $^{205}T\ell$ and 13.6 with 123 observations for $^{203}T\ell$. The curve for $^{203}T\ell$ is identical to Fig. III-5 except that the curve is shifted upward by 39 MHz. For N near 1 we have Na''' = -1.051(230) $\times 10^3$ MHz for $^{205}T\ell$ and Na''' = 1.090(240) $\times 10^3$ MHz for $^{203}T\ell$. Runs 151 and 152 were very sensitive to $\Delta\nu$ and very insensitive to the other parameters. $\Delta\nu$ for both $T\ell$ isotopes were fitted with runs 151 and 152 using the other five fitted parameters. The results for $^{205}T\ell$ are $\Delta\nu_{3/2}$ = 530.07655(10) MHz, and for $^{203}T\ell$ $\Delta\nu_{3/2}$ = 524.05994(10) MHz. For these two runs the Ramsey method of separated loops was used employing just the 4-1/2 in. box hairpin shown in Fig. II-4. The half width of the central maximum was 1.5 kHz. On the basis of only s→s' mode configuration interaction and the measured a-values we calculated the expected a''' values. The results were

$$a''' = -1930 \text{ MHz for } ^{205}T\ell \text{ and}$$
$$a''' = -1910 \text{ MHz for } ^{203}T\ell.$$

If N = 1 then our observed values are about 44(12)% lower than the theoretical values. The agreement is very poor.

The nuclear g-factors are -195(800) ppm and -431(780) ppm below the respective NMR values[31] for $^{205}T\ell$ and $^{203}T\ell$ respectively which were done on thallous aqueous solutions. The chemical shifts from the NMR values seem reasonable.

Table 2. Thallium g_J Comparison

		With Exchange	Without Exchange
$P_{3/2}$	Δg_{Rel}	$= +72.5 \times 10^{-6}$	$+20.0 \times 10^{-6}$
	Δg_{Lamb}	$= +27.3 \times 10^{-6}$	$+27.1 \times 10^{-6}$
	$\Delta g_{orbit\text{-}orbit}$	$= +76.9 \times 10^{-6}$	$+72.5 \times 10^{-6}$
	Δg_{total}	$= +176.7 \times 10^{-6}$	$+119.6 \times 10^{-6}$
	g_{theory}	$= -1.3339297$	-1.3339868
	$g_{observed}$	$= -1.3341045$	-1.3341045
	Discrepancy	$= +0.0001748$	$+0.0001177$
		$= +131$ ppm	$+88$ ppm
$P_{1/2}$	Δg_{Rel}	$= +72.5 \times 10^{-6}$	$+20.0 \times 10^{-6}$
	Δg_{Lamb}	$= +2.5 \times 10^{-6}$	$+4.7 \times 10^{-6}$
	$\Delta g_{orbit\text{-}orbit}$	$= +153.7 \times 10^{-6}$	$+145.1 \times 10^{-6}$
	Δg_{total}	$= +228.7 \times 10^{-6}$	$+169.8 \times 10^{-6}$
	g_{theory}	$= -0.6656649$	-0.6657238
	$g_{observed}$	$= -0.6656922$	-0.6656922
	Discrepancy	$= -0.0000273$	$+0.000032$
		$= -41$ ppm	$+48$ ppm

Now for the electronic g-factors. As expected, there is no isotope effect. Table 2 shows the correction factors for two wave functions. Both were derived from Herman's HFSSC atomic wave function program[32] one with the free electron exchange and the other with no exchange approximation at all (i.e. RUEXCH(I) was set to zero in the program). The two results seem to bracket the observed values for $^2P_{1/2}$ leading one to suspect that better wave functions including exchange effects will predict $g_{1/2}$ rather well. For the $^2P_{3/2}$ state, however, the situation appears quite different. It appears that an unknown effect has decreased $g_{3/2}$ by some one part in 10^4. As has been mentioned above, configuration interaction in 4^{th} order probably decreases $g_{3/2}$ slightly. This may be due to this effect. It seems reasonable that the small a''' value observed is related to this also. Of course, N too may be significantly perturbed. The ground state doublet wave functions with respect to configuration interaction are so poorly known that no calculations are possible at this time. In any case, it is clear that much theoretical work remains to be done for an understanding of atomic structure to the accuracy of present experimental results.

IV. CONCLUSIONS

The results of the analysis of the Gallium data agree reasonably well with the current theory of hyperfine structure of the subgroup III elements. The off-diagonal dipole and quadrupole elements are 11% smaller and 4.8% larger than their corresponding theoretical values. These discrepancies seem reasonable in the light of the many approximations used in calculating the theoretical values. The same conclusions hold for the electronic g factors where the agreement between theory and experiment is as good as one could expect which is about one part in 10^5. Although there is no theoretical value for the uncorrected free atom value of g_I, the experimental value, 778 ppm below the NMR value, seems reasonable in the light of other measured diamagnetic shifts, notably those in Thallic ion solutions.

The Thallium results, on the other hand, indicate some rather large discrepancies. The value of the off-diagonal dipole element can not be inferred until N is known. If N is one then the observed value of a''' is 44% below the theoretical value which would indicate that at Z equal to 81 the $s \rightarrow s'$ mode of configuration interaction is not sufficient by itself to account for most of the observed value. $g_{1/2}$ and g_I agree very well with what one would expect whereas the one part in 10^4 discrepancy in $g_{3/2}$ between theory and experiment would indicate an additional configuration interaction effect discussed by Phillips[16] that is not seen in $g_{1/2}$.

ACKNOWLEDGMENTS

It is a pleasure to thank Professor Howard A. Shugart for his boundless enthusiasm for all aspects of this work. Special thanks must also go to Professor Vernon J. Ehlers and Doctor Paul A. Vanden Bout whose assistance during many of the runs was greatly appreciated. I would also like to thank Mr. Dana Vance for his assistance and willingness to work late into the night and during many weekends. Finally, I would like to thank the entire Berkeley Atomic Beam Group for making this work possible.

This research was supported by the United States Atomic Energy Commission.

APPENDICES

A. ^{69}Ga ^{2}P Doublet Parameters

Parameter	Previous Value	Reference	This Work
$a_{3/2}$	190.79428(15)* MHz	(33)	190.79436(11) MHz
b	62.52247(30)* MHz	(33)	62.52319(11) MHz
c	.000094(6)* MHz	(44)	0.000090(6) MHz
$\Delta\nu_{1/2}$	2677.9875(10) MHz	(24)	2677.98716(20) MHz
δ	826.24 cm^{-1}	(2)	Not Measured
η	1.04	(14)	1.0886(290)
a'''	----	----	-107.76(98) MHz
N	1	----	Not Measured
$g_{1/2}$	-0.66582(40)	(28)	-0.66579172(28)
$g_{3/2}$	-1.333920(11)	(28)	-1.33405731(60)
$g_{I_{uncorr}}$**	7.300982×10^{-4}	(26)	$7.29530(33) \times 10^{-4}$

* Corrected for off-diagonal elements and $s \rightarrow s'$ configuration interaction. As pointed out by Schwartz[44] (who corrected the value of c) there was an error in the analysis used by Holloway[33]. Consequently, the values of $a_{3/2}$ and b quoted by Holloway are still slightly in error.

** All g_I's are uncorrected for diamagnetism.

B. $^{205}Tl\ ^{2}P$ Doublet Parameters

Parameter	Previous Value	Reference	This Work
$\Delta\nu_{3/2}$	530.0766(2) MHz	(34)	530.07655(10) MHz
$\Delta\nu_{1/2}$	21310.8339459(2) MHz	(23)	Not Measured
N	-----	----	
a'''	-----	----	Na''' = -1.051(230) GHz
δ	7992.7 cm^{-1}	(1)	Not Measured
$g_{1/2}$	-----	----	-0.6656924(18)
$g_{3/2}$	-----	----	-1.33410447(20)
$g_{I_{uncorr}}$	17.55242×10^{-4}	(31)	$17.549(14) \times 10^{-4}$

C. $^{203}Tl\ ^{2}P$ Doublet Parameters

Parameter	Previous Value	Reference	This Work
$\Delta\nu_{3/2}$	524.0601(2) MHz	(34)	524.05994(10) MHz
$\Delta\nu_{1/2}$	21105.447(5) MHz	(24)	Not Measured
N	-----	----	$Na''' = -1.090(240)$ GHz
a'''	-----	----	
δ	7992.7 cm^{-1}	(1)	Not Measured
$g_{1/2}$	-----	----	-0.6656920(18)
$g_{3/2}$	-----	----	-1.3341044(11)
$g_{I_{uncorr}}$	17.38250×10^{-4}	(31)	$17.375(14) \times 10^{-4}$

D. Values of Physical Constants Assumed

General

$$\mu_o/h = 1.399613(14)^{35}$$

$$M/m = 1836.10(12)^{36}$$

^{39}K

$$I = 3/2$$

$$g_J = -2.0022954(22)^{37}$$

$$\mu_{I_{uncorr}} = +0.39088\ nm^{38}$$

$$\Delta\nu = 461.719723(30)\ MHz^{39}$$

^{85}Rb

$$I = 5/2$$

$$g_J = -2.0023319(20)^{37}$$

$$\mu_{I_{uncorr}} = +1.34817\ nm^{38}$$

$$\Delta\nu = 3035.732439(5)\ MHz^{40}$$

^{87}Rb

$$I = 3/2$$

$$g_J = -2.0023319(20)^{37}$$

$$\mu_{I_{uncorr}} = +2.7413\ nm^{38}$$

$$\Delta\nu = 6834.682614(3)\ MHz^{40}$$

^{133}Cs

$$I = 7/2$$

$$g_J = -2.0025417(24)^{37}$$

$$\mu_{I_{uncorr}} = +2.5641\ nm^{38}$$

$$\Delta\nu = 9192.631770\ MHz^{41}$$

APPENDIX E. ^{69}GA RUN SUMMARY

RUN	ISOTOPE	CALIBRATION FREQUENCY (MHZ)	FREQUENCY ERROR (MHZ)	FIELD (GAUSS)	FIELD ERROR (GAUSS)	TRANSITION F 1	TRANSITION M 1	TRANSITION F 2	TRANSITION M 2	EXPERIMENTAL FREQUENCY (MHZ)	FREQUENCY ERROR (MHZ)	RESIDUAL (MHZ)	WEIGHT FACTOR
116A1	RB85	3584.1937	.020	2069.9808	.0077	3	-1	3	-2	3583.088800	.0200	-.02083	1.65E+03
116A2	RB85	3584.2031	.020	2069.9844	.0077	3	-1	3	-2	3583.091900	.0200	-.02446	1.65E+03
116A3	RB85	3584.2309	.020	2069.9951	.0077	3	-1	3	-2	3583.115700	.0200	-.02056	1.65E+03
116A4	RB85	3584.2483	.020	2070.0018	.0077	3	-1	3	-2	3583.127600	.0200	-.02112	1.65E+03
116A5	RB85	3584.2461	.020	2070.0009	.0077	3	-1	3	-2	3583.132600	.0200	-.01455	1.65E+03
116A6	RB85	3584.2352	.020	2069.9967	.0077	3	-1	3	-2	3583.128700	.0200	-.01064	1.65E+03
116A7	RB85	3584.2388	.020	2069.9981	.0077	3	-1	3	-2	3583.126000	.0200	-.01592	1.65E+03
116A8	RB85	3584.2413	.020	2069.9991	.0077	3	-1	3	-2	3583.124300	.0200	-.01941	1.65E+03
116A0	RB85	3584.2360	.020	2069.9970	.0077	3	-1	3	-2	3583.121000	.0200	-.01892	1.65E+03
116A1	RB85	3584.2368	.020	2069.9973	.0077	3	-1	3	-2	3583.115400	.0200	-.02509	1.65E+03
116A2	RB85	3584.2101	.020	2069.9871	.0077	3	-1	3	-2	3583.107800	.0200	-.01357	1.65E+03
116A3	RB85	3584.1882	.020	2069.9787	.0077	3	-1	3	-2	3583.093200	.0200	-.01249	1.65E+03
116A4	RB85	3584.1870	.020	2069.9782	.0077	3	-1	3	-2	3583.085200	.0200	-.01963	1.65E+03
116A5	RB85	3584.1797	.020	2069.9754	.0077	3	-1	3	-2	3583.084200	.0200	-.01540	1.65E+03
116A6	RB85	3584.1658	.020	2069.9701	.0077	3	-1	3	-2	3583.076100	.0200	-.01359	1.65E+03
116A7	RB85	3584.1389	.020	2069.9597	.0077	3	-1	3	-2	3583.044900	.0200	-.02549	1.65E+03
119A1	RB87	9652.5727	.008	4998.4596	.0030	3	-1	3	-2	9048.029600	.0080	.00140	1.04E+04
119A1	RB87	9652.5714	.008	4998.4591	.0030	3	-1	3	-2	9048.032500	.0080	.00523	1.04E+04
119A1	RB87	9652.5701	.008	4998.4586	.0030	3	-1	3	-2	9048.030400	.0080	.00409	1.04E+04
119A1	RB87	9652.5675	.008	4998.4576	.0030	3	-1	3	-2	9048.028600	.0080	.00410	1.04E+04
119A1	RB87	9652.5636	.008	4998.4562	.0030	3	-1	3	-2	9048.027900	.0080	.00618	1.04E+04
119A1	RB87	9652.5636	.008	4998.4562	.0030	3	-1	3	-2	9048.026900	.0080	.00508	1.04E+04
119A1	RB87	9652.5649	.008	4998.4566	.0030	3	-1	3	-2	9048.027900	.0080	.00525	1.04E+04
119A1	RB87	9652.5636	.008	4998.4562	.0030	3	-1	3	-2	9048.025400	.0080	.00368	1.04E+04
119A2	RB87	9652.5610	.008	4998.4552	.0030	3	-1	3	-2	9048.024700	.0080	.00483	1.04E+04
119A2	RB87	9652.5610	.008	4998.4552	.0030	3	-1	3	-2	9048.024100	.0080	.00423	1.04E+04
119A2	RB87	9652.5623	.008	4998.4557	.0030	3	-1	3	-2	9048.024200	.0080	.00340	1.04E+04
119A2	RB87	9652.5597	.008	4998.4547	.0030	3	-1	3	-2	9048.023300	.0080	.00435	1.04E+04
119A2	RB87	9652.5584	.008	4998.4542	.0030	3	-1	3	-2	9048.022700	.0080	.00468	1.04E+04
119A2	RB87	9652.5584	.008	4998.4542	.0030	3	-1	3	-2	9048.021200	.0080	.00318	1.04E+04
119A2	RB87	9652.5571	.008	4998.4537	.0030	3	-1	3	-2	9048.021500	.0080	.00440	1.04E+04
119A2	RB87	9652.5636	.008	4998.4562	.0030	3	-1	3	-2	9048.025500	.0080	.00378	1.04E+04
117A1	RB85	6071.1409	.016	2999.5994	.0059	3	-1	3	-2	5317.060100	.0160	-.01466	2.66E+03
117A2	RB85	6071.1394	.016	2999.5988	.0059	3	-1	3	-2	5317.063100	.0160	-.01063	2.66E+03
117A3	RB85	6071.1405	.016	2999.5993	.0059	3	-1	3	-2	5317.060700	.0160	-.01378	2.66E+03
117A4	RB85	6071.1415	.016	2999.5996	.0059	3	-1	3	-2	5317.062200	.0160	-.01297	2.66E+03
117A5	RB85	6071.1408	.016	2999.5994	.0059	3	-1	3	-2	5317.061400	.0160	-.01329	2.66E+03
117A6	RB85	6071.1385	.016	2999.5985	.0059	3	-1	3	-2	5317.060700	.0160	-.01241	2.66E+03
117A7	RB85	6071.1389	.016	2999.5987	.0059	3	-1	3	-2	5317.061100	.0160	-.01224	2.66E+03
117A8	RB85	6071.1420	.016	2999.5998	.0059	3	-1	3	-2	5317.062300	.0160	-.01321	2.66E+03
117A9	RB85	6071.1384	.016	2999.5985	.0059	3	-1	3	-2	5317.060300	.0160	-.01274	2.66E+03
117A0	RB85	6071.1384	.016	2999.5985	.0059	3	-1	3	-2	5317.058900	.0160	-.01414	2.66E+03
117A1	RB85	6071.1388	.016	2999.5986	.0059	3	-1	3	-2	5317.059400	.0160	-.01392	2.66E+03
117A2	RB85	6071.1397	.016	2999.5990	.0059	3	-1	3	-2	5317.059200	.0160	-.01473	2.66E+03
117A3	RB85	6071.1420	.016	2999.5998	.0059	3	-1	3	-2	5317.059500	.0160	-.01601	2.66E+03
117A4	RB85	6071.1431	.016	2999.6002	.0059	3	-1	3	-2	5317.061700	.0160	-.01457	2.66E+03
117A5	RB85	6071.1416	.016	2999.5997	.0059	3	-1	3	-2	5317.061900	.0160	-.01334	2.66E+03
117A6	RB85	6071.1417	.016	2999.5997	.0059	3	-1	3	-2	5317.059800	.0160	-.01551	2.66E+03
118A1	RB87	7482.8842	.020	4159.3704	.0079	3	-1	3	-2	7481.643400	.0200	-.01187	1.62E+03
118A2	RB87	7482.8837	.020	4159.3702	.0079	3	-1	3	-2	7481.639000	.0200	-.01590	1.62E+03
118A3	RB87	7482.8821	.020	4159.3695	.0079	3	-1	3	-2	7481.640900	.0200	-.01283	1.62E+03
118A4	RB87	7482.8804	.020	4159.3689	.0079	3	-1	3	-2	7481.641900	.0200	-.01058	1.62E+03
118A5	RB87	7482.8814	.020	4159.3693	.0079	3	-1	3	-2	7481.638300	.0200	-.01491	1.62E+03
118A6	RB87	7482.8816	.020	4159.3693	.0079	3	-1	3	-2	7481.636500	.0200	-.01686	1.62E+03
118A8	RB87	7482.8882	.020	4159.3719	.0079	3	-1	3	-2	7481.641000	.0200	-.01721	1.62E+03
118A9	RB87	7482.8865	.020	4159.3713	.0079	3	-1	3	-2	7481.636800	.0200	-.02016	1.62E+03
118A0	RB87	7482.8840	.020	4159.3703	.0079	3	-1	3	-2	7481.641700	.0200	-.01342	1.62E+03
118A1	RB87	7482.8736	.020	4159.3662	.0079	3	-1	3	-2	7481.630400	.0200	-.01708	1.62E+03
118A2	RB87	7482.8731	.020	4159.3660	.0079	3	-1	3	-2	7481.629300	.0200	-.01781	1.62E+03
118A3	RB87	7482.8727	.020	4159.3658	.0079	3	-1	3	-2	7481.633800	.0200	-.01302	1.62E+03
118A4	RB87	7482.8677	.020	4159.3639	.0079	3	-1	3	-2	7481.632400	.0200	-.01074	1.62E+03
118A5	RB87	7482.8500	.020	4159.3569	.0079	3	-1	3	-2	7481.623100	.0200	-.00703	1.62E+03
118A6	RB87	7482.8312	.020	4159.3495	.0079	3	-1	3	-2	7481.597400	.0200	-.01891	1.62E+03
118B1	RB87	7488.6513	.016	4161.6413	.0063	3	-1	3	-2	7485.899800	.0150	.00555	2.75E+03
118B2	RB87	7488.6507	.016	4161.6410	.0063	3	-1	3	-2	7485.896700	.0150	.00289	2.75E+03
118B3	RB87	7488.6496	.016	4161.6406	.0063	3	-1	3	-2	7485.898000	.0150	.00500	2.75E+03
118B4	RB87	7488.6494	.016	4161.6405	.0063	3	-1	3	-2	7485.897900	.0150	.00504	2.75E+03
118B5	RB87	7488.6505	.016	4161.6409	.0063	3	-1	3	-2	7485.896000	.0150	.00233	2.75E+03
118B6	RB87	7488.6517	.016	4161.6414	.0063	3	-1	3	-2	7485.898100	.0150	.00355	2.75E+03
118B7	RB87	7488.6522	.016	4161.6416	.0063	3	-1	3	-2	7485.898800	.0150	.00388	2.75E+03
118B8	RB87	7488.6514	.016	4161.6413	.0063	3	-1	3	-2	7485.898700	.0150	.00437	2.75E+03
118B9	RB87	7488.6518	.016	4161.6415	.0063	3	-1	3	-2	7485.899200	.0150	.00458	2.75E+03
118B0	RB87	7488.6524	.016	4161.6417	.0063	3	-1	3	-2	7485.899200	.0150	.00414	2.75E+03
118B1	RB87	7488.6504	.016	4161.6409	.0063	3	-1	3	-2	7485.899700	.0150	.00611	2.75E+03
118B2	RB87	7488.6510	.016	4161.6411	.0063	3	-1	3	-2	7485.902100	.0150	.00807	2.75E+03
118B3	RB87	7488.6526	.016	4161.6418	.0063	3	-1	3	-2	7485.898100	.0150	.00289	2.75E+03
118B4	RB87	7488.6512	.016	4161.6412	.0063	3	-1	3	-2	7485.897200	.0150	.00302	2.75E+03
118B5	RB87	7488.6500	.016	4161.6408	.0063	3	-1	3	-2	7485.897300	.0150	.00400	2.75E+03
118B6	RB87	7488.6506	.016	4161.6410	.0063	3	-1	3	-2	7485.898500	.0150	.00476	2.75E+03
116B1	RB85	3584.2216	.020	2069.9915	.0077	2	-1	2	-2	821.200300	.0120	-.00820	6.10E+03
116B2	RB85	3584.2375	.020	2069.9976	.0077	2	-1	2	-2	821.203200	.0120	-.00885	6.10E+03
116B3	RB85	3584.2876	.020	2070.0169	.0077	2	-1	2	-2	821.212600	.0120	-.01063	6.10E+03
116B5	RB85	3584.2924	.020	2070.0187	.0077	2	-1	2	-2	821.217400	.0120	-.00690	6.10E+03
116B6	RB85	3584.2869	.020	2070.0166	.0077	2	-1	2	-2	821.216700	.0120	-.00637	6.10E+03

XBL 687-1277

APPENDIX E. ^{69}GA RUN SUMMARY

RUN	ISOTOPE	CALIBRATION FREQUENCY (MHZ)	FREQUENCY ERROR (MHZ)	FIELD (GAUSS)	FIELD ERROR (GAUSS)	TRANSITION F 1	TRANSITION M 1	TRANSITION F 2	TRANSITION M 2	EXPERIMENTAL FREQUENCY (MHZ)	FREQUENCY ERROR (MHZ)	RESIDUAL (MHZ)	WEIGHT FACTOR
11687	RB85	3584.2744	.020	2070.0118	.0077	2	-1	2	-2	821.212400	.0120	-.00788	6.10E+03
11688	RB85	3584.2766	.020	2070.0126	.0077	2	-1	2	-2	821.215600	.0120	-.00517	6.10E+03
11689	RB85	3584.2796	.020	2070.0138	.0077	2	-1	2	-2	821.215500	.0120	-.00594	6.10E+03
11680	RB85	3584.2723	.020	2070.0110	.0077	2	-1	2	-2	821.216800	.0120	-.00301	6.10E+03
11681	RB85	3584.2724	.020	2070.0110	.0077	2	-1	2	-2	821.213600	.0120	-.00623	6.10E+03
11682	RB85	3584.2718	.020	2070.0108	.0077	2	-1	2	-2	821.211600	.0120	-.00810	6.10E+03
11683	RB85	3584.2684	.020	2070.0095	.0077	2	-1	2	-2	821.211700	.0120	-.00724	6.10E+03
11684	RB85	3584.2634	.020	2070.0076	.0077	2	-1	2	-2	821.211300	.0120	-.00653	6.10E+03
11685	RB85	3584.2580	.020	2070.0055	.0077	2	-1	2	-2	821.212300	.0120	-.00432	6.10E+03
11686	RB85	3584.2576	.020	2070.0053	.0077	2	-1	2	-2	821.217800	.0120	.00127	6.10E+03
11687	RB85	3584.2557	.020	2070.0046	.0077	2	-1	2	-2	821.208100	.0120	-.00801	6.10E+03
11688	RB85	3584.2527	.020	2070.0034	.0077	2	-1	2	-2	821.210300	.0120	-.00514	6.10E+03
11689	RB85	3584.2530	.020	2070.0036	.0077	2	-1	2	-2	821.209100	.0120	-.00641	6.10E+03
11680	RB85	3584.2532	.020	2070.0036	.0077	2	-1	2	-2	821.212200	.0120	-.00335	6.10E+03
11781	RB85	6071.1471	.016	2999.6017	.0059	2	-1	2	-2	1427.112900	.0100	-.00810	8.50E+03
11782	RB85	6071.1436	.016	2999.6004	.0059	2	-1	2	-2	1427.111200	.0100	-.00888	8.50E+03
11783	RB85	6071.1428	.016	2999.6001	.0059	2	-1	2	-2	1427.113800	.0100	-.00607	8.50E+03
11784	RB85	6071.1460	.016	2999.6013	.0059	2	-1	2	-2	1427.112600	.0100	-.00811	8.50E+03
11785	RB85	6071.1486	.016	2999.6022	.0059	2	-1	2	-2	1427.113400	.0100	-.00799	8.50E+03
11786	RB85	6071.1443	.016	2999.6006	.0059	2	-1	2	-2	1427.113400	.0100	-.00687	8.50E+03
11787	RB85	6071.1444	.016	2999.6007	.0059	2	-1	2	-2	1427.114600	.0100	-.00569	8.50E+03
11788	RB85	6071.1502	.016	2999.6028	.0059	2	-1	2	-2	1427.114500	.0100	-.00731	8.50E+03
11789	RB85	6071.1494	.016	2999.6025	.0059	2	-1	2	-2	1427.114400	.0100	-.00720	8.50E+03
11780	RB85	6071.1480	.016	2999.6020	.0059	2	-1	2	-2	1427.113800	.0100	-.00744	8.50E+03
11781	RB85	6071.1584	.016	2999.6058	.0059	2	-1	2	-2	1427.116400	.0100	-.00756	8.50E+03
11782	RB85	6071.1678	.016	2999.6093	.0059	2	-1	2	-2	1427.120400	.0100	-.00603	8.50E+03
11783	RB85	6071.1644	.016	2999.6080	.0059	2	-1	2	-2	1427.119400	.0100	-.00614	8.50E+03
11784	RB85	6071.1598	.016	2999.6063	.0059	2	-1	2	-2	1427.117500	.0100	-.00683	8.50E+03
11785	RB85	6071.1588	.016	2999.6060	.0059	2	-1	2	-2	1427.118500	.0100	-.00557	8.50E+03
11786	RB85	6071.1590	.016	2999.6060	.0059	2	-1	2	-2	1427.118000	.0100	-.00612	8.50E+03
11787	RB85	6071.1592	.016	2999.6061	.0059	2	-1	2	-2	1427.117000	.0100	-.00717	8.50E+03
11788	RB85	6071.1621	.016	2999.6072	.0059	2	-1	2	-2	1427.118100	.0100	-.00683	8.50E+03
11789	RB85	6071.1655	.016	2999.6084	.0059	2	-1	2	-2	1427.121100	.0100	-.00473	8.50E+03
11780	RB85	6071.1652	.016	2999.6083	.0059	2	-1	2	-2	1427.118500	.0100	-.00725	8.50E+03
118C1	RB87	7488.6485	.019	4161.6402	.0075	2	-1	2	-2	2318.879500	.0090	.00150	8.49E+03
118C2	RB87	7488.6512	.019	4161.6412	.0075	2	-1	2	-2	2318.879100	.0090	.00024	8.49E+03
118C3	RB87	7488.6522	.019	4161.6416	.0075	2	-1	2	-2	2318.880000	.0090	.00082	8.49E+03
118C4	RB87	7488.6516	.019	4161.6414	.0075	2	-1	2	-2	2318.879800	.0090	.00081	8.49E+03
118C5	RB87	7488.6504	.019	4161.6409	.0075	2	-1	2	-2	2318.880200	.0090	.00160	8.49E+03
118C6	RB87	7488.6487	.019	4161.6402	.0075	2	-1	2	-2	2318.879500	.0090	.00144	8.49E+03
118C7	RB87	7488.6490	.019	4161.6404	.0075	2	-1	2	-2	2318.879500	.0090	.00134	8.49E+03
118C8	RB87	7488.6490	.019	4161.6404	.0075	2	-1	2	-2	2318.879300	.0090	.00114	8.49E+03
118C9	RB87	7488.6469	.019	4161.6395	.0075	2	-1	2	-2	2318.878700	.0090	.00121	8.49E+03
118C0	RB87	7488.6460	.019	4161.6392	.0075	2	-1	2	-2	2318.879000	.0090	.00180	8.49E+03
118C1	RB87	7488.6462	.019	4161.6393	.0075	2	-1	2	-2	2318.878500	.0090	.00124	8.49E+03
118C2	RB87	7488.6446	.019	4161.6386	.0075	2	-1	2	-2	2318.878800	.0090	.00205	8.49E+03
118C3	RB87	7488.6450	.019	4161.6388	.0075	2	-1	2	-2	2318.879000	.0090	.00212	8.49E+03
118C4	RB87	7488.6442	.019	4161.6385	.0075	2	-1	2	-2	2318.878400	.0090	.00177	8.49E+03
118C5	RB87	7488.6414	.019	4161.6374	.0075	2	-1	2	-2	2318.877900	.0090	.00217	8.49E+03
118C6	RB87	7488.6428	.019	4161.6379	.0075	2	-1	2	-2	2318.878800	.0090	.00262	8.49E+03
13101	RB87	7487.1762	.010	4161.0604	.0039	2	-1	2	-2	2318.403600	.0050	-.00479	2.84E+04
13102	RB87	7487.1762	.010	4161.0604	.0039	2	-1	2	-2	2318.403900	.0050	-.00449	2.84E+04
13103	RB87	7487.1786	.010	4161.0614	.0039	2	-1	2	-2	2318.405300	.0050	-.00386	2.84E+04
13104	RB87	7487.1794	.010	4161.0617	.0039	2	-1	2	-2	2318.404900	.0050	-.00452	2.84E+04
13105	RB87	7487.1786	.010	4161.0614	.0039	2	-1	2	-2	2318.406000	.0050	-.00316	2.84E+04
13106	RB87	7487.1781	.010	4161.0612	.0039	2	-1	2	-2	2318.404500	.0050	-.00450	2.84E+04
13107	RB87	7487.1779	.010	4161.0611	.0039	2	-1	2	-2	2318.405300	.0050	-.00364	2.84E+04
13108	RB87	7487.1769	.010	4161.0607	.0039	2	-1	2	-2	2318.403500	.0050	-.00512	2.84E+04
13109	RB87	7487.1761	.010	4161.0604	.0039	2	-1	2	-2	2318.403500	.0050	-.00486	2.84E+04
13111	RB87	7486.6007	.010	4160.8338	.0039	2	-1	2	-2	2318.222700	.0050	-.00213	2.84E+04
13112	RB87	7486.6030	.010	4160.8347	.0039	2	-1	2	-2	2318.220000	.0050	-.00557	2.84E+04
13113	RB87	7486.6045	.010	4160.8353	.0039	2	-1	2	-2	2318.221000	.0050	-.00505	2.84E+04
13114	RB87	7486.6057	.010	4160.8358	.0039	2	-1	2	-2	2318.221200	.0050	-.00523	2.84E+04
13115	RB87	7487.4592	.010	4161.1719	.0039	2	-1	2	-2	2318.493700	.0050	-.00496	2.84E+04
13116	RB87	7487.4580	.010	4161.1714	.0039	2	-1	2	-2	2318.493400	.0050	-.00488	2.84E+04
13117	RB87	7487.4577	.010	4161.1713	.0039	2	-1	2	-2	2318.493400	.0050	-.00478	2.84E+04
13118	RB87	7487.4568	.010	4161.1709	.0039	2	-1	2	-2	2318.492900	.0050	-.00499	2.84E+04
13119	RB87	7487.4563	.010	4161.1707	.0039	2	-1	2	-2	2318.492300	.0050	-.00543	2.84E+04
13120	RB87	7487.4564	.010	4161.1708	.0039	2	-1	2	-2	2318.492500	.0050	-.00527	2.84E+04
13121	RB87	7483.6772	.008	4159.6826	.0032	2	-1	2	-2	2317.303600	.0070	.01122	1.80E+04
13122	RB87	7483.6754	.008	4159.6819	.0032	2	-1	2	-2	2317.300300	.0070	.00850	1.80E+04
13123	RB87	7483.6738	.008	4159.6813	.0032	2	-1	2	-2	2317.300300	.0070	.00901	1.80E+04
13124	RB87	7483.6730	.008	4159.6810	.0032	2	-1	2	-2	2317.299300	.0070	.00826	1.80E+04
13125	RB87	7483.6703	.008	4159.6799	.0032	2	-1	2	-2	2317.298100	.0070	.00792	1.80E+04
13126	RB87	7483.6684	.008	4159.6792	.0032	2	-1	2	-2	2317.296300	.0070	.00673	1.80E+04
13127	RB87	7483.6694	.008	4159.6796	.0032	2	-1	2	-2	2317.297900	.0070	.00801	1.80E+04
13128	RB87	7483.6679	.008	4159.6790	.0032	2	-1	2	-2	2317.296900	.0070	.00749	1.80E+04
13129	RB87	7483.6658	.008	4159.6781	.0032	2	-1	2	-2	2317.297300	.0070	.00856	1.80E+04
13130	RB87	7483.6662	.008	4159.6783	.0032	2	-1	2	-2	2317.296900	.0070	.00803	1.80E+04
13131	RB87	7489.8800	.008	4162.1251	.0031	2	-1	2	-2	2319.275100	.0070	.00430	1.80E+04
13132	RB87	7489.8867	.008	4162.1277	.0031	2	-1	2	-2	2319.280600	.0070	.00766	1.80E+04
13133	RB87	7489.8937	.008	4162.1304	.0031	2	-1	2	-2	2319.278800	.0070	.00363	1.80E+04
13134	RB87	7489.8972	.008	4162.1318	.0031	2	-1	2	-2	2319.280500	.0070	.00421	1.80E+04
13135	RB87	7489.8959	.008	4162.1313	.0031	2	-1	2	-2	2319.279900	.0070	.00403	1.80E+04
13136	RB87	7489.8915	.008	4162.1296	.0031	2	-1	2	-2	2319.279600	.0070	.00513	1.80E+04

XBL 687-1276

APPENDIX E. ^{69}GA RUN SUMMARY

RUN	ISOTOPE	CALIBRATION FREQUENCY (MHZ)	FREQUENCY ERROR (MHZ)	FIELD (GAUSS)	FIELD ERROR (GAUSS)	TRANSITION F 1	TRANSITION M 1	TRANSITION F 2	TRANSITION M 2	EXPERIMENTAL FREQUENCY (MHZ)	FREQUENCY ERROR (MHZ)	RESIDUAL (MHZ)	WEIGHT FACTOR
13137	RB87	7489.8912	.008	4162.1295	.0031	2	-1	2	-2	2319.279900	.0070	.00553	1.80E+04
13138	RB87	7489.8925	.008	4162.1300	.0031	2	-1	2	-2	2319.279700	.0070	.00491	1.80E+04
13139	RB87	7489.8955	.008	4162.1312	.0031	2	-1	2	-2	2319.278000	.0070	.00225	1.80E+04
13140	RB87	7486.2956	.008	4160.7137	.0032	2	-1	2	-2	2318.132600	.0070	.00508	1.80E+04
13140	RB87	7486.2961	.008	4160.7139	.0032	2	-1	2	-2	2318.130000	.0070	.00232	1.80E+04
11981	RB87	9652.5506	.008	4998.4512	.0030	2	-1	2	-2	3013.892900	.0050	.00135	3.16E+04
11981	RB87	9652.5480	.008	4998.4502	.0030	2	-1	2	-2	3013.891300	.0050	.00059	3.16E+04
11981	RB87	9652.5480	.008	4998.4502	.0030	2	-1	2	-2	3013.890800	.0050	.00009	3.16E+04
11981	RB87	9652.5467	.008	4998.4497	.0030	2	-1	2	-2	3013.890200	.0050	-.00009	3.16E+04
11981	RB87	9652.5428	.008	4998.4482	.0030	2	-1	2	-2	3013.888800	.0050	-.00023	3.16E+04
11981	RB87	9652.5389	.008	4998.4467	.0030	2	-1	2	-2	3013.888000	.0050	.00023	3.16E+04
11981	RB87	9652.5402	.008	4998.4472	.0030	2	-1	2	-2	3013.886400	.0050	-.00179	3.16E+04
11981	RB87	9652.5389	.008	4998.4467	.0030	2	-1	2	-2	3013.889500	.0050	.00173	3.16E+04
11982	RB87	9652.5454	.008	4998.4492	.0030	2	-1	2	-2	3013.893300	.0050	.00343	3.16E+04
11982	RB87	9652.5441	.008	4998.4487	.0030	2	-1	2	-2	3013.891800	.0050	.00235	3.16E+04
11982	RB87	9652.5428	.008	4998.4482	.0030	2	-1	2	-2	3013.891700	.0050	.00267	3.16E+04
11982	RB87	9652.5428	.008	4998.4482	.0030	2	-1	2	-2	3013.891400	.0050	.00237	3.16E+04
11982	RB87	9652.5428	.008	4998.4482	.0030	2	-1	2	-2	3013.891300	.0050	.00227	3.16E+04
11982	RB87	9652.5415	.008	4998.4477	.0030	2	-1	2	-2	3013.891700	.0050	.00309	3.16E+04
11982	RB87	9652.5402	.008	4998.4472	.0030	2	-1	2	-2	3013.890000	.0050	.00181	3.16E+04
11982	RB87	9652.5402	.008	4998.4472	.0030	2	-1	2	-2	3013.890600	.0050	.00241	3.16E+04
13201	GA69	2773.8400	.200	4713.5641	.2389	2	0	3	-1	117.814597	.0001	-.00002	1.00E+08
13202	GA69	2773.8400	.200	4713.5641	.2389	2	0	3	-1	117.814597	.0001	-.00002	1.00E+08
13203	GA69	2773.8400	.200	4713.5641	.2389	2	0	3	-1	117.814597	.0001	-.00002	9.99E+07
13204	GA69	2773.8400	.200	4713.5641	.2389	2	0	3	-1	117.814597	.0001	-.00002	9.97E+07
13205	GA69	2773.8400	.200	4713.5641	.2389	2	0	3	-1	117.814597	.0001	-.00002	1.00E+08
13206	GA69	2773.9410	.200	4713.6848	.2389	2	0	3	-1	117.814596	.0001	-.00002	1.00E+08
13207	GA69	2773.9410	.200	4713.6848	.2389	2	0	3	-1	117.814596	.0001	-.00002	9.99E+07
13208	GA69	2773.9410	.200	4713.6848	.2389	2	0	3	-1	117.814596	.0001	-.00002	1.00E+08
13209	GA69	2773.8740	.200	4713.6047	.2389	2	0	3	-1	117.814590	.0001	-.00002	1.00E+08
13210	GA69	2773.8740	.200	4713.6047	.2389	2	0	3	-1	117.814590	.0001	-.00002	1.00E+08
13211	GA69	2773.7550	.200	4713.4626	.2389	2	0	3	-1	117.814621	.0001	.00001	1.00E+08
13212	GA69	2773.7550	.200	4713.4626	.2389	2	0	3	-1	117.814621	.0001	.00001	9.98E+07
13213	GA69	2773.7150	.200	4713.4148	.2389	2	0	3	-1	117.814623	.0001	.00001	1.00E+08
13214	GA69	2773.7150	.200	4713.4148	.2389	2	0	3	-1	117.814623	.0001	.00001	1.00E+08
13215	GA69	2773.9660	.200	4713.7146	.2389	2	0	3	-1	117.814640	.0001	.00003	9.99E+07
13216	GA69	2773.9660	.200	4713.7146	.2389	2	0	3	-1	117.814640	.0001	.00003	1.00E+08
13217	GA69	2773.9660	.200	4713.7146	.2389	2	0	3	-1	117.814640	.0001	.00003	1.00E+08
13218	GA69	2773.6340	.200	4713.3180	.2389	2	0	3	-1	117.814631	.0001	.00002	9.95E+07
13219	GA69	2773.6340	.200	4713.3180	.2389	2	0	3	-1	117.814637	.0001	.00002	9.98E+07
13220	GA69	2773.6340	.200	4713.3180	.2389	2	0	3	-1	117.814637	.0001	.00002	9.96E+07
13301	CS133	333.8500	.030	765.8395	.0557	2	-1	1	0	2587.513610	.0002	.00002	2.50E+07
13302	CS133	333.8500	.030	765.8395	.0557	2	-1	1	0	2587.513596	.0002	.00001	2.50E+07
13303	CS133	333.8530	.030	765.8451	.0557	2	-1	1	0	2587.513558	.0002	-.00003	2.50E+07
13304	CS133	333.8500	.030	765.8395	.0557	2	-1	1	0	2587.513617	.0002	.00003	2.50E+07
13305	CS133	333.8500	.030	765.8395	.0557	2	-1	1	0	2587.513603	.0002	.00001	2.50E+07
13306	CS133	333.8500	.030	765.8395	.0557	2	-1	1	0	2587.513617	.0002	.00003	2.50E+07
13307	CS133	333.8500	.030	765.8395	.0557	2	-1	1	0	2587.513623	.0002	.00003	2.50E+07
13308	CS133	333.8500	.030	765.8395	.0557	2	-1	1	0	2587.513595	.0002	.00001	2.50E+07
13309	CS133	333.8500	.030	765.8395	.0557	2	-1	1	0	2587.513620	.0002	.00003	2.50E+07
13310	CS133	333.8500	.030	765.8395	.0557	2	-1	1	0	2587.513604	.0002	.00001	2.50E+07
13311	CS133	333.8500	.030	765.8395	.0557	2	-1	1	0	2587.513591	.0002	.00000	2.50E+07
13312	CS133	333.8530	.030	765.8451	.0557	2	-1	1	0	2587.513568	.0002	-.00002	2.50E+07
13313	CS133	333.8530	.030	765.8451	.0557	2	-1	1	0	2587.513568	.0002	-.00002	2.50E+07
13314	CS133	333.8530	.030	765.8451	.0557	2	-1	1	0	2587.513568	.0002	-.00002	2.50E+07
13315	CS133	333.8530	.030	765.8451	.0557	2	-1	1	0	2587.513566	.0002	-.00002	2.50E+07
13316	CS133	333.8530	.030	765.8451	.0557	2	-1	1	0	2587.513570	.0002	-.00002	2.50E+07
13317	CS133	333.8530	.030	765.8451	.0557	2	-1	1	0	2587.513563	.0002	-.00003	2.50E+07
13318	CS133	333.8530	.030	765.8451	.0557	2	-1	1	0	2587.513570	.0002	-.00002	2.50E+07
13319	CS133	333.8530	.030	765.8451	.0557	2	-1	1	0	2587.513586	.0002	-.00000	2.50E+07
13320	CS133	333.8530	.030	765.8451	.0557	2	-1	1	0	2587.513562	.0002	-.00003	2.50E+07
13321	CS133	337.6060	.030	772.8003	.0555	2	0	1	-1	2585.953303	.0002	.00001	2.50E+07
13322	CS133	337.6060	.030	772.8003	.0555	2	0	1	-1	2585.953295	.0002	.00000	2.50E+07
13323	CS133	337.6060	.030	772.8003	.0555	2	0	1	-1	2585.953286	.0002	-.00001	2.50E+07
13324	CS133	337.6060	.030	772.8003	.0555	2	0	1	-1	2585.953300	.0002	.00001	2.50E+07
13325	CS133	337.6060	.030	772.8003	.0555	2	0	1	-1	2585.953286	.0002	-.00001	2.50E+07
13326	CS133	337.6060	.030	772.8003	.0555	2	0	1	-1	2585.953305	.0002	.00001	2.50E+07
13327	CS133	337.6060	.030	772.8003	.0555	2	0	1	-1	2585.953311	.0002	.00002	2.50E+07
13328	CS133	337.6060	.030	772.8003	.0555	2	0	1	-1	2585.953291	.0002	-.00000	2.50E+07
13329	CS133	337.6060	.030	772.8003	.0555	2	0	1	-1	2585.953307	.0002	.00001	2.50E+07
13330	CS133	337.6060	.030	772.8003	.0555	2	0	1	-1	2585.953285	.0002	-.00001	2.50E+07
13331	CS133	337.6400	.030	772.8632	.0555	2	0	1	-1	2585.953304	.0002	.00000	2.50E+07
13332	CS133	337.6400	.030	772.8632	.0555	2	0	1	-1	2585.953319	.0002	.00002	2.50E+07
13333	CS133	337.6400	.030	772.8632	.0555	2	0	1	-1	2585.953296	.0002	-.00000	2.50E+07
13334	CS133	337.6400	.030	772.8632	.0555	2	0	1	-1	2585.953297	.0002	-.00000	2.50E+07
13335	CS133	337.6400	.030	772.8632	.0555	2	0	1	-1	2585.953309	.0002	.00001	2.50E+07
13336	CS133	337.6400	.030	772.8632	.0555	2	0	1	-1	2585.953294	.0002	-.00001	2.50E+07
13337	CS133	337.6400	.030	772.8632	.0555	2	0	1	-1	2585.953294	.0002	-.00001	2.50E+07
13338	CS133	337.6400	.030	772.8632	.0555	2	0	1	-1	2585.953301	.0002	.00000	2.50E+07
13339	CS133	337.6400	.030	772.8632	.0555	2	0	1	-1	2585.953286	.0002	-.00001	2.50E+07
13340	CS133	337.6400	.030	772.8632	.0555	2	0	1	-1	2585.953291	.0002	-.00001	2.50E+07
133A	RB87	.1660	.010	.2373	.0143	2	0	1	0	2677.987172	.0002	.00000	2.50E+07
144				.0000	.0000	3	0	2	0	634.901800	.0002	.00000	2.50E+07
145				.0000	.0000	2	0	1	0	319.067100	.0002	.00000	2.50E+07
146				.0000	.0000	1	0	0	0	128.277300	.0002	.00000	2.50E+07

XBL 687-1275

APPENDIX F. 205 TL RUN SUMMARY

RUN	ISOTOPE	CALIBRATION FREQUENCY (MHZ)	FREQUENCY ERROR (MHZ)	FIELD (GAUSS)	FIELD ERROR (GAUSS)	TRANSITION F 1	TRANSITION M 1	TRANSITION F 2	TRANSITION M 2	EXPERIMENTAL FREQUENCY (MHZ)	FREQUENCY ERROR (MHZ)	RESIDUAL (MHZ)	WEIGHT FACTOR
96 1+	CS133	2739.9875	.004	2999.8692	.0025	1	0	1	-1	1485.568200	.0018	.00108	2.03E+05
96 3+	CS133	2739.9849	.004	2999.8677	.0025	1	0	1	-1	1485.567200	.0018	.00087	2.03E+05
96 5+	CS133	2739.9829	.004	2999.8666	.0025	1	0	1	-1	1485.565800	.0018	.00007	2.03E+05
96 7+	CS133	2739.9821	.004	2999.8661	.0025	1	0	1	-1	1485.566300	.0018	.00081	2.03E+05
96 9+	CS133	2739.9795	.004	2999.8646	.0025	1	0	1	-1	1485.565600	.0018	.00090	2.03E+05
9611+	CS133	2739.9795	.004	2999.8646	.0025	1	0	1	-1	1485.565300	.0018	.00060	2.03E+05
9613+	CS133	2739.9790	.004	2999.8643	.0025	1	0	1	-1	1485.565200	.0018	.00065	2.03E+05
9615+	CS133	2739.9783	.004	2999.8638	.0025	1	0	1	-1	1485.564800	.0018	.00055	2.03E+05
9617+	CS133	2739.9775	.004	2999.8635	.0025	1	0	1	-1	1485.565000	.0018	.00090	2.03E+05
9619+	CS133	2739.9760	.004	2999.8626	.0025	1	0	1	-1	1485.564300	.0018	.00065	2.03E+05
9622+	CS133	2740.1400	.004	2999.9569	.0025	1	0	1	-1	1485.613400	.0018	.00022	2.03E+05
9624+	CS133	2740.1367	.004	2999.9550	.0025	1	0	1	-1	1485.611700	.0018	-.00048	2.03E+05
9626+	CS133	2740.1345	.004	2999.9537	.0025	1	0	1	-1	1485.611800	.0018	.00028	2.03E+05
9628+	CS133	2740.1318	.004	2999.9521	.0025	1	0	1	-1	1485.611000	.0018	.00030	2.03E+05
9630+	CS133	2740.1307	.004	2999.9515	.0025	1	0	1	-1	1485.610600	.0018	.00023	2.03E+05
9635+	CS133	2740.0638	.004	2999.9131	.0025	1	0	1	-1	1485.590600	.0018	.00044	2.03E+05
9637+	CS133	2740.0638	.004	2999.9131	.0025	1	0	1	-1	1485.590400	.0018	.00024	2.03E+05
9639+	CS133	2740.0639	.004	2999.9131	.0025	1	0	1	-1	1485.590700	.0018	.00051	2.03E+05
9641+	CS133	2740.0639	.004	2999.9131	.0025	1	0	1	-1	1485.590200	.0018	.00001	2.03E+05
97 1+	CS133	5881.3156	.005	4499.3359	.0022	1	0	1	-1	2295.800500	.0025	.00001	1.28E+05
97 3+	CS133	5881.3066	.005	4499.3321	.0022	1	0	1	-1	2295.797800	.0025	-.00057	1.28E+05
97 5+	CS133	5881.2957	.005	4499.3275	.0022	1	0	1	-1	2295.796100	.0025	.00029	1.28E+05
97 8+	CS133	5881.0161	.005	4499.2091	.0022	1	0	1	-1	2295.729000	.0025	-.00110	1.28E+05
9710+	CS133	5880.9956	.005	4499.2004	.0022	1	0	1	-1	2295.724800	.0025	-.00048	1.28E+05
9712+	CS133	5880.9735	.005	4499.1911	.0022	1	0	1	-1	2295.719600	.0025	-.00048	1.28E+05
9714+	CS133	5880.9548	.005	4499.1831	.0022	1	0	1	-1	2295.715200	.0025	-.00049	1.28E+05
9716+	CS133	5880.9392	.005	4499.1765	.0022	1	0	1	-1	2295.711500	.0025	-.00042	1.28E+05
9718+	CS133	5880.9235	.005	4499.1699	.0022	1	0	1	-1	2295.707900	.0025	-.00043	1.28E+05
9720+	CS133	5880.9046	.005	4499.1619	.0022	1	0	1	-1	2295.703600	.0025	-.00029	1.28E+05
9723+	CS133	5881.1328	.005	4499.2585	.0022	1	0	1	-1	2295.757400	.0025	-.00012	1.28E+05
9725+	CS133	5881.1157	.005	4499.2513	.0022	1	0	1	-1	2295.753100	.0025	-.00040	1.28E+05
9727+	CS133	5881.0937	.005	4499.2420	.0022	1	0	1	-1	2295.747600	.0025	-.00073	1.28E+05
9729+	CS133	5880.9479	.005	4499.1802	.0022	1	0	1	-1	2295.713300	.0025	-.00077	1.28E+05
9731+	CS133	5880.9440	.005	4499.1786	.0022	1	0	1	-1	2295.712300	.0025	-.00085	1.28E+05
9733+	CS133	5880.9398	.005	4499.1768	.0022	1	0	1	-1	2295.710900	.0025	-.00126	1.28E+05
9735+	CS133	5880.9336	.005	4499.1742	.0022	1	0	1	-1	2295.709900	.0025	-.00080	1.28E+05
9737+	CS133	5880.9307	.005	4499.1729	.0022	1	0	1	-1	2295.709300	.0025	-.00072	1.28E+05
9739+	CS133	5880.9272	.005	4499.1714	.0022	1	0	1	-1	2295.708800	.0025	-.00240	1.28E+05
9741+	CS133	5880.9235	.005	4499.1699	.0022	1	0	1	-1	2295.707500	.0025	-.00073	1.28E+05
98 1+	CS133	9629.4434	.008	5999.6623	.0031	1	0	1	-1	3149.972500	.0024	.00021	1.11E+05
98 3+	CS133	9629.4262	.008	5999.6557	.0031	1	0	1	-1	3149.970300	.0024	.00187	1.11E+05
98 6+	CS133	9629.4061	.008	5999.6479	.0031	1	0	1	-1	3149.966600	.0024	.00069	1.11E+05
98 8+	CS133	9629.3957	.008	5999.6439	.0031	1	0	1	-1	3149.957800	.0024	-.00378	1.11E+05
9810+	CS133	9629.4064	.008	5999.6481	.0031	1	0	1	-1	3149.963900	.0024	-.00008	1.11E+05
9812+	CS133	9629.3817	.008	5999.6385	.0031	1	0	1	-1	3149.961700	.0024	.00327	1.11E+05
9814+	CS133	9629.3720	.008	5999.6348	.0031	1	0	1	-1	3149.955100	.0024	-.00115	1.11E+05
9816+	CS133	9629.3842	.008	5999.6395	.0031	1	0	1	-1	3149.958800	.0024	-.00019	1.11E+05
9818+	CS133	9629.3767	.008	5999.6366	.0031	1	0	1	-1	3149.958100	.0024	.00079	1.11E+05
9820+	CS133	9629.3686	.008	5999.6335	.0031	1	0	1	-1	3149.956400	.0024	.00091	1.11E+05
9822+	CS133	9630.9821	.008	6000.2550	.0031	1	0	1	-1	3150.317200	.0024	-.00086	1.11E+05
9824+	CS133	9630.9614	.008	6000.2470	.0031	1	0	1	-1	3150.312800	.0024	-.00061	1.11E+05
9826+	CS133	9630.9638	.008	6000.2479	.0031	1	0	1	-1	3150.313400	.0024	-.00055	1.11E+05
9828+	CS133	9630.9728	.008	6000.2514	.0031	1	0	1	-1	3150.316700	.0024	.00073	1.11E+05
9830+	CS133	9630.9635	.008	6000.2478	.0031	1	0	1	-1	3150.313500	.0024	-.00038	1.11E+05
9832+	CS133	9630.9464	.008	6000.2412	.0031	1	0	1	-1	3150.308800	.0024	-.00124	1.11E+05
9834+	CS133	9630.9304	.008	6000.2350	.0031	1	0	1	-1	3150.306500	.0024	.00005	1.11E+05
9836+	CS133	9630.9179	.008	6000.2302	.0031	1	0	1	-1	3150.302400	.0024	-.00124	1.11E+05
9838+	CS133	9630.9245	.008	6000.2328	.0031	1	0	1	-1	3150.305000	.0024	-.00012	1.11E+05
9840+	CS133	9630.9281	.008	6000.2342	.0031	1	0	1	-1	3150.305300	.0024	-.00063	1.11E+05
10 1+	CS133	5880.9020	.005	4499.1608	.0021	1	0	1	-1	2295.703200	.0025	-.00008	1.31E+05
10 3+	CS133	5880.9111	.005	4499.1646	.0021	1	0	1	-1	2295.704900	.0025	-.00052	1.31E+05
10 5+	CS133	5880.9192	.005	4499.1681	.0021	1	0	1	-1	2295.707200	.0025	-.00012	1.31E+05
10 7+	CS133	5880.9124	.005	4499.1652	.0021	1	0	1	-1	2295.705300	.0025	-.00042	1.31E+05
1019+	CS133	5880.9009	.005	4499.1603	.0021	1	0	1	-1	2295.702600	.0025	-.00042	1.31E+05
1013+	CS133	5880.9888	.005	4499.1975	.0021	1	0	1	-1	2295.723100	.0025	-.00058	1.31E+05
1015+	CS133	5880.9923	.005	4499.1990	.0021	1	0	1	-1	2295.724200	.0025	-.00030	1.31E+05
1017+	CS133	5880.9943	.005	4499.1999	.0021	1	0	1	-1	2295.724200	.0025	-.00077	1.31E+05
1019+	CS133	5880.9835	.005	4499.1953	.0021	1	0	1	-1	2295.721900	.0025	-.00053	1.31E+05
1021+	CS133	5880.9838	.005	4499.1954	.0021	1	0	1	-1	2295.722100	.0025	-.00040	1.31E+05
1025+	CS133	5882.2488	.005	4499.7311	.0021	1	0	1	-1	2296.019700	.0025	-.00012	1.31E+05
1027+	CS133	5882.2435	.005	4499.7289	.0021	1	0	1	-1	2296.018200	.0025	-.00037	1.31E+05
1029+	CS133	5882.2472	.005	4499.7304	.0021	1	0	1	-1	2296.019400	.0025	-.00004	1.31E+05
1031+	CS133	5882.2506	.005	4499.7319	.0021	1	0	1	-1	2296.020200	.0025	-.00004	1.31E+05
1033+	CS133	5882.2543	.005	4499.7334	.0021	1	0	1	-1	2296.021100	.0025	-.00001	1.31E+05
1035+	CS133	5882.2548	.005	4499.7336	.0021	1	0	1	-1	2296.021200	.0025	-.00003	1.31E+05
1037+	CS133	5882.2510	.005	4499.7320	.0021	1	0	1	-1	2296.020100	.0025	-.00024	1.31E+05
1039+	CS133	5882.2482	.005	4499.7308	.0021	1	0	1	-1	2296.019300	.0025	-.00038	1.31E+05
1041+	CS133	5882.2531	.005	4499.7329	.0021	1	0	1	-1	2296.020800	.0025	-.00003	1.31E+05
1043+	CS133	5882.2566	.005	4499.7344	.0021	1	0	1	-1	2296.021800	.0025	.00015	1.31E+05
11 1+	K39	12266.3921	.008	4499.4575	.0029	1	0	1	-1	2295.868400	.0023	.00041	1.28E+05
11 3+	K39	12266.3915	.008	4499.4573	.0029	1	0	1	-1	2295.869100	.0023	.00123	1.28E+05
11 5+	K39	12266.3859	.008	4499.4553	.0029	1	0	1	-1	2295.867400	.0023	.00064	1.28E+05
11 7+	K39	12266.3755	.008	4499.4516	.0029	1	0	1	-1	2295.864700	.0023	-.00000	1.28E+05
11 9+	K39	12266.3739	.008	4499.4510	.0029	1	0	1	-1	2295.864700	.0023	.00032	1.28E+05
1111+	K39	12266.3760	.008	4499.4518	.0029	1	0	1	-1	2295.864800	.0023	-.00000	1.28E+05
1113+	K39	12266.3749	.008	4499.4514	.0029	1	0	1	-1	2295.864800	.0023	.00022	1.28E+05
1115+	K39	12266.3666	.008	4499.4486	.0029	1	0	1	-1	2295.863000	.0023	.00006	1.28E+05
1117+	K39	12266.3556	.008	4499.4445	.0029	1	0	1	-1	2295.861200	.0023	.00044	1.28E+05
1119+	K39	12266.3488	.008	4499.4421	.0029	1	0	1	-1	2295.860500	.0023	.00109	1.28E+05

XBL 687-1274

APPENDIX F. ^{205}TL RUN SUMMARY

RUN	ISOTOPE	CALIBRATION FREQUENCY (MHZ)	FREQUENCY ERROR (MHZ)	FIELD (GAUSS)	FIELD ERROR (GAUSS)	TRANSITION F 1	M 1	F 2	M 2	EXPERIMENTAL FREQUENCY (MHZ)	FREQUENCY ERROR (MHZ)	RESIDUAL (MHZ)	WEIGHT FACTOR
1122+	K39	12267.0952	.008	4499.7085	.0029	1	0	1	-1	2296.007800	.0023	.00053	1.28E+05
1124+	K39	12267.0934	.008	4499.7079	.0029	1	0	1	-1	2296.007800	.0023	.00088	1.28E+05
1126+	K39	12267.0962	.008	4499.7089	.0029	1	0	1	-1	2296.008300	.0023	.00083	1.28E+05
1128+	K39	12267.0981	.008	4499.7095	.0029	1	0	1	-1	2296.008600	.0023	.00075	1.28E+05
1130+	K39	12267.0918	.008	4499.7073	.0029	1	0	1	-1	2296.007700	.0023	.00110	1.28E+05
1132+	K39	12267.0818	.008	4499.7037	.0029	1	0	1	-1	2296.006200	.0023	.00158	1.28E+05
1134+	K39	12267.0852	.008	4499.7049	.0029	1	0	1	-1	2296.006500	.0023	.00121	1.28E+05
1136+	K39	12267.0910	.008	4499.7070	.0029	1	0	1	-1	2296.007000	.0023	.00056	1.28E+05
1138+	K39	12267.0957	.008	4499.7087	.0029	1	0	1	-1	2296.007300	.0023	-.00007	1.28E+05
1140+	K39	12267.0913	.008	4499.7070	.0029	1	0	1	-1	2296.006800	.0023	.00036	1.28E+05
D1++	TL205	2711.1200	.200	5238.1944	.3514	1	1	2	0	106.915348	.0002	-.00010	2.50E+07
D2+-	TL205	2711.1800	.200	5238.2998	.3514	1	1	2	0	106.915390	.0002	-.00006	2.50E+07
D3-+	TL205	2711.1200	.200	5238.1944	.3514	1	1	2	0	106.915417	.0002	-.00004	2.50E+07
D4--	TL205	2711.1800	.200	5238.2998	.3514	1	1	2	0	106.915372	.0002	-.00008	2.50E+07
D5+-	TL205	2746.4000	.200	5300.1166	.3507	1	1	2	0	106.912733	.0002	.00002	2.46E+07
D6--	TL205	2746.5760	.200	5300.4252	.3507	1	1	2	0	106.912663	.0002	-.00003	2.46E+07
D7+-	TL205	2803.2400	.200	5399.6136	.3495	1	1	2	0	106.901250	.0002	.00021	2.32E+07
D8--	TL205	2803.2000	.200	5399.5437	.3495	1	1	2	0	106.901177	.0002	.00012	2.32E+07
D9+-	TL205	2679.4950	.200	5182.5786	.3520	1	1	2	0	106.914844	.0002	.00002	2.49E+07
D10-	TL205	2679.4950	.200	5182.5786	.3520	1	1	2	0	106.914690	.0002	-.00014	2.49E+07
D11+	TL205	2621.3000	.200	5079.9655	.3533	1	1	2	0	106.905771	.0002	.00009	2.35E+07
D12-	TL205	2621.3000	.200	5079.9655	.3533	1	1	2	0	106.905739	.0002	.00006	2.35E+07
D13+	TL205	2700.5160	.200	5219.5577	.3516	1	1	2	0	106.915593	.0002	.00002	2.50E+07
D14-	TL205	2700.5760	.200	5219.6631	.3516	1	1	2	0	106.915505	.0002	-.00007	2.50E+07
3801-	TL205	1495.6967	.002	3019.1368	.0038	2	0	2	-1	5508.434000	.0046	.01394	1.40E+04
38002	TL205	1495.6968	.002	3019.1370	.0038	2	0	2	-1	5508.418500	.0046	-.00191	1.40E+04
38003	TL205	1495.6972	.002	3019.1377	.0038	2	0	2	-1	5508.421500	.0046	-.00033	1.40E+04
38004	TL205	1495.6985	.002	3019.1402	.0038	2	0	2	-1	5508.427100	.0046	.00065	1.40E+04
38005	TL205	1495.6995	.002	3019.1421	.0038	2	0	2	-1	5508.431700	.0046	.00171	1.40E+04
38006	TL205	1495.6993	.002	3019.1417	.0038	2	0	2	-1	5508.427200	.0046	-.00298	1.40E+04
38007	TL205	1495.6988	.002	3019.1408	.0038	2	0	2	-1	5508.426000	.0046	-.00151	1.40E+04
38008	TL205	1495.6978	.002	3019.1389	.0038	2	0	2	-1	5508.423000	.0046	-.00096	1.40E+04
38009	TL205	1495.6966	.002	3019.1366	.0038	2	0	2	-1	5508.418200	.0046	-.00151	1.40E+04
38010	TL205	1495.6959	.002	3019.1353	.0038	2	0	2	-1	5508.415600	.0046	-.00162	1.40E+04
38011	TL205	1495.6960	.002	3019.1354	.0038	2	0	2	-1	5508.410900	.0046	-.00668	1.40E+04
38012	TL205	1495.6958	.002	3019.1351	.0038	2	0	2	-1	5508.416800	.0046	-.00007	1.40E+04
38013	TL205	1495.6962	.002	3019.1358	.0038	2	0	2	-1	5508.420500	.0046	.00221	1.40E+04
38014	TL205	1495.6972	.002	3019.1377	.0038	2	0	2	-1	5508.421600	.0046	-.00023	1.40E+04
38015	TL205	1495.6981	.002	3019.1394	.0038	2	0	2	-1	5508.425800	.0046	.00077	1.40E+04
4301+	TL205	1490.6353	.002	3009.5110	.0036	2	0	2	-1	5490.471000	.0040	.01207	1.63E+04
4302+	TL205	1490.6354	.002	3009.5112	.0036	2	0	2	-1	5490.463400	.0040	.00411	1.63E+04
4303+	TL205	1490.6346	.002	3009.5097	.0036	2	0	2	-1	5490.450700	.0040	-.00575	1.63E+04
4304+	TL205	1490.6332	.002	3009.5070	.0036	2	0	2	-1	5490.448600	.0040	-.00288	1.63E+04
4305+	TL205	1490.6327	.002	3009.5060	.0036	2	0	2	-1	5490.444000	.0040	-.00570	1.63E+04
4306+	TL205	1490.6312	.002	3009.5032	.0036	2	0	2	-1	5490.448600	.0040	.00422	1.63E+04
4307+	TL205	1490.6293	.002	3009.4996	.0036	2	0	2	-1	5490.445200	.0040	.00757	1.63E+04
4308+	TL205	1490.6274	.002	3009.4960	.0036	2	0	2	-1	5490.426700	.0040	-.00419	1.63E+04
4309+	TL205	1490.6256	.002	3009.4925	.0036	2	0	2	-1	5490.415700	.0040	-.00880	1.63E+04
4310+	TL205	1490.6251	.002	3009.4916	.0036	2	0	2	-1	5490.415800	.0040	-.00693	1.63E+04
4301-	TL205	1490.6487	.002	3009.5365	.0036	2	0	2	-1	5490.501800	.0040	-.00469	1.63E+04
4302-	TL205	1490.6443	.002	3009.5281	.0036	2	0	2	-1	5490.481200	.0040	-.00967	1.63E+04
4303-	TL205	1490.6400	.002	3009.5199	.0036	2	0	2	-1	5490.469200	.0040	-.00641	1.63E+04
4304-	TL205	1490.6368	.002	3009.5138	.0036	2	0	2	-1	5490.459600	.0040	-.00465	1.63E+04
4305-	TL205	1490.7775	.002	3009.7815	.0036	2	0	2	-1	5490.958100	.0040	-.00594	1.63E+04
4306-	TL205	1490.7785	.002	3009.7834	.0036	2	0	2	-1	5490.960400	.0040	-.00679	1.63E+04
4307-	TL205	1490.7788	.002	3009.7839	.0036	2	0	2	-1	5490.959900	.0040	-.00835	1.63E+04
4308-	TL205	1490.7790	.002	3009.7843	.0036	2	0	2	-1	5490.961900	.0040	-.00706	1.63E+04
4309-	TL205	1490.7794	.002	3009.7851	.0036	2	0	2	-1	5490.962600	.0040	-.00778	1.63E+04
4310-	TL205	1490.7800	.002	3009.7862	.0036	2	0	2	-1	5490.965000	.0040	-.00751	1.63E+04
4201-	TL205	2296.8518	.002	4501.2300	.0040	2	0	2	-1	8274.582600	.0045	-.00445	1.33E+04
4202-	TL205	2296.8515	.002	4501.2295	.0040	2	0	2	-1	8274.582400	.0045	-.00364	1.33E+04
4203-	TL205	2296.8513	.002	4501.2291	.0040	2	0	2	-1	8274.581400	.0045	-.00397	1.33E+04
4204-	TL205	2296.8513	.002	4501.2291	.0040	2	0	2	-1	8274.581100	.0045	-.00427	1.33E+04
4205-	TL205	2296.8511	.002	4501.2287	.0040	2	0	2	-1	8274.580600	.0045	-.00410	1.33E+04
4206-	TL205	2296.8510	.002	4501.2286	.0040	2	0	2	-1	8274.580300	.0045	-.00406	1.33E+04
4207-	TL205	2296.8508	.002	4501.2282	.0040	2	0	2	-1	8274.579300	.0045	-.00439	1.33E+04
4208-	TL205	2296.8505	.002	4501.2277	.0040	2	0	2	-1	8274.577000	.0045	-.00568	1.33E+04
4209-	TL205	2296.8495	.002	4501.2259	.0040	2	0	2	-1	8274.575100	.0045	-.00422	1.33E+04
4210-	TL205	2296.8473	.002	4501.2219	.0040	2	0	2	-1	8274.568800	.0045	-.00312	1.33E+04
4201+	TL205	2296.9088	.002	4501.3327	.0040	2	0	2	-1	8274.775200	.0045	-.00355	1.33E+04
4202+	TL205	2296.9097	.002	4501.3343	.0040	2	0	2	-1	8274.777300	.0045	-.00447	1.33E+04
4203+	TL205	2296.9103	.002	4501.3354	.0040	2	0	2	-1	8274.779400	.0045	-.00439	1.33E+04
4204+	TL205	2296.9109	.002	4501.3365	.0040	2	0	2	-1	8274.781600	.0045	-.00421	1.33E+04
4205+	TL205	2296.9110	.002	4501.3367	.0040	2	0	2	-1	8274.781100	.0045	-.00505	1.33E+04
4206+	TL205	2296.9108	.002	4501.3363	.0040	2	0	2	-1	8274.781600	.0045	-.00387	1.33E+04
4207+	TL205	2296.9105	.002	4501.3359	.0040	2	0	2	-1	8274.781500	.0045	-.00330	1.33E+04
4208+	TL205	2296.9106	.002	4501.3359	.0040	2	0	2	-1	8274.780500	.0045	-.00430	1.33E+04
4209+	TL205	2296.9104	.002	4501.3356	.0040	2	0	2	-1	8274.780800	.0045	-.00333	1.33E+04
4210+	TL205	2296.9097	.002	4501.3343	.0040	2	0	2	-1	8274.775300	.0045	-.00647	1.33E+04
4901-	TL205	2296.8353	.002	4501.2003	.0036	2	0	2	-1	8274.531700	.0050	.00014	1.42E+04
4902-	TL205	2296.8362	.002	4501.2019	.0036	2	0	2	-1	8274.536100	.0050	.00151	1.42E+04
4903-	TL205	2296.8372	.002	4501.2037	.0036	2	0	2	-1	8274.539300	.0050	.00135	1.42E+04
4904-	TL205	2296.8369	.002	4501.2032	.0036	2	0	2	-1	8274.537900	.0050	.00096	1.42E+04
4905-	TL205	2296.8366	.002	4501.2026	.0036	2	0	2	-1	8274.535500	.0050	-.00043	1.42E+04
4906-	TL205	2296.8369	.002	4501.2032	.0036	2	0	2	-1	8274.537800	.0050	.00086	1.42E+04
4907-	TL205	2296.8378	.002	4501.2049	.0036	2	0	2	-1	8274.541100	.0050	.00113	1.42E+04
4908-	TL205	2296.8391	.002	4501.2071	.0036	2	0	2	-1	8274.544500	.0050	.00016	1.42E+04
4909-	TL205	2296.8398	.002	4501.2084	.0036	2	0	2	-1	8274.547400	.0050	.00071	1.42E+04
4910-	TL205	2296.8401	.002	4501.2089	.0036	2	0	2	-1	8274.547900	.0050	.00020	1.42E+04

XBL 687-1273

APPENDIX F . ^{205}TL RUN SUMMARY

RUN	ISOTOPE	CALIBRATION FREQUENCY (MHZ)	FREQUENCY ERROR (MHZ)	FIELD (GAUSS)	FIELD ERROR (GAUSS)	TRANSITION F 1	TRANSITION M 1	TRANSITION F 2	TRANSITION M 2	EXPERIMENTAL FREQUENCY (MHZ)	FREQUENCY ERROR (MHZ)	RESIDUAL (MHZ)	WEIGHT FACTOR
4001+	TL205	2296.7837	.002	4501.1073	.0036	2	0	2	-1	8274.357600	.0050	-.00042	1.42E+04
4002+	TL205	2296.7835	.002	4501.1069	.0036	2	0	2	-1	8274.356200	.0050	-.00115	1.42E+04
4003+	TL205	2296.7829	.002	4501.1059	.0036	2	0	2	-1	8274.355300	.0050	-.00093	1.42E+04
4004+	TL205	2296.7821	.002	4501.1044	.0036	2	0	2	-1	8274.352600	.0050	-.00004	1.42E+04
4005+	TL205	2296.7815	.002	4501.1035	.0036	2	0	2	-1	8274.351400	.0050	.00044	1.42E+04
4006+	TL205	2296.7813	.002	4501.1030	.0036	2	0	2	-1	8274.349900	.0050	-.00005	1.42E+04
4007+	TL205	2296.7810	.002	4501.1024	.0036	2	0	2	-1	8274.348800	.0050	-.00014	1.42E+04
4008+	TL205	2296.7810	.002	4501.1024	.0036	2	0	2	-1	8274.349200	.0050	.00026	1.42E+04
4009+	TL205	2296.7813	.002	4501.1030	.0036	2	0	2	-1	8274.350200	.0050	.00025	1.42E+04
4010+	TL205	2296.7816	.002	4501.1035	.0036	2	0	2	-1	8274.350700	.0050	-.00026	1.42E+04
4001+	TL205	3150.5922	.003	6000.7254	.0043	2	0	2	-1	11073.906900	.0067	.01896	9.18E+03
4002+	TL205	3150.5960	.003	6000.7319	.0043	2	0	2	-1	11073.914700	.0067	.01460	9.18E+03
4003+	TL205	3150.6000	.003	6000.7387	.0043	2	0	2	-1	11073.926400	.0067	.01350	9.18E+03
4004+	TL205	3150.3370	.003	6000.2880	.0043	2	0	2	-1	11073.084000	.0067	.01266	9.18E+03
4005+	TL205	3150.3351	.003	6000.2847	.0043	2	0	2	-1	11073.076200	.0067	.01094	9.18E+03
4006+	TL205	3150.3329	.003	6000.2809	.0043	2	0	2	-1	11073.073600	.0067	.01538	9.18E+03
4007+	TL205	3150.3311	.003	6000.2779	.0043	2	0	2	-1	11073.066000	.0067	.00814	9.18E+03
4008+	TL205	3150.3299	.003	6000.2758	.0043	2	0	2	-1	11073.065400	.0067	.00678	9.18E+03
4009+	TL205	3150.3300	.003	6000.2760	.0043	2	0	2	-1	11073.061900	.0067	.01296	9.18E+03
4010+	TL205	3150.3314	.003	6000.2784	.0043	2	0	2	-1	11073.063200	.0067	.00978	9.18E+03
4011+	TL205	3150.3332	.003	6000.2815	.0043	2	0	2	-1	11073.071000	.0067	.01182	9.18E+03
4012+	TL205	3150.3346	.003	6000.2839	.0043	2	0	2	-1	11073.077500	.0067	.01384	9.18E+03
4013+	TL205	3150.3356	.003	6000.2856	.0043	2	0	2	-1	11073.080100	.0067	.01324	9.18E+03
4014+	TL205	3150.3369	.003	6000.2878	.0043	2	0	2	-1	11073.077500	.0067	.00648	9.18E+03
4001-	TL205	3150.5459	.003	6000.6460	.0043	2	0	2	-1	11073.752200	.0067	.01241	9.18E+03
4002-	TL205	3150.5472	.003	6000.6482	.0043	2	0	2	-1	11073.754800	.0067	.01085	9.18E+03
4003-	TL205	3150.5494	.003	6000.6520	.0043	2	0	2	-1	11073.763900	.0067	.01291	9.18E+03
4004-	TL205	3150.5512	.003	6000.6551	.0043	2	0	2	-1	11073.767800	.0067	.01105	9.18E+03
4005-	TL205	3150.5530	.003	6000.6582	.0043	2	0	2	-1	11073.774300	.0067	.01179	9.18E+03
4006-	TL205	3150.5546	.003	6000.6609	.0043	2	0	2	-1	11073.782100	.0067	.01447	9.18E+03
4007-	TL205	3150.5547	.003	6000.6611	.0043	2	0	2	-1	11073.783400	.0067	.01545	9.18E+03
4008-	TL205	3150.5544	.003	6000.6606	.0043	2	0	2	-1	11073.782100	.0067	.01511	9.18E+03
4009-	TL205	3150.5544	.003	6000.6606	.0043	2	0	2	-1	11073.779500	.0067	.01251	9.18E+03
4010-	TL205	3150.5533	.003	6000.6587	.0043	2	0	2	-1	11073.775500	.0067	.01213	9.18E+03
4011-	TL205	3150.5513	.003	6000.6553	.0043	2	0	2	-1	11073.770400	.0067	.01333	9.18E+03
4012-	TL205	3150.5503	.003	6000.6530	.0043	2	0	2	-1	11073.767800	.0067	.01489	9.18E+03
4001-	TL205	3151.2052	.002	6001.7760	.0039	2	0	2	-1	11075.850000	.0048	.00061	1.30E+04
4002-	TL205	3151.2052	.002	6001.7760	.0039	2	0	2	-1	11075.849100	.0048	-.00029	1.30E+04
4003-	TL205	3151.2049	.002	6001.7755	.0039	2	0	2	-1	11075.848600	.0048	.00017	1.30E+04
4004-	TL205	3151.2046	.002	6001.7750	.0039	2	0	2	-1	11075.846800	.0048	-.00067	1.30E+04
4005-	TL205	3151.2042	.002	6001.7743	.0039	2	0	2	-1	11075.847300	.0048	.00111	1.30E+04
4006-	TL205	3151.2040	.002	6001.7739	.0039	2	0	2	-1	11075.844700	.0048	-.00085	1.30E+04
4007-	TL205	3151.2041	.002	6001.7741	.0039	2	0	2	-1	11075.846000	.0048	.00013	1.30E+04
4008-	TL205	3151.2044	.002	6001.7746	.0039	2	0	2	-1	11075.846500	.0048	-.00033	1.30E+04
4009-	TL205	3151.2050	.002	6001.7757	.0039	2	0	2	-1	11075.849400	.0048	.00065	1.30E+04
4010-	TL205	3151.2060	.002	6001.7774	.0039	2	0	2	-1	11075.852200	.0048	.00025	1.30E+04
4001+	TL205	3150.9224	.002	6001.2913	.0038	2	0	2	-1	11074.943100	.0049	-.00141	1.36E+04
4002+	TL205	3150.9226	.002	6001.2917	.0038	2	0	2	-1	11074.942600	.0049	-.00255	1.36E+04
4003+	TL205	3150.9246	.002	6001.2951	.0038	2	0	2	-1	11074.944700	.0049	-.00285	1.36E+04
4004+	TL205	3150.9272	.002	6001.2995	.0038	2	0	2	-1	11074.958200	.0049	-.00167	1.36E+04
4005+	TL205	3150.9292	.002	6001.3030	.0038	2	0	2	-1	11074.964800	.0049	-.00147	1.36E+04
4006+	TL205	3150.9302	.002	6001.3047	.0038	2	0	2	-1	11074.966700	.0049	-.00277	1.36E+04
4007+	TL205	3150.9302	.002	6001.3047	.0038	2	0	2	-1	11074.968500	.0049	-.00097	1.36E+04
4008+	TL205	3150.9297	.002	6001.3038	.0038	2	0	2	-1	11074.964800	.0049	-.00307	1.36E+04
4009+	TL205	3150.9290	.002	6001.3026	.0038	2	0	2	-1	11074.963900	.0049	-.00173	1.36E+04
4010+	TL205	3150.9281	.002	6001.3011	.0038	2	0	2	-1	11074.960000	.0049	-.00275	1.36E+04
4001-	TL205	3562.3326	.003	6698.7501	.0049	2	0	2	-1	12377.074500	.0057	-.00229	8.70E+03
4002-	TL205	3562.3330	.003	6698.7508	.0049	2	0	2	-1	12377.075600	.0057	-.00244	8.70E+03
4003-	TL205	3562.3330	.003	6698.7508	.0049	2	0	2	-1	12377.075700	.0057	-.00234	8.70E+03
4004-	TL205	3562.3326	.003	6698.7501	.0049	2	0	2	-1	12377.072800	.0057	-.00399	8.70E+03
4005-	TL205	3562.3335	.003	6698.7516	.0049	2	0	2	-1	12377.077000	.0057	-.00261	8.70E+03
4006-	TL205	3562.3341	.003	6698.7526	.0049	2	0	2	-1	12377.080500	.0057	-.00099	8.70E+03
4007-	TL205	3562.3307	.003	6698.7469	.0049	2	0	2	-1	12377.067200	.0057	-.00364	8.70E+03
4008-	TL205	3562.3297	.003	6698.7452	.0049	2	0	2	-1	12377.066600	.0057	-.00111	8.70E+03
4009-	TL205	3562.3290	.003	6698.7441	.0049	2	0	2	-1	12377.059600	.0057	-.00592	8.70E+03
4001+	TL205	3562.7334	.003	6699.4223	.0049	2	0	2	-1	12378.338000	.0057	.00618	8.70E+03
4002+	TL205	3562.7334	.003	6699.4223	.0049	2	0	2	-1	12378.337500	.0057	.00568	8.70E+03
4003+	TL205	3562.7333	.003	6699.4221	.0049	2	0	2	-1	12378.336600	.0057	.00509	8.70E+03
4004+	TL205	3562.7329	.003	6699.4215	.0049	2	0	2	-1	12378.337700	.0057	.00745	8.70E+03
4005+	TL205	3562.7324	.003	6699.4206	.0049	2	0	2	-1	12378.336300	.0057	.00761	8.70E+03
4006+	TL205	3562.7327	.003	6699.4211	.0049	2	0	2	-1	12378.337100	.0057	.00747	8.70E+03
4007+	TL205	3562.7333	.003	6699.4221	.0049	2	0	2	-1	12378.337000	.0057	.00549	8.70E+03
4008+	TL205	3562.7339	.003	6699.4231	.0049	2	0	2	-1	12378.341600	.0057	.00822	8.70E+03
4009+	TL205	3562.7345	.003	6699.4242	.0049	2	0	2	-1	12378.342000	.0057	.00674	8.70E+03
4010+	TL205	3562.7352	.003	6699.4253	.0049	2	0	2	-1	12378.342600	.0057	.00515	8.70E+03
4701+	TL205	3561.3338	.002	6697.0749	.0037	2	0	2	-1	12373.954000	.0048	.00487	1.42E+04
4702+	TL205	3561.3339	.002	6697.0750	.0037	2	0	2	-1	12373.950600	.0048	.00116	1.42E+04
4703+	TL205	3561.3339	.002	6697.0750	.0037	2	0	2	-1	12373.950200	.0048	.00076	1.42E+04
4704+	TL205	3561.3340	.002	6697.0752	.0037	2	0	2	-1	12373.952900	.0048	.00315	1.42E+04
4705+	TL205	3561.3349	.002	6697.0767	.0037	2	0	2	-1	12373.956200	.0048	.00363	1.42E+04
4706+	TL205	3561.3370	.002	6697.0802	.0037	2	0	2	-1	12373.960700	.0048	.00155	1.42E+04
4707+	TL205	3561.3396	.002	6697.0846	.0037	2	0	2	-1	12373.967300	.0048	.00001	1.42E+04
4708+	TL205	3561.3420	.002	6697.0886	.0037	2	0	2	-1	12373.977900	.0048	.00310	1.42E+04
4709+	TL205	3561.3442	.002	6697.0923	.0037	2	0	2	-1	12373.985400	.0048	.00371	1.42E+04
4710+	TL205	3561.3455	.002	6697.0945	.0037	2	0	2	-1	12373.985100	.0048	-.00066	1.42E+04
4711+	TL205	3561.3464	.002	6697.0960	.0037	2	0	2	-1	12373.990500	.0048	.00192	1.42E+04
4701-	TL205	3560.9703	.002	6696.4651	.0039	2	0	2	-1	12372.810900	.0060	.00009	1.14E+04
4702-	TL205	3560.9696	.002	6696.4640	.0039	2	0	2	-1	12372.808500	.0060	-.00012	1.14E+04
4703-	TL205	3560.9686	.002	6696.4623	.0039	2	0	2	-1	12372.805700	.0060	.00021	1.14E+04

XBL 687-1272

APPENDIX F. ^{205}TL RUN SUMMARY

RUN	ISOTOPE	CALIBRATION FREQUENCY (MHZ)	FREQUENCY ERROR (MHZ)	FIELD (GAUSS)	FIELD ERROR (GAUSS)	TRANSITION F 1	M 1	F 2	M 2	EXPERIMENTAL FREQUENCY (MHZ)	FREQUENCY ERROR (MHZ)	RESIDUAL (MHZ)	WEIGHT FACTOR
4704-	TL205	3560.9675	.002	6696.4605	.0039	2	0	2	-1	12372.797700	.0060	-.00435	1.14E+04
4705-	TL205	3560.9674	.002	6696.4603	.0039	2	0	2	-1	12372.796600	.0060	-.00513	1.14E+04
4706-	TL205	3560.9680	.002	6696.4613	.0039	2	0	2	-1	12372.804200	.0060	.00059	1.14E+04
4707-	TL205	3560.9693	.002	6696.4635	.0039	2	0	2	-1	12372.805600	.0060	-.00208	1.14E+04
4708-	TL205	3560.9705	.002	6696.4657	.0039	2	0	2	-1	12372.809600	.0060	-.00215	1.14E+04
4709-	TL205	3560.9714	.002	6696.4670	.0039	2	0	2	-1	12372.813100	.0060	-.00116	1.14E+04
4710-	TL205	3560.9680	.002	6696.4613	.0039	2	0	2	-1	12372.813800	.0060	.01019	1.14E+04
150N	TL205	258.4189	.002	549.5270	.0040	2	0	2	-1	918.358900	.0043	-.00417	1.41E+04
150N	TL205	258.4196	.002	549.5285	.0040	2	0	2	-1	918.362500	.0043	-.00325	1.41E+04
150N	TL205	258.4210	.002	549.5314	.0040	2	0	2	-1	918.367800	.0043	-.00329	1.41E+04
150N	TL205	258.4218	.002	549.5331	.0040	2	0	2	-1	918.371800	.0043	-.00235	1.41E+04
150N	TL205	258.4222	.002	549.5339	.0040	2	0	2	-1	918.371400	.0043	-.00427	1.41E+04
150N	TL205	258.4228	.002	549.5352	.0040	2	0	2	-1	918.373900	.0043	-.00406	1.41E+04
150N	TL205	258.4229	.002	549.5354	.0040	2	0	2	-1	918.375400	.0043	-.00295	1.41E+04
150N	TL205	258.4213	.002	549.5321	.0040	2	0	2	-1	918.369700	.0043	-.00254	1.41E+04
150N	TL205	258.4195	.002	549.5283	.0040	2	0	2	-1	918.361200	.0043	-.00416	1.41E+04
150N	TL205	258.4171	.002	549.5232	.0040	2	0	2	-1	918.358300	.0043	.00210	1.41E+04
150N	TL205	258.4173	.002	549.5236	.0040	2	0	2	-1	918.359000	.0043	.00204	1.41E+04
150R	TL205	258.4007	.002	549.4888	.0036	2	0	2	-1	918.290900	.0040	-.00268	1.72E+04
150R	TL205	258.4011	.002	549.4896	.0036	2	0	2	-1	918.296100	.0040	.00099	1.72E+04
150R	TL205	258.4006	.002	549.4886	.0036	2	0	2	-1	918.290000	.0040	-.00320	1.72E+04
150R	TL205	258.3986	.002	549.4843	.0036	2	0	2	-1	918.283300	.0040	-.00226	1.72E+04
150R	TL205	258.3979	.002	549.4829	.0036	2	0	2	-1	918.280700	.0040	-.00219	1.72E+04
150R	TL205	258.3975	.002	549.4822	.0036	2	0	2	-1	918.280000	.0040	-.00174	1.72E+04
150R	TL205	258.3975	.002	549.4820	.0036	2	0	2	-1	918.278300	.0040	-.00306	1.72E+04
150R	TL205	258.3992	.002	549.4856	.0036	2	0	2	-1	918.288000	.0040	.00015	1.72E+04
150R	TL205	258.4005	.002	549.4886	.0036	2	0	2	-1	918.289500	.0040	-.00370	1.72E+04
4501+	TL205	378.0202	.002	799.5108	.0040	2	0	2	-1	1376.499300	.0037	-.00996	1.50E+04
4502+	TL205	378.0197	.002	799.5097	.0040	2	0	2	-1	1376.498000	.0037	-.00935	1.50E+04
4503+	TL205	378.0196	.002	799.5095	.0040	2	0	2	-1	1376.497300	.0037	-.00966	1.50E+04
4504+	TL205	378.0195	.002	799.5093	.0040	2	0	2	-1	1376.497500	.0037	-.00908	1.50E+04
4505+	TL205	378.0194	.002	799.5091	.0040	2	0	2	-1	1376.494700	.0037	-.01150	1.50E+04
4506+	TL205	378.0195	.002	799.5093	.0040	2	0	2	-1	1376.498100	.0037	-.00848	1.50E+04
4507+	TL205	378.0196	.002	799.5095	.0040	2	0	2	-1	1376.497700	.0037	-.00926	1.50E+04
4508+	TL205	378.0196	.002	799.5095	.0040	2	0	2	-1	1376.497200	.0037	-.00976	1.50E+04
4509+	TL205	378.0194	.002	799.5091	.0040	2	0	2	-1	1376.498300	.0037	-.00790	1.50E+04
4510+	TL205	378.0192	.002	799.5087	.0040	2	0	2	-1	1376.497100	.0037	-.00833	1.50E+04
4501-	TL205	378.0015	.002	799.4719	.0040	2	0	2	-1	1376.428600	.0037	-.00898	1.50E+04
4502-	TL205	378.0015	.002	799.4719	.0040	2	0	2	-1	1376.429200	.0037	-.00838	1.50E+04
4503-	TL205	378.0009	.002	799.4707	.0040	2	0	2	-1	1376.425000	.0037	-.01028	1.50E+04
4504-	TL205	378.0004	.002	799.4696	.0040	2	0	2	-1	1376.423800	.0037	-.00957	1.50E+04
4505-	TL205	378.0003	.002	799.4694	.0040	2	0	2	-1	1376.424100	.0037	-.00888	1.50E+04
4506-	TL205	378.0002	.002	799.4692	.0040	2	0	2	-1	1376.423900	.0037	-.00870	1.50E+04
4507-	TL205	378.0002	.002	799.4692	.0040	2	0	2	-1	1376.418500	.0037	-.01410	1.50E+04
4508-	TL205	378.0001	.002	799.4690	.0040	2	0	2	-1	1376.421900	.0037	-.01032	1.50E+04
4509-	TL205	377.9997	.002	799.4682	.0040	2	0	2	-1	1376.421000	.0038	-.00968	1.48E+04
4510-	TL205	377.9995	.002	799.4677	.0040	2	0	2	-1	1376.420900	.0038	-.00902	1.48E+04
4401-	TL205	719.6885	.002	1499.4580	.0036	2	0	2	-1	2675.066000	.0040	-.01064	1.62E+04
4402-	TL205	719.6875	.002	1499.4560	.0036	2	0	2	-1	2675.061200	.0040	-.01168	1.62E+04
4403-	TL205	719.6868	.002	1499.4544	.0036	2	0	2	-1	2675.059400	.0040	-.01048	1.62E+04
4404-	TL205	719.6852	.002	1499.4511	.0036	2	0	2	-1	2675.053800	.0040	-.01007	1.62E+04
4405-	TL205	719.6840	.002	1499.4487	.0036	2	0	2	-1	2675.049400	.0040	-.00996	1.62E+04
4406-	TL205	719.6850	.002	1499.4507	.0036	2	0	2	-1	2675.054200	.0040	-.00891	1.62E+04
4407-	TL205	719.6862	.002	1499.4531	.0036	2	0	2	-1	2675.060800	.0040	-.00682	1.62E+04
4408-	TL205	719.6867	.002	1499.4542	.0036	2	0	2	-1	2675.060100	.0040	-.00940	1.62E+04
4401+	TL205	719.6294	.002	1499.3385	.0036	2	0	2	-1	2674.842700	.0035	-.01147	1.72E+04
4402+	TL205	719.6298	.002	1499.3393	.0036	2	0	2	-1	2674.844700	.0035	-.01097	1.72E+04
4403+	TL205	719.6306	.002	1499.3409	.0036	2	0	2	-1	2674.848000	.0035	-.01067	1.72E+04
4404+	TL205	719.6285	.002	1499.3366	.0036	2	0	2	-1	2674.852700	.0035	.00192	1.72E+04
4405+	TL205	719.6293	.002	1499.3383	.0036	2	0	2	-1	2674.856100	.0035	.00231	1.72E+04
4406+	TL205	719.6332	.002	1499.3461	.0036	2	0	2	-1	2674.858300	.0035	-.01015	1.72E+04
4407+	TL205	719.6337	.002	1499.3471	.0036	2	0	2	-1	2674.859700	.0035	-.01062	1.72E+04
4408+	TL205	719.6341	.002	1499.3479	.0036	2	0	2	-1	2674.859900	.0035	-.01193	1.72E+04
4409+	TL205	719.6341	.002	1499.3479	.0036	2	0	2	-1	2674.861700	.0035	-.01013	1.72E+04
4410+	TL205	719.6337	.002	1499.3471	.0036	2	0	2	-1	2674.860800	.0035	-.00952	1.72E+04
4411+	TL205	719.6326	.002	1499.3449	.0036	2	0	2	-1	2674.856900	.0035	-.00929	1.72E+04
4412+	TL205	719.6317	.002	1499.3431	.0036	2	0	2	-1	2674.851400	.0035	-.01141	1.72E+04
4413+	TL205	719.6308	.002	1499.3413	.0036	2	0	2	-1	2674.848500	.0035	-.01093	1.72E+04
4414+	TL205	719.6311	.002	1499.3419	.0036	2	0	2	-1	2674.849630	.0035	-.01095	1.72E+04
4415+	TL205	719.6317	.002	1499.3431	.0036	2	0	2	-1	2674.851200	.0035	-.01161	1.72E+04
4409-	TL205	719.6283	.002	1499.3362	.0036	2	0	2	-1	2674.841200	.0040	-.00883	1.62E+04
4410-	TL205	719.6289	.002	1499.3374	.0036	2	0	2	-1	2674.842500	.0040	-.00979	1.62E+04
4411-	TL205	719.6298	.002	1499.3393	.0036	2	0	2	-1	2674.845300	.0040	-.01037	1.62E+04
4412-	TL205	719.6301	.002	1499.3399	.0036	2	0	2	-1	2674.847900	.0040	-.00890	1.62E+04
4413-	TL205	719.6302	.002	1499.3401	.0036	2	0	2	-1	2674.849000	.0040	-.00817	1.62E+04
4414-	TL205	719.6304	.002	1499.3405	.0036	2	0	2	-1	2674.848400	.0040	-.00952	1.62E+04
4415-	TL205	719.6300	.002	1499.3397	.0036	2	0	2	-1	2674.848200	.0040	-.00822	1.62E+04
4416-	TL205	719.6293	.002	1499.3383	.0036	2	0	2	-1	2674.845400	.0040	-.00839	1.62E+04
4417-	TL205	719.6283	.002	1499.3362	.0036	2	0	2	-1	2674.840700	.0040	-.00933	1.62E+04
4418-	TL205	719.6278	.002	1499.3352	.0036	2	0	2	-1	2674.839600	.0040	-.00855	1.62E+04
4416+	TL205	719.6290	.002	1499.3376	.0036	2	0	2	-1	2674.843230	.0040	-.00943	1.62E+04
4417+	TL205	719.6295	.002	1499.3389	.0036	2	0	2	-1	2674.845400	.0040	-.00952	1.62E+04
4418+	TL205	719.6300	.002	1499.3397	.0036	2	0	2	-1	2674.846830	.0040	-.00962	1.62E+04
4419+	TL205	719.6302	.002	1499.3401	.0036	2	0	2	-1	2674.847900	.0040	-.00927	1.62E+04
4420+	TL205	719.6303	.002	1499.3403	.0036	2	0	2	-1	2674.848960	.0040	-.00865	1.62E+04
4421+	TL205	719.6305	.002	1499.3407	.0036	2	0	2	-1	2674.847700	.0040	-.01060	1.62E+04
4422+	TL205	719.6307	.002	1499.3411	.0036	2	0	2	-1	2674.849200	.0040	-.00985	1.62E+04
4423+	TL205	719.6304	.002	1499.3405	.0036	2	0	2	-1	2674.849000	.0040	-.00892	1.62E+04
4424+	TL205	719.6295	.002	1499.3387	.0036	2	0	2	-1	2674.846200	.0040	-.00834	1.62E+04
151	TL205	.1353	.002	.2906	.0043	2	0	1	0	530.076825	.0001	.00000	9.93E+07

XBL 687-1271

G. ^{69}Ga Reduced Submatrix for $m_F = -2$

F	3	2
3	$A(1,1) - \varepsilon$	$A(1,2)$
2	$A(1,2)$	$A(2,2) - \varepsilon$

Where

$$A(1,1) = (9a_{3/2} + b)/4 + 7.25c + \mu_o H(g_{3/2} + g_I)/h + (\mu_o HN)^2/9\delta h^2$$

$$A(1,2) = \mu_o H(g_{3/2} - g_I)/2h + (\mu_o HN/h)(3a'' - \eta b/2 - \mu_o HN/3h)/3\delta$$

$$A(2,2) = -3(a_{3/2} + b + c)/4 + \mu_o H(g_{3/2} + g_I)/h$$

$$+ (3a''' - \eta b/2 - \mu_o HN/3h)^2/\delta$$

H. ^{69}Ga Reduced Submatrix for $m_F = -1$

F	3	2	1
3	$A(1,1) - \varepsilon$	$A(1,2)$	$A(1,3)$
2	$A(1,2)$	$A(2,2) - \varepsilon$	$A(2,3)$
1	$A(1,3)$	$A(2,3)$	$A(3,3) - \varepsilon$

Where

$$A(1,1) = (9a_{3/2} + b)/4 + 7.25c + \mu_o H(g_{3/2} + g_I)/2h + 8(\mu_o HN/h)^2/45\delta$$

$$A(1,2) = 2\mu_o H(g_{3/2} - g_I)/\sqrt{10}h + (2\sqrt{2}\mu_o HN/3\sqrt{5}h)(3a''' - \eta b/2 - \mu_o HN/6h)/\delta$$

$$A(1,3) = -2(\mu_o HN/h)^2/15\sqrt{6}\delta$$

$$A(2,2) = -3(a_{3/2} + b + c)/4 + \mu_o H(g_{3/2} + g_I)/2h$$

$$+(\mu_o HN/h)^2/12\delta + (3a''' - \eta b/2 - \mu_o HN/6h)^2/\delta$$

$$A(2,3) = \sqrt{3}\mu_o H(g_{3/2} - g_I)/\sqrt{5}h + (\sqrt{3}\mu_o HN/6h)(\sqrt{5}a''' + \sqrt{5}\eta b/2 - \sqrt{5}\mu_o HN/6h)/\delta$$

$$-(3a''' - \eta b/2 - \mu_o HN/6h)(\mu_o HN/\sqrt{60}h)/\delta$$

$$A(3,3) = (-11a_{3/2} + b)/4 + 27.25c + \mu_o H(g_{3/2} + g_I)/2h$$

$$+(\sqrt{5}a''' + \sqrt{5}\eta b/2 - \sqrt{5}\mu_o HN/6h)^2/\delta + (\mu_o HN/h)^2/60\delta$$

I. ^{69}Ga Reduced Submatrix for $m_F = 0$

F	3	2	1	0
3	$A(1,1) - \varepsilon$	$A(1,2)$	$A(1,3)$	0
2	$A(1,2)$	$A(2,2) - \varepsilon$	$A(2,3)$	$A(2,4)$
1	$A(1,3)$	$A(2,3)$	$A(3,3) - \varepsilon$	$A(3,4)$
0	0	$A(2,4)$	$A(3,4)$	$A(4,4) - \varepsilon$

Where

$$A(1,1) = (9a_{3/2} + b)/4 + 7.25c + (\mu_o HN/h)^2/5\delta$$

$$A(1,2) = 3\mu_o H(g_{3/2} - g_I)/2\sqrt{5}h + (\mu_o HN/\sqrt{5}h)(3a''' - \eta b/2)/\delta$$

$$A(1,3) = -(\mu_o HN/h)^2/15\delta$$

$$A(2,2) = -3(a_{3/2} + b + c)/4 + (\mu_o HN/h)^2/9\delta + (3a''' - \eta b/2)^2/\delta$$

$$A(2,3) = 2\mu_o H(g_{3/2} - g_I)/\sqrt{5}h + (\mu_o HN/3h)(\sqrt{5}a''' + \sqrt{5}\eta b/2)/\delta$$
$$-(\mu_o HN/3\sqrt{5}h)(3a''' - \eta b/2)/\delta$$

$$A(2,4) = -(\mu_o HN/h)^2/9\delta$$

$$A(3,3) = (-11a_{3/2} + b)/4 + 27.25c + (\sqrt{5}a''' + \sqrt{5}\eta b/2)^2/\delta + (\mu_o HN/3\sqrt{5}h)^2/\delta$$

$$A(3,4) = \sqrt{5}\mu_o H(g_{3/2} - g_I)/2h - (\mu_o HN/3h)(\sqrt{5}a''' + \sqrt{5}\, b/2)/\delta$$

$$A(4,4) = (-15a_{3/2} + 5b)/4 - 28.75c + (\mu_o HN/h)^2/9\delta$$

REFERENCES

[1] Charlotte E. Moore, Atomic Energy Levels, Vol. III, (U.S. Government Printing Office; Washington, D.C., 1958) p. 202.

[2] Ibid, Vol. II, p. 130.

[3] Charles Schwartz, Theory of Hyperfine Structure, Phys. Rev. 97, 380 (1955).

[4] Aage Bohr and V. E. Weisskopf, The Influence of Nuclear Structure on The Hyperfine Structure of Heavy Elements, Phys. Rev. 77, 94 (1950).

[5] H. B. G. Casimir, On The Interaction Between Atomic Nuclei and Electrons, (W. H. Freeman and Company, 1963).

[6] W. W. Clendenin, Gyromagnetic Ratio in the Hyperfine Structure of Doublet States, Phys. Rev. 94, 1590 (1954).

[7] Henry Margenau, Relativistic Magnetic Moment of a Charged Particle, Phys. Rev. 57, 383 (1940).

[8] J. Scarborough, Numerical Mathematical Analysis, (The Johns Hopkins Press, Baltimore, 1962).

[9] A. Lurio, Ph.D. Thesis, Columbia University (1955) [unpublished].

[10] T. G. Eck and P. Kusch, Octupole Interactions in Stable Isotopes of In, Phys. Rev. 106, 958 (1957).

[11] B. Poole, F2 BC HOQR -- Eigenvalues and Eigenvectors of a Real Symmetric Matrix, Computer Center, University of California, Berkeley (1966).

[12] M. Phillips, The Effect of Nuclear Motion on Atomic Magnetic Moments, Phys. Rev. 76, 1803 (1949).

[13] A. Abragam and J. H. Van Vleck, Theory of the Microwave Zeeman Effect in Atomic Oxygen, Phys. Rev. 92, 1448 (1953).

[14] Charles Schwartz, Theory of Hyperfine Structure, Phys. Rev. 105, 173 (1957).

[15] Charles Schwartz, Hyperfine Structure Anomaly in Atomic P-States, Phys. Rev. 99, 1035 (1955).

[16] M. Phillips, Perturbations of Atomic g Values, Phys. Rev. 88, 202 (1952).

[17] P. A. Vanden Bout, Ph.D. Thesis, Lawrence Radiation Laboratory Report No. 16757, March 31, 1966 (unpublished).

[18] Y. Chan, Observation of the Field Dependent Ramsey Resonance Without Extremely Homogeneous Magnetic Fields, Brookhaven National Laboratory Report No. 10294 (1968).

[19] Norman Ramsey, Molecular Beams, (Oxford University Press, London, 1956).

[20] G. O. Brink and W. A. Nierenberg, Expérience de Double Résonance Dans un Jet Atomique, J. Phys. Rad. 19, 816 (1958).

[21] G. K. Woodgate and P. G. H. Sandars, Measurement of Nuclear Magnetic Moments in Atomic Beams, Nature 181, 1395 (1958).

[22] M. N. McDermott and R. Novick, Optical Double Resonance in Radio-Active Atoms: Spin and Nuclear Moments of the Ground State of Cd^{109}, Phys. Rev. 131, 707 (1963).

[23] R. E. Beehler and D. J. Glaze, Evaluation of a Thallium Atomic Beam Frequency Standard at the National Bureau of Standards, IEEE Transactions on Instrumentation and Measurement IM-15, 55 (1966).

[24] A. Lurio and A. G. Prodell, Hfs Separations and Hfs Anomalies in The $^2P_{1/2}$ State of Ga^{69}, Ga^{71}, $T\ell^{203}$ and $T\ell^{205}$, Phys. Rev. 101, 79 (1956).

[25] Charles Schwartz, Private Communication.

[26] H. Walchli, Oak Ridge National Laboratory Report No. 1775 (1954).

[27] J. W. Emsley, J. Feeney, and L. H. Sutcliffe, High Resolution Nuclear Magnetic Resonance Spectroscopy, Vol. 2, (Permagon Press, Oxford, 1966).

[28] Reference 19, p. 261.

[29] W. Hartree, D. Hartree, and M. Manning, Self-Consistent Field Calculations for Zn, Ga, Ga^{+}, Ga^{+++}, As, As^{+}, As^{++}, As^{+++}, Phys. Rev. 59, 299 (1941).

[30] Frank Herman and Sherwood Skillman, Atomic Structure Calculations, (Prentice-Hall, Inc., Englewood Cliffs, 1963).

[31] Edward B. Baker and L. W. Burd, Frequency-Swept and Proton-Stabilized NMR Spectrometer for All Nucleii using a Frequency Synthesizer, Rev. Sci. Instr. 34, 238 (1963).

[32] Frank Herman and Sherwood Skillman, Share Program ZO ML HFSS, International Business Machines (1963).

[33] R. T. Daley, Jr. and J. H. Holloway, Nuclear Magnetic Octupole Moments of the Stable Gallium Isotopes, Phys. Rev. 96, 539 (1954).

[34] Gordon Gould, Hfs Separations and Hfs Anomaly in the $6^2P_{3/2}$ Metastable Level of $T\ell^{203}$ and $T\ell^{205}$, Phys. Rev. 101, 1828 (1956).

[35] L. C. Balling and F. M. Pipkin, Gyromagnetic Ratios of Hydrogen, Tritium, Free Electrons, and Rb^{85}, Phys. Rev. 139, A19 (1965).

[36] New Values of the Physical Constants as Recommended by the NAS-NRC, Physics Today 17, No. 2, 48 (1964).

[37] Paul A. Vanden Bout, Erol Aygun, Vernon J. Ehlers, Tuncay Incesu, Adnan Saplakoglu, and Howard A. Shugart, Precision Measurement of the Electronic g Factors of the Alkali Metals, Phys. Rev. 165, 88 (1968).

[38] I. Lindgren, Table of Nuclear Spins and Moments in Alpha-, Beta-, and Gamma-Ray Sepctroscopy, Vol. 2, K. Siegbahn, ed., (North-Holland Publishing Company, Amsterdam, 1965) p. 1621.

[39] S. Penselin, Private Communication.

[40] S. Penselin, T. Moran, V. W. Cohen, and G. Winkley, Hyperfine Structure of the Electronic Ground States of Rb^{85} and Rb^{87}, Phys. Rev. 127, 524 (1962).

[41] $\Delta\nu$ of ^{133}Cs is the presently accepted frequency standard.

[42] D. T. Wilkinson and H. R. Crane, Precision Measurement of the g-Factor of the Free Electron, Phys. Rev. 130, 852 (1963): Arthur Rich, Correction to the Experimental Value for the Electron g-Factor Anomaly, Phys. Rev. Letters 20, 967 (1968).

[43] K. Kambe and J. H. Van Vleck, Improved Theory of the Zeeman Effect of Atomic Oxygen, Phys. Rev. 96, 66 (1954).

[44] Charles Schwartz, Theory of Hyperfine Structure, Phys. Rev. 105, 173 (1957).

[45] Brian R. Judd, Operator Techniques in Atomic Spectroscopy, (McGraw-Hill, New York, 1963).

This report was prepared as an account of Government sponsored work. Neither the United States, nor the Commission, nor any person acting on behalf of the Commission:

A. Makes any warranty or representation, expressed or implied, with respect to the accuracy, completeness, or usefulness of the information contained in this report, or that the use of any information, apparatus, method, or process disclosed in this report may not infringe privately owned rights; or

B. Assumes any liabilities with respect to the use of, or for damages resulting from the use of any information, apparatus, method, or process disclosed in this report.

As used in the above, "person acting on behalf of the Commission" includes any employee or contractor of the Commission, or employee of such contractor, to the extent that such employee or contractor of the Commission, or employee of such contractor prepares, disseminates, or provides access to, any information pursuant to his employment or contract with the Commission, or his employment with such contractor.